AN ABSTRACT OF THE THESIS OF

ADRIANA HUYER (Name) for the DOCTOR OF PHILOSOPHY (Degree)

in OCEANOGRAPHY (Major) presented on November 15, 1973 (Date)

TITLE: OBSERVATIONS OF THE COASTAL UPWELLING REGION OFF OREGON DURING 1972

Abstract approved: Redacted for privacy
Robert L. Smith

Observations of wind, currents, sea level and hydrography obtained during the 1972 Coastal Upwelling Experiment (CUE-I) are described. Only phenomena with periods longer than a day are considered. One section describes the changes observed during a period of variable winds in early July 1972. Another describes a ribbon of relatively cool water observed early in the upwelling season and attributes its existence to advection of Subarctic water by the coastal jet associated with upwelling. A third section describes the seasonal development of the upwelling regime between April and October 1972. These studies are combined with other studies of CUE-I data to provide a partial description of the upwelling regime which is compared to the conceptual model developed prior to CUE-I.

It is concluded that the vertical and onshore velocity fields are as yet largely unknown. The alongshore velocity field includes southward surface flow with a coastal jet, a persistent vertical shear

with deeper velocities northward relative to the surface and high coherence with the wind and sea level at periods of several days. A poleward undercurrent is observed, but it may not be an integral part of the upwelling regime.

The hydrography has a strong seasonal cycle. Differences between any two sections between April and October 1972 are smaller than between any of these and a section occupied in January 1973. Oscillations in the wind with periods of several days cause significant changes in the region inshore of 10 km and in the upper 20 m further offshore. Subsurface temperature observations are not coherent with the wind at periods of several days.

Observations of the Coastal Upwelling Region off Oregon during 1972

by

Adriana Huyer

A THESIS

submitted to

Oregon State University

in partial fulfillment of
the requirements for the
degree of

Doctor of Philosophy

June 1974

APPROVED:

Redacted for privacy

Associate Professor of Oceanography
in charge of major

Redacted for privacy

Dean of School of Oceanography

Redacted for privacy

Dean of Graduate School

Date thesis is presented: November 15, 1973

Typed by Suelynn Williams for Adriana Huyer.

ACKNOWLEDGMENTS

All members of the CUE family at Oregon State University contributed in one way or another to this dissertation. CUE participants from other institutions also contributed significantly. CUE was funded by the Office for the International Decade of Ocean Exploration, National Science Foundation. During my studies, I have been supported by the Marine Sciences Branch, Environment Canada.

Three sections of the dissertation comprise papers with one or more co-authors. Section II has been presented at the Second Conference "Analyse de l'Ecosysteme des 'Upwellings'" in Marseille and will be published in Tethys as part of the proceedings of that meeting with R. L. Smith and R. D. Pillsbury as co-authors. An earlier draft of Section III has been submitted to Journal of Physical Oceanography with R. L. Smith as co-author, and is currently undergoing revision. Section IV will be revised and submitted with R. D. Pillsbury and R. L. Smith as co-authors.

The controversial manuscript by Chris Mooers, Curt Collins and Bob Smith contributed immeasurably both to the design of CUE and to my own thinking. The CUE Theoretical Workshop led by John Allen and Chris Mooers provided a great deal of food for thought.

Fred Barber, June Pattullo and Robert Smith have guided my development as an oceanographer; I suspect my work will always show their influence.

TABLE OF CONTENTS

I. Introduction 1
The 1972 Coastal Upwelling Experiment 2
Organization 4
The Oceanography off Oregon - Literature Review 4

II. Observations During a Period of Variable Winds, July 1972 10
The Observations 10
Results 14
Discussion 25
The Hydrographic Regime 25
Currents 30
Stability 35
Conclusions 37

III. Observations of a Subsurface Ribbon of Cool Water over the Continental Shelf off Oregon 39
The Observations 39
Results 42
Discussion 50
Seasonal Evolution of the Ribbon 50
Spatial Extent of the Ribbon 51
The Ribbon as a permanent Feature of the Upwelling Regime 54
Source of the Ribbon 59
Other Temperature Inversions in the Region 61
Conclusions 67

IV. Seasonal Evolution of the Upwelling Regime, 1972 69
The Observations 69
Results 73
Discussion 79
Wind 79
Hydrography 85
Currents 96
(1) The Surface Jet 97
(2) The Poleward Uncercurrent 99
(3) Geostrophy of Alongshore Flow 105
(4) Comparison between Wind and Current 107
Sea Level 111
Conclusions 113

TABLE OF CONTENTS (CONTINUED)

V. Discussion 117
Partial Description of the Upwelling Regime off Oregon 117
Boundaries 118
Density Field 119
Velocity Field 121
Distribution of Tracers 127
Exchange Across the Boundaries 128
Comparison with Previous Description 129
Completing the Description 136
Defining Upwelling 137

VI. Conclusions 139

VII. References 142

LIST OF TABLES

Table		Page
I	Oceanographic observations during the 1972 Coastal Upwelling Experiment.	3
II	Estimates of minimum Richardson number, 5-20 July 1972.	34
III	Dates of hydrographic surveys by R/V YAQUINA of the grid adjacent to the Oregon coast, 1972.	41
IV	Values of the upwelling index at 45°N, 125°W and observations of the presence of the cool ribbon during the upwelling season of Oregon, 1961-1971. A (*) indicates the ribbon was observed; a (°) indicates observations were made but there was no evidence of the ribbon. Units of the upwelling index are m^3/sec/ 100 m.	58
V	Dates of hydrographic surveys off the coast of Oregon, 1972.	73
VI	Comparison of means of local wind stress and wind stress computed from Bakun's values of Ekman transport.	84
VII	Mean velocities from the moored current meter array, 0000 Z, 25 July to 0000 Z, 5 August 1972. Components are eastward (u), northward (v), cross-isobath (u'), and along-isobath (v').	125

LIST OF FIGURES

Figure		Page
1	Positions and depths of the current meters from which data were obtained during the period of variable winds, 5-20 July 1972. The position of the anemometer is indicated by A.	11
2	Low-passed time series of sea level and of eastward (u) and northward (v) components of the wind and currents, 5-20 July 1972. Units for wind are m sec^{-1}, for sea level are cm, and for current are cm sec^{-1}.	13
3	Vertical distributions of temperature, salinity and sigma-t: (a) 6 and 9 July, (b) 13-14 and 14-15 July, (c) 16 and 17 July 1972.	15-17
4	Low passed wind and current vectors for shallow (thin) and deep (thick) current meters, 1200 Z, 6-19 July 1972. The large dot represents Yaquina Head and separates wind and current vectors.	19
5	Vertical distributions of the eastward and northward components of the low passed current observations along 44°40'N.	22
6	Bottom profiles in the vicinity of Stonewall Bank, between 44°25' and 44°40'N.	29
7	Comparison between observed and geostrophic differences in the northward component of the current between the top and bottom current meters at NH-10, NH-15, and NH-20.	29
8	Northward component of the surface current versus distance offshore.	34
9	Location of the grid surveyed by YAQUINA, summer 1972. Lines show the position and length of sections occupied several times during the summer	40

LIST OF FIGURES (CONTINUED)

Figure		Page
10	Vertical distributions of temperature and salinity during the YAQUINA survey of 21-22 June, along 44°40'N, 44°50'N, and 45°00'N.	43
11	Vertical distributions of temperature at 45°00'N, 20-21 May, 7 July and 2 August 1972, and at 44°55'N, 27 August 1972.	44
12	Properties of the cool ribbon observed during surveys in May, June and early July 1972: (a) thickness and depth (b) temperature and salinity.	45, 46
13	Properties of a relative temperature minimum layer during surveys in August. Areas where more than one relative minimum were observed are shaded.	48
14	Distribution of the correlation between a reference station (*) and each other station of the May, June and early July surveys. Cross-hatched areas show regions where the maximum salinity was too small to compute the correlation. The nearshore area had minimum salinities too large to compute the correlation.	53
15	Station positions for YAQUINA cruise Y6806C, 24 June-3 July 1968.	55
16	Vertical distributions of temperature and salinity for two sections of YAQUINA cruise Y6806C.	56
17	The vertical distributions of both temperature and the northward component of velocity at 44°40'N, 9 July 1972.	62
18	Temperature-salinity characteristics both offshore and along the cool ribbon, June 1968.	64
19	Temperature-salinity curves for selected stations from the June 1972 grid survey.	64

LIST OF FIGURES (CONTINUED)

Figure		Page
20	Positions of the moored current meter arrays, April to October 1972.	71
21	Periods of moored current meter operation off Oregon, April to October, 1972.	72
22	Low passed time series of wind and currents measured at locations off Yaquina Head, and sea level at Depoe Bay, April to October 1972. (a) eastward component of wind and currents, (b) northward component of wind and currents, and sea level.	74, 75
23	Low passed time series of the currents measured off Depoe Bay, July and August, 1972. Wind and sea level are repeated from Figure 22.	76
24	Hydrographic sections along 44°55'N showing vertical distributions of temperature, salinity and sigma-t.	78
25	Low passed time series of temperature from the deepest current meter at each moored array except NH-3.	80
26	Zonal Ekman transport per 100 m of coastline, in the vicinity of 45°N, 125°W.	81
27	Monthly mean values of the upwelling index at 45°N, 125°W, from Bakun (1972). Heavy solid line indicates the twenty-year mean; lighter lines show the standard deviation. The dashed line shows the 1972 values.	83
28	Monthly means and standard deviations of the low passed wind measured at Newport, May to October 1972.	83
29	Autospectra and the coherence-squared spectrum for the local wind stress and the wind stress computed from Bakun's values of the Ekman transport, 22 April to 31 October 1972. The dashed line shows the 99% significance level for coherence squared.	86

LIST OF FIGURES (CONTINUED)

Figure		Page
30	Vertical distributions of temperature, salinity and sigma-t along 44°45'N, 2-3 January 1973.	87
31	Distance vs. time plots of the depth and temperature of isohalines at 44°55'N, May to October 1972.	89
32	Distance vs. time plots of the depth and temperature of isohalines at 44°40'N, 6-18 July 1972.	91
33	Autospectra and the coherence squared spectrum of the wind at Newport and the temperature at 80 m, NH-15, 24 April to 26 October 1972. The dashed line shows coherence squared significantly different from zero at the 95% level.	94
34	Coherence squared spectra between the wind at Newport and three temperature records at 20 m, DB-7; 20 m, NH-20; and 80 m, NH-15, 10 July-26 August 1973. The dashed line shows coherence squared significantly different from zero at the 95% level.	95
35	Time vs. distance plots of the northward component of velocity along 44°40'N, 10-29 July and 13-27 August 1972.	98
36	Northward velocity and sigma-t at 20 m, along 44°40'N, vs. distance offshore.	100
37	Monthly mean values of the northward component of the relative velocity between the deepest and shallowest current meter at each station, April to October 1972.	103
38	Monthly mean values of the northward component of the current at the deepest current meter of each array, April to October 1972.	103
39	Comparison between measured and geostrophic relative velocities: (a) geostrophic vs. measured velocity, (b) difference between measured and geostrophic relative velocity for each date.	106

LIST OF FIGURES (CONTINUED)

Figure		Page
40	Coherence squared spectra for currents vs. wind at Newport, 10 July-27 August 1972. The dashed line shows coherence squared significantly different from zero at the 95% level.	109
41	Autospectra and coherence squared spectrum for the wind at Newport and current at 40 m, NH 15, 23 June to 26 October 1972. The dashed line shows coherence squared different from zero at the 95% level.	110
42	The spectrum of low passed sea level at Depoe Bay, 23 June to 26 October 1972, and the coherence squared spectra of Depoe Bay sea level vs. Newport wind and current at 40 m, NH-15, 23 June to 26 October 1972. The dashed line shows coherence squared significantly different from zero at the 95% level.	112
43	The monthly mean sea level at Newport, Oregon. Solid line shows the 10 year mean sea level (Brunson, 1973). Dashed line shows values from the 1972 upwelling season.	114
44	The conceptual model tested in the 1972 Coastal Upwelling Experiment (from Mooers et al., 1973, their Figure 14).	131

OBSERVATIONS OF THE COASTAL UPWELLING REGION OFF OREGON DURING 1972

1. INTRODUCTION

Upwelling has been defined (Smith, 1968) to mean ascending motion of some minimum duration and extent by which water from the subsurface layers is brought into the surface layer and is removed from the area of upwelling by horizontal flow. In general, upwelling is the result of divergence in the surface layer; coastal upwelling occurs when the prevailing winds carry the surface water away from the coast.

Seasonal coastal upwelling is a dominant feature of the oceanographic regime off Oregon; the process has been the subject of a great deal of research at Oregon State University and elsewhere. Several years of study of upwelling off Oregon resulted in the development of a conceptual model of the regime. The 1972 Coastal Upwelling Experiment (CUE-I) off Oregon was an effort to test the model, and to obtain new kinds of observations to learn more about the regime.

The purpose of this dissertation is to present some of the results of CUE-I, particularly those that have traditionally been referred to as "descriptive physical oceanography". This dissertation is by no means exhaustive even within this limited area; several more man-years of

work will be required before that is possible. Instead, it presents some features of the oceanographic regime of particular importance or of special interest to the author.

The 1972 Coastal Upwelling Experiment (CUE-I)

Several kinds of observations were made by different institutions within the CUE-I area during the summer of 1972. The area designated for study was about a 50 km square: from the coast (about 124°00'W) to about 124°30'W and from 44°35'N to 45°00'N. Hydrographic surveys were made primarily from two ships: the R/V OCEANOGRAPHER by Pacific Oceanographic Laboratory, and from R/V YAQUINA by Oregon State University. Moored current meter observations were made primarily by Oregon State University. The remaining types of oceanographic observations of CUE-I are listed in Table I. In addition, routine measurements of wind speed and direction and atmospheric pressure were made at Newport, Oregon and sea level was measured at Newport and Depoe Bay, Oregon. This dissertation utilizes mainly the hydrographic and current meter data obtained by Oregon State University.

The observations were initially planned to test the conceptual model of the upwelling regime formulated by Mooers, Collins and Smith (1973). The observations described in this dissertation are compared as much as possible to this conceptual model.

Table I. Oceanographic observations during the 1972 Coastal Upwelling Experiment.

Type of Observations	Institution	Reference
Hydrography	OSU	Anon. 1972a-e; 1973a-c
	POL	Halpern and Holbrook, 1972
	IATTC	Stevenson and Wyatt, 1973
	UM	
Moored current meters	OSU	Pillsbury, Bottero and Still, 1973
	POL	Halpern, Holbrook and Reynolds, 1973
Vertical current meters	WHOI/OSU	Deckard, 1974
Sea surface temperatures	FSU	O'Brien, 1972
Subsurface drogues	IATTC	Stevenson, 1972a, b
Surface drogues	UC	Garvine, 1972
Nutrients	OSU	Tomlinson et al., 1973
Optics	OSU	Plank and Pak, 1973
Phytoplankton	OSU	Small, 1972
Profiling current meters	UM	

Acronyms for institutions are: OSU - Oregon State University; POL - Pacific Oceanographic Laboratory, National Oceanic and Atmospheric Administration; IATTC - Inter-American Tropical Tuna Commission; UM - University of Miami; WHOI - Woods Hole Oceanographic Institution; FSU - Florida State University; UC - University of Connecticut.

Organization

The dissertation has three relatively independent sections which each describe one aspect of the observations in detail. The first describes the effect of variable wind (several day period) on the regime. The second describes a mesoscale feature of the hydrographic regime and relates it to the presence of upwelling. The third explores the evolution of the upwelling regime during the season. Each of these sections is complete with discussion and conclusions. These results are then combined with other studies of CUE-I data to provide a partial description of the coastal upwelling regime, which is compared to the earlier description and the conceptual model provided by Mooers et al. (1973).

The Oceanography off Oregon - Literature Review

The water off Oregon is generally believed to lie within the transition region of the North Pacific Ocean, between the Subarctic Region and the Central Region (e.g., Dodimead, Favorite and Hirano, 1963). The general circulation in the region is dominated by the California Current system, which flows southeastward between a cell of high atmospheric pressure to the west and a cell of low pressure on the landward side (Reid, Roden and Wyllie, 1958). Changes in strength and location of these high and low pressure cells cause seasonal changes in

the winds; from spring through fall, the winds have a northerly (southward) component, causing upwelling along the coast.

The water which is brought south by the California Current is cooler than the water further offshore (Reid et al., 1958). Rosenberg (1962) in a study of the water masses off Oregon, found that modified subarctic water was identified with the main stream of the California Current system. Beneath the modified subarctic water, he found modified equatorial water which indicated northward flow at depth. The data examined by Rosenberg did not allow detailed study of the nearshore region. Processes affecting the sea water characteristics in the nearshore region were described by Pattullo and Denner (1965).

The first paper dealing explicitly with the nearshore oceanography off Oregon (Pattullo and McAlister, 1962) has caused confusion about the role of fronts in the upwelling regime. Pattullo and McAlister showed a front sloping downward toward the coast (at 100 m deep 15 miles offshore and 30 m deep at 35 miles offshore). The front was inferred from bathythermographs obtained in October 1960; an apparently simultaneous hydrographic section shows isohalines sloping upward toward the coast (Wyatt and Kujala, 1962, p. 46). The isotherms can be drawn in an alternative way which is more consistent with the salinity distribution. The front seems to be inferred from temperature inversions at only two locations, occurring at very different salinities. The front described probably did not exist, and the paper should be

neglected in subsequent studies of the upwelling regime.

Park, Pattullo and Wyatt (1962) showed that chemical properties are better indicators of upwelling than are temperature and salinity. Smith, Pattullo and Lane (1966) estimated the vertical velocity from displacement of isopycnals for a short period early in the upwelling season, finding it to be larger nearshore (7×10^{-3} cm sec^{-1} at 5 nautical miles offshore) than further offshore (2×10^{-4} cm sec^{-1} at 35 n.m.).

Collins (1964) described the upwelling regime in terms of the permanent oceanic front. He defined the permanent front from observations at a single location (105 miles west of Newport, Oregon) during 1962. He found that water between 50 m and 150 m always lay within the front, and that sigma-t values between 25.3 and 26.3 were always within the front. He then defined sigma-t values of 25.5 and 26.0 as delineating the front. During intense upwelling, the front frequently intersects the sea surface.

Pattullo, Burt and Kulm (1969) showed the heat storage in the upper 100 m is lower in the summer than in the winter for the nearshore region (up to 65 miles from shore). The cold water near the coast in summer is principally the result of upwelling.

Observations of temperature inversions in the upwelling region were frequent (Collins et al., 1968; Mooers et al., 1968). One of these was studied in detail using optical as well as the usual temperature

and salinity observations (Pak, Beardsley and Smith, 1970); the temperature inversion coincided with a turbidity maximum and seemed to be due to the sinking of modified upwelled water as it moved offshore. Mooers et al. (1973) pursued the relation between the temperature inversions and the circulation in the frontal region of the upwelling regime. They concluded that the sinking occurred at the base of the permanent pycnocline and inferred a two-celled onshore-offshore circulation.

Early studies of chemical parameters off Oregon described the distributions at locations well offshore (Steffanson and Richards, 1964; Pytkowicz, 1964; Park, 1967a, b). Park (1968) describes the seasonal variation in the vertical distribution of alkaline pH and salinity nearer shore and shows the effect of coastal upwelling. Hager (1969), in a study of the Columbia River plume showed that the silicate distribution at 30 m depth off Oregon is determined mostly by coastal upwelling, with values over 50 μM nearshore and less than 2 μM offshore. Cissell (1969) showed that isograms of several parameters (dissolved oxygen, phosphate, nitrate, silicate, pH, and carbonates) slope upward toward the coast from depths exceeding 200 m. Ball (1970) described the seasonal variation in the distribution of nutrients. Kantz (1973) in a comparison between conditions during March and June 1971, showed that on both occasions the regime was highly influenced by meteorological conditions occurring during the week or so prior to the

observations. Atlas (1973) describes three occupations of the same hydrographic line made just before, during and after a five day period of strong southward winds in June 1973. He computed the vertical distribution of the onshore velocity from successive salinity distributions and found that most of the offshore flow was restricted to about the upper 20 m and that onshore velocities were generally less than 2 cm sec^{-1}. Gordon (1973) described the distribution of the partial pressure of carbon dioxide in the upwelling regions, and found some evidence of the existence of a carbon trap, resulting from a recycling of the carbon dioxide entering the upwelling region at depth.

Direct current observations off the Oregon coast began with drift bottles (Burt and Wyatt, 1964) which showed evidence of nearshore northward flow in winter (the Davidson Current) and southward flow in summer. Percentage returns were found to be lower in summer, as expected from the offshore surface flow during the upwelling season. Drogue observations (Stevenson, Pattullo and Wyatt, 1969) showed that current direction was relatively constant with depth during a particular cruise, but highly variable from cruise to cruise at the same depth. Sea level data were used to infer the presence of continental shelf waves along the Oregon coast (Mooers and Smith, 1968). Moored current meters were deployed off Oregon each year from 1965 to 1969; data from these moorings form the basis for a number of studies: Collins et al., 1968; Collins and Pattullo, 1970; Mooers,

1970; Huyer and Pattullo, 1972; and Cutchin and Smith, 1973. Pillsbury (1972) summarized the results obtained up to and including 1972. He showed that there is a shear between the shallow and deep currents during the upwelling season, with deep currents always being northward relative to the shallow currents; late in the upwelling season (August and September) flow is often northward in the deeper layer. The longshore current is mainly geostrophic and seems to be fairly well correlated with the local wind. Cutchin and Smith (1973) showed that continental shelf waves may be present.

The upwelling regime off Oregon has been compared with other upwelling regions and appears to be similar (Smith, 1968; Smith, Mooers and Enfield, 1971).

The manuscript by Mooers et al. (1973) contains the most complete description of the coastal upwelling regime off Oregon prior to the Coastal Upwelling Experiment. Their conceptual model includes schematics of both the alongshore flow regime and the cross-stream circulation. The alongshore flow regime includes an equatorward surface current with a coastal jet, and a poleward undercurrent. The cross-stream circulation consists of two cells, with sinking at the base of the permanent pycnocline. Since their model provided much of the basis for CUE-I, it will be described in detail and compared to the results of studies of CUE-I data.

II. OBSERVATIONS DURING A PERIOD OF VARIABLE WINDS, JULY 1972

The coastal upwelling regime off Oregon has generally been described in terms of the mean wind field. The wind is generally not steady and significant departures from the mean occur on time scales of days or weeks. Intense oceanographic observations were made during a period of variable winds in early July 1972. The measurements included wind, sea level, current and hydrographic observations.

The purpose of this section is to describe variations in the parameters observed, and to determine whether they are related. The data are not adequate to describe variations in the three-dimensional fields, and attention will be focused on the two-dimensional (vertical and offshore) fields. Our interest in this section is primarily in the low frequency variations and no attempt is made to describe tidal, inertial or higher frequency variations.

THE OBSERVATIONS

The wind was measured from the south jetty at Newport, Oregon (Figure 1) with a Bendix-Freize anemometer. The system records wind speed and direction continuously. Hourly values of speed and direction were obtained by averaging over a twenty-minute interval

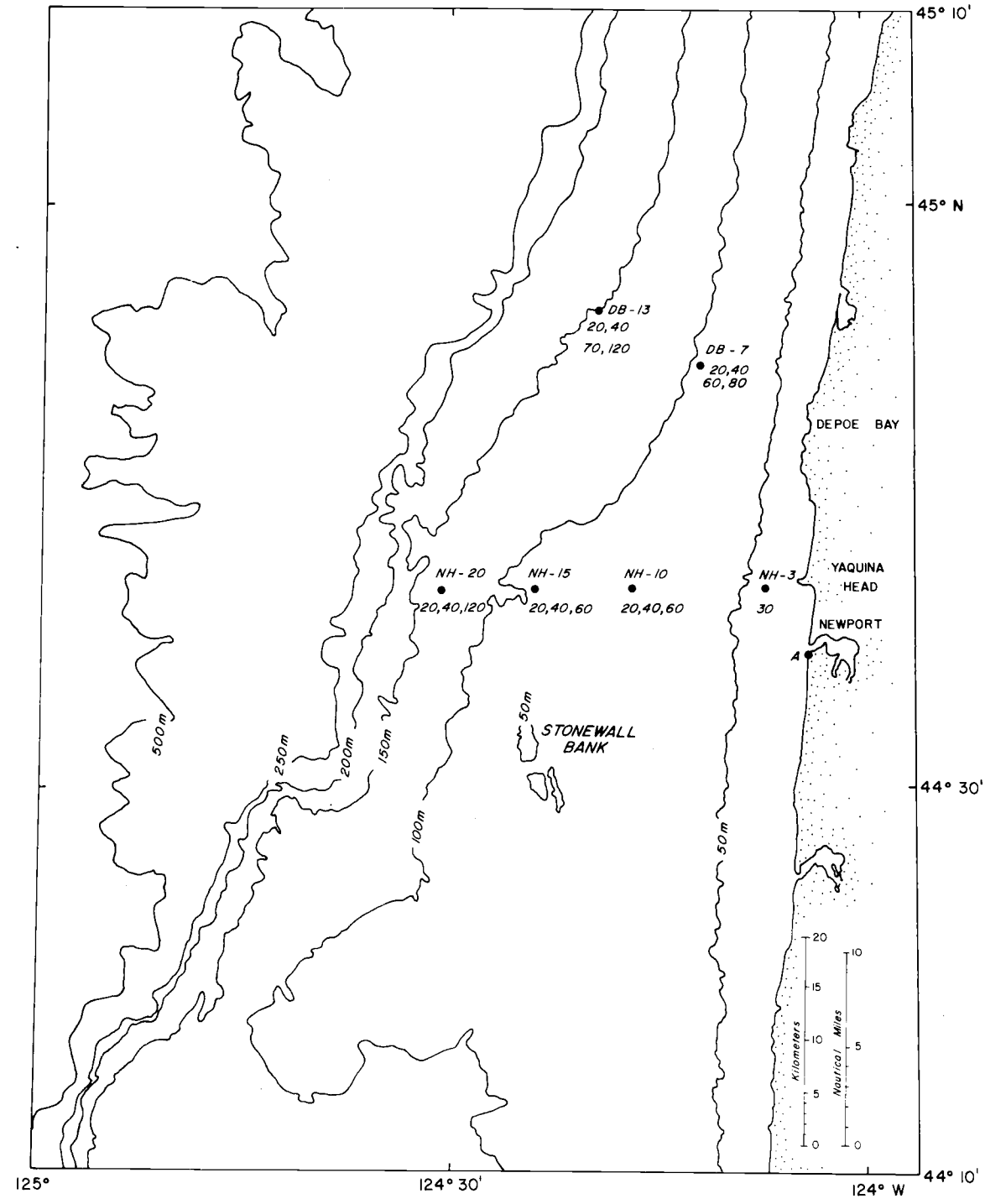

Figure 1. Positions and depths of the current meters from which data were obtained during the period of variable winds, 5-20 July 1972. The position of the anemometer is indicated by A.

centered at the hour. Sea level was measured by a permanently maintained tide gauge at Newport. The data are automatically recorded every 6 minutes to within 0.3 cm and the series were decimated to hourly values. Atmospheric pressure is recorded at Newport and an hourly data series was obtained.

During this period, currents were measured from six moored arrays: at 3, 10, 15 and 20 nautical miles off Yaquina Head and 7 and 13 miles off Depoe Bay (Figure 1). Aanderaa current meters recorded speed, direction, and temperature at 5 minute intervals. The deepest current meter in each array also recorded pressure. The five minute observations were filtered to obtain hourly time series; these series and the details of the current meter operation and data processing are reported by Pillsbury et al. (1973). The array at NH-15 was moored on 20 June 1972, recovered on 18 July and replaced with another array the same day. The array at NH-3 was moored on 5 July; the arrays at NH-10 and NH-20 were moored on 6 July. The arrays at DB-7 and DB-13 were moored on 7 July 1972; the entire array at DB-13 was unknowingly released on 18 July.

The hourly wind, sea level, atmospheric pressure, and current data were filtered to suppress tidal and inertial oscillations; we used a symmetrical Cosine filter spanning 121 hours with a half-power point of 40 hours. The average sea level and the "inverted barometer" effect of atmospheric pressure on sea level (a 1 mb increase in

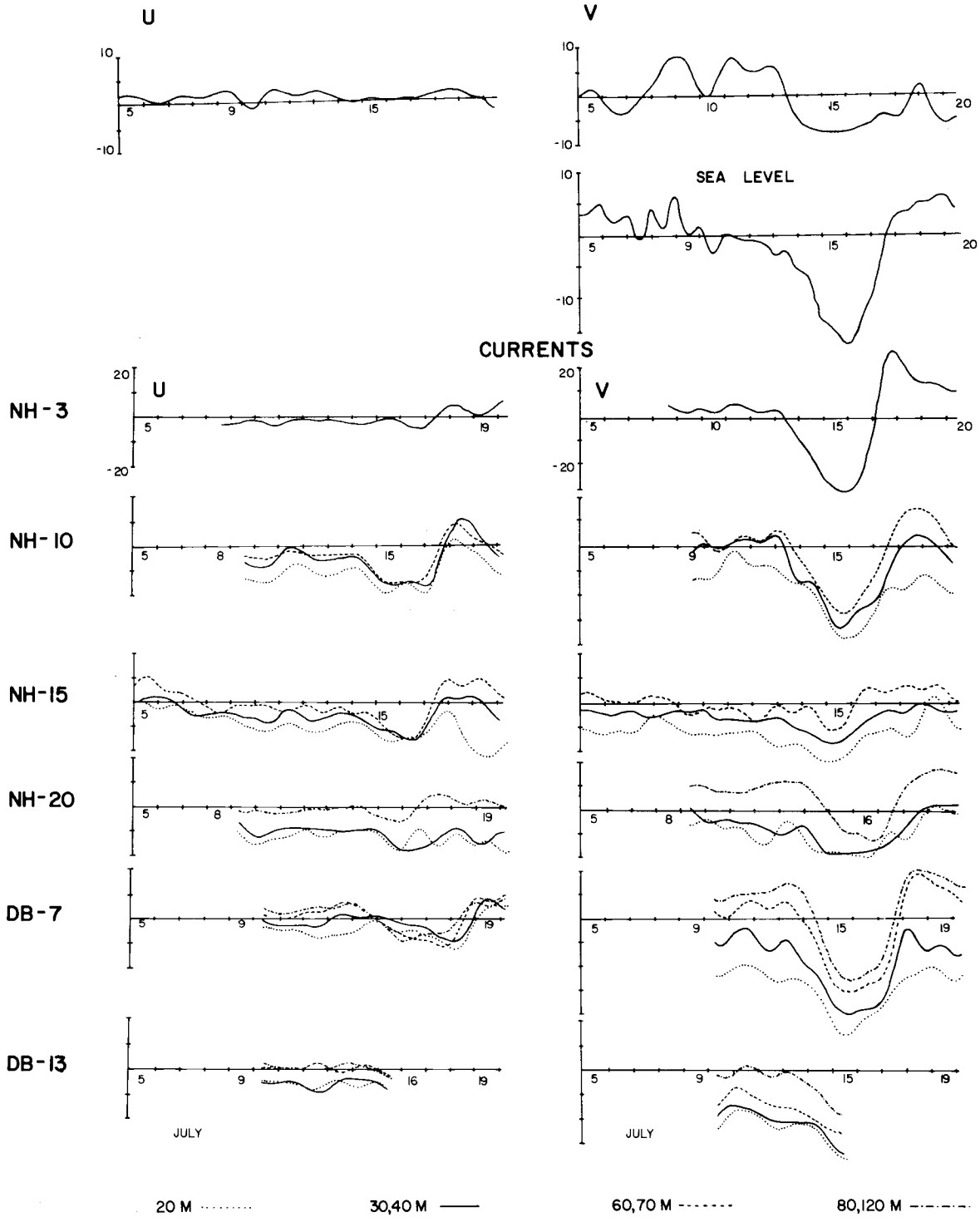

Figure 2. Low-passed time series of sea level and of eastward (u) and northward (v) components of the wind and currents, 5-20 July 1972. Units for wind are m sec^{-1}, for sea level are cm, and for current are cm sec^{-1}.

atmospheric pressure decreases sea level by 1 cm) were removed. The resulting low passed series of wind, adjusted sea level and currents are shown for the period from 5 to 20 July 1972 (Figure 2).

A line of hydrographic stations seaward of Yaquina Head (along 44°40'N) was occupied six times by R/V YAQUINA between 6 and 17 July. The maximum separation between stations was 7.9 km; usually the separation between inshore stations was less. The line ended at about 50 km offshore (124°42'W); on one occasion it was extended to about 75 km (125°00'W). The line was covered as quickly as possible; usually in less than eight hours. Observations were made with a Geodyne conductivity-temperature-depth (CTD) unit. Sampling techniques and data processing procedures are described in the hydrographic data reports (Anon., 1972b, c). Salinity and sigma-t were computed for each observed depth. Vertical sections of temperature, salinity and sigma-t (Figure 3) were contoured from the vertical profiles of each parameter. The position and maximum depth of each CTD cast are shown in the sections.

A few vertical current meters were also deployed during this period. These observations were analyzed separately by Deckard (1974) and are discussed in section V of this dissertation.

RESULTS

The wind had been blowing southward (the direction favorable to

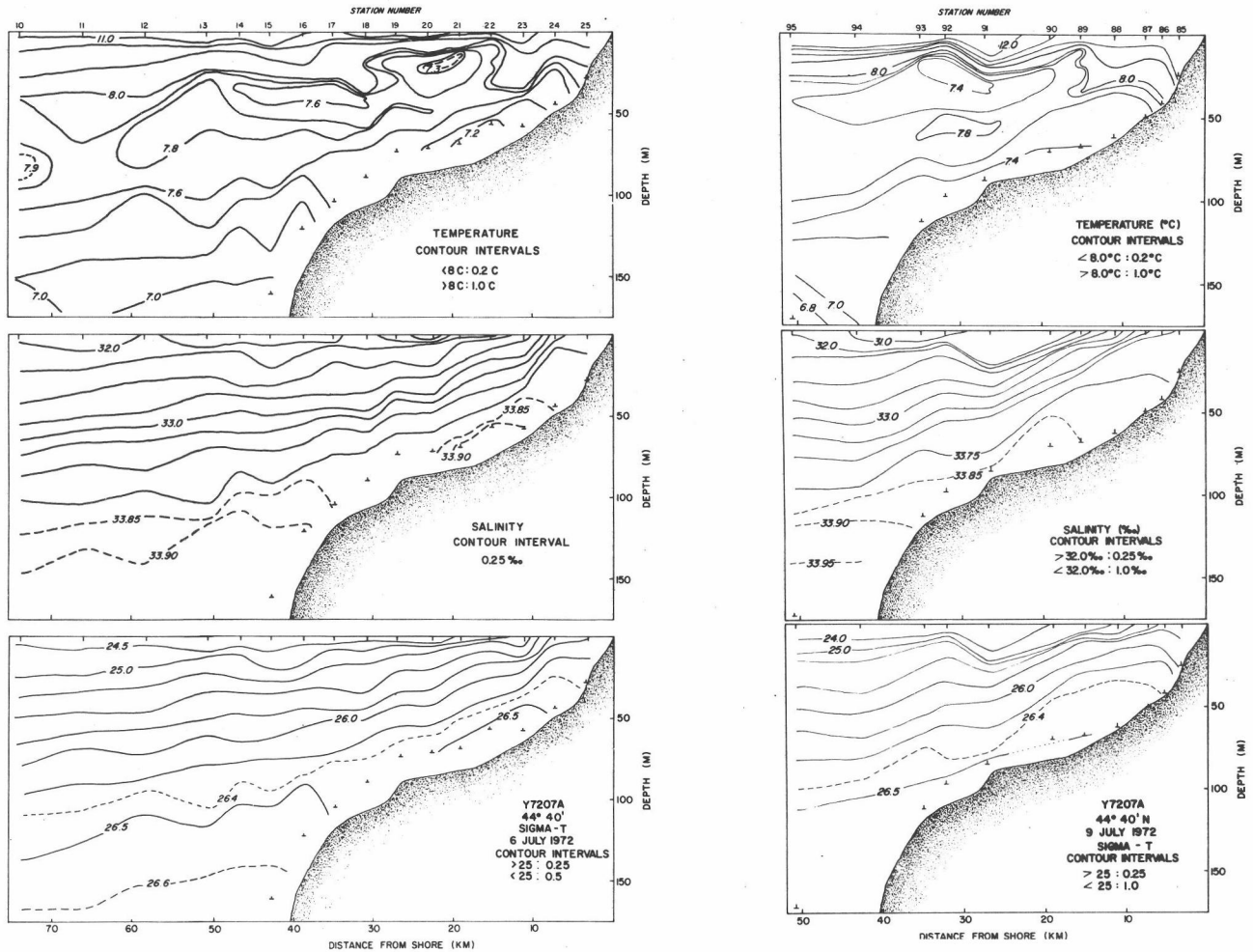

Figure 3(a). Vertical distributions of temperature, salinity and sigma-t, 6 and 9 July 1972.

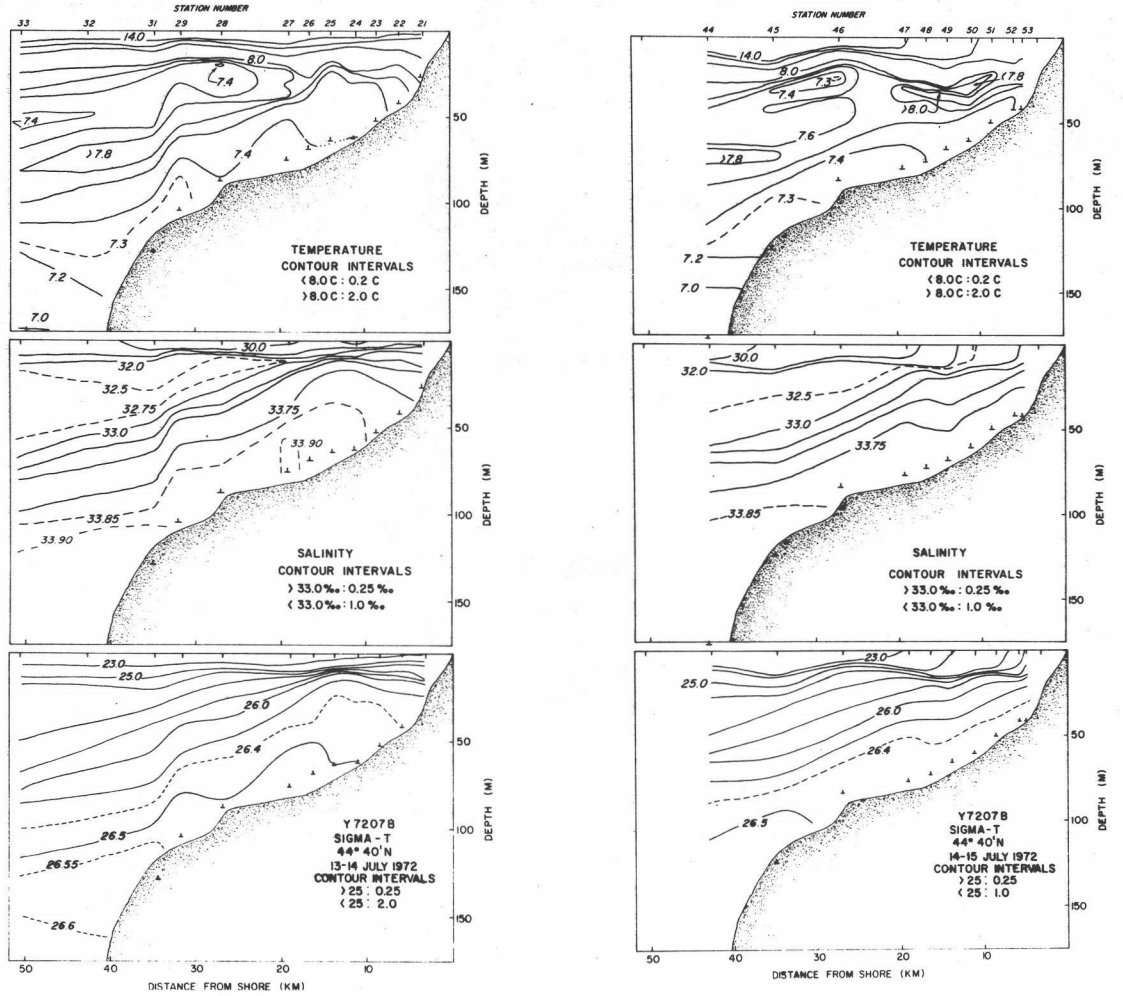

Figure 3(b). Vertical distributions of temperature, salinity and sigma-t, 13-14 and 14-15 July 1972.

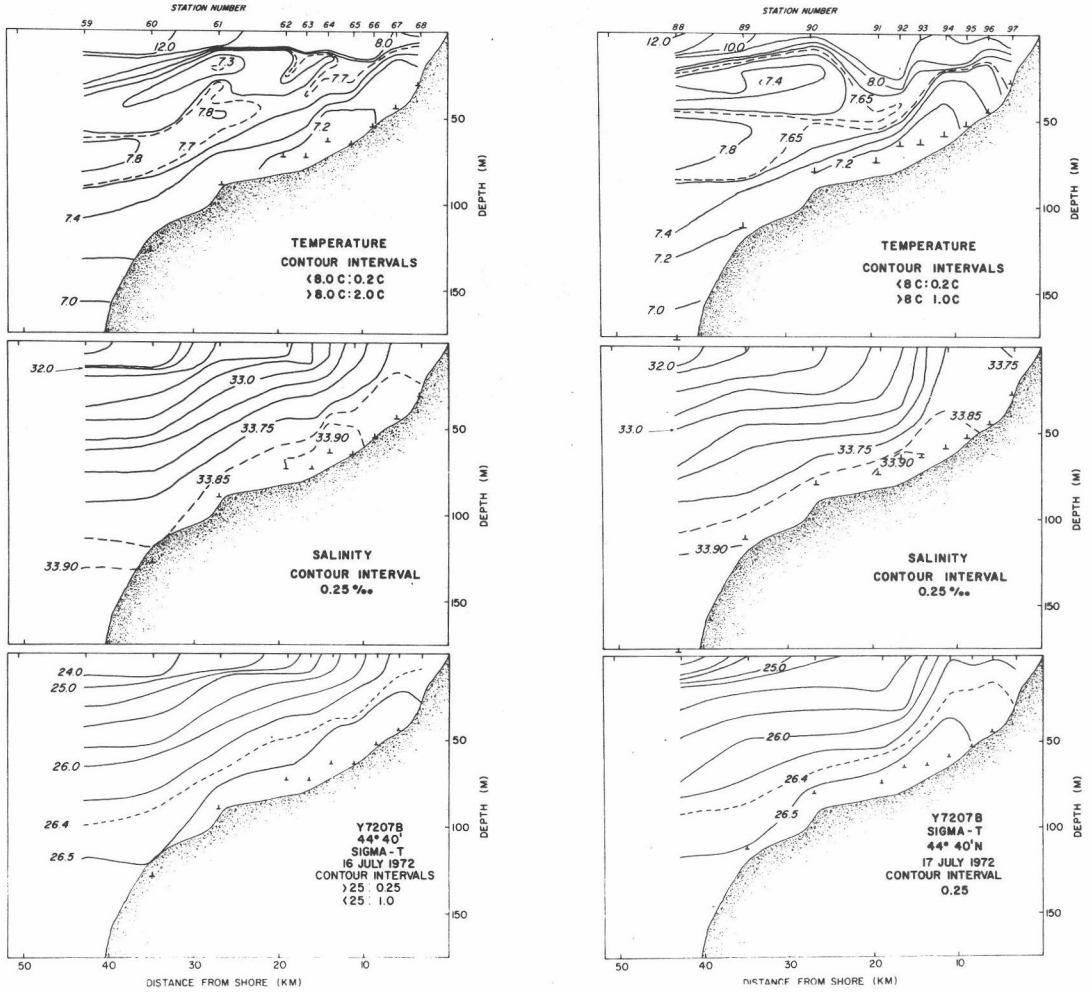

Figure 3(c). Vertical distributions of temperature, salinity and sigma-t, 16 and 17 July 1972.

upwelling) from 25 June to 3 July. Between 3 and 7 July, the wind was weak (< 5 m sec^{-1}), first northward, and then southward. On 8 July, the wind became strong northward (up to 10 m sec^{-1}) and remained so until 13 July, except for a brief calm period on 10 July. On 13 July, the wind became southward at about 8 m sec^{-1}, and remained so until late on 18 July.

Sea level was close to the 1972 summer mean on 5 July. Sea level decreased slowly until 13 July, and then rapidly until 16 July. On 16 July, sea level began to rise rapidly until 18 July and reached a peak on 19 July. The depression of sea level on 13 July was apparently related to the wind shift to southward occurring on that date. However, the rise in sea level on 16 and 17 July precedes the wind reversal to northward that occurs on 18 July.

Current fluctuations also appeared to be related to fluctuations in the wind, as suggested by Huyer and Pattullo (1972) and others. However, there is an even greater similarity between the sea level and the northward component of the current (Figure 2). A vertical shear in the current persisted during the entire period, with the shallower current always being southward relative to the deeper current.

Values of the low passed current at 1200 Z (Figure 4) each day are shown for the shallowest and deepest current meters at each location, except that the 60 m rather than the 80 m current meter is shown for DB-7. The shallow currents are larger at DB-7 and DB-13

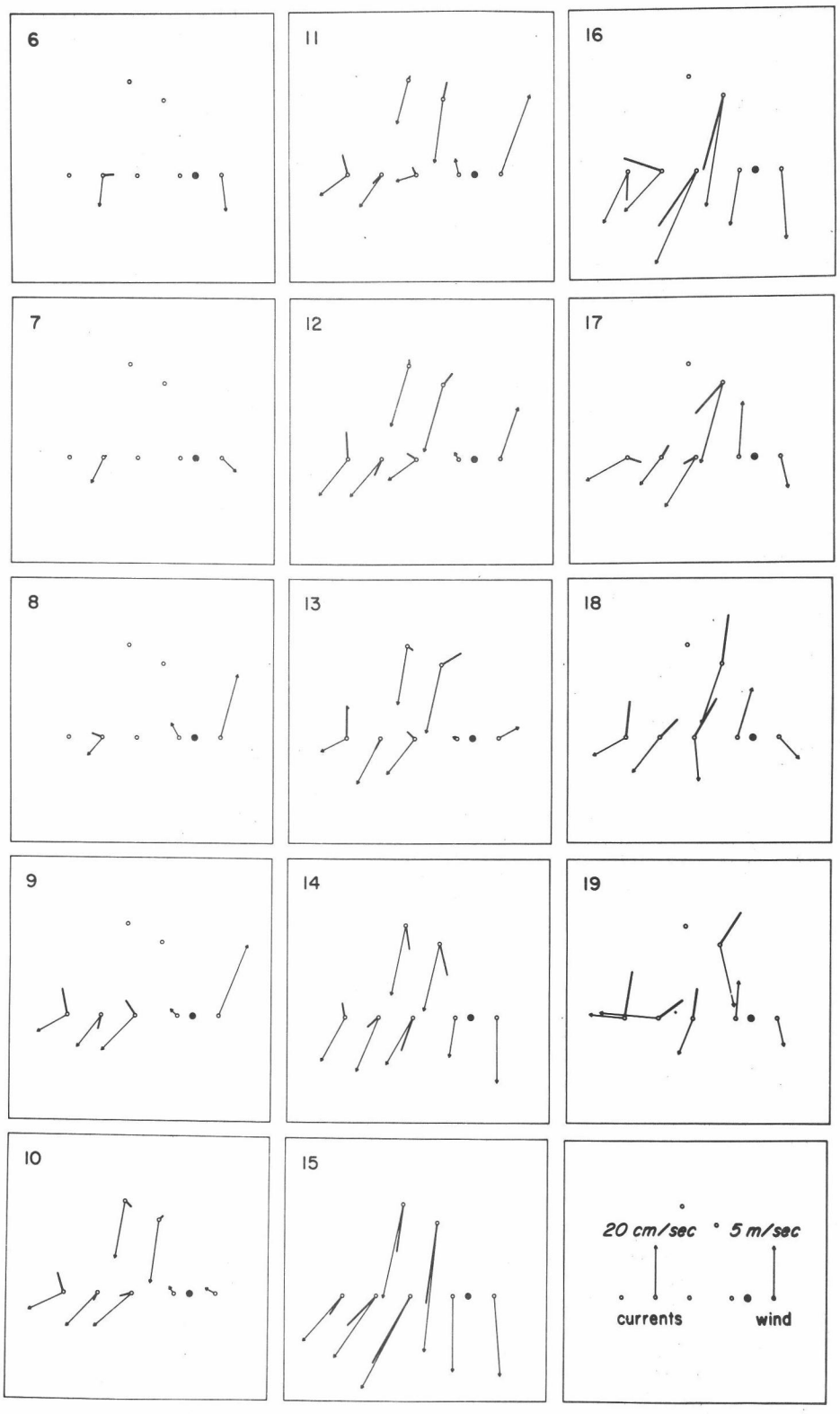

Figure 4. Low passed wind and current vectors for shallow (thin) and deep (thick) current meters, 1200 Z, 6-19 July 1972. The large dot represents Yaquina Head and separates wind and current vectors.

than along the line off Yaquina Head; it appears that the longshore current diverges as the shelf widens. A maximum in the longshore current along the line off Yaquina Head usually occurs at NH-10, but it is also observed at NH-15; this corresponds to the "alongshore jet" described by Mooers et al., 1973. A poleward undercurrent (Mooers et al., 1973) is observed at most locations until 14 July, and again after 18 July. The deepest current observed at NH-15 (60 m) is qualitatively more similar to an intermediate than to a deep current. On 14, 15 and 16 July, during the period of strong southward winds, almost all observed currents are southward. The shallow currents reach a maximum during this period, and the vertical shear at the inshore stations is less during this time.

Only the deep currents at DB-7 and DB-13 have an obviously onshore component. Because of the complex bottom topography, it is usually not apparent whether the currents observed along the line seaward of Yaquina Head have an offshore or an onshore component. Certainly, none of these currents have a very large onshore component.

The first hydrographic section, on 6 July (Figure 3) clearly shows the effects of upwelling. Isopycnals rise gradually offshore and steepen as they approach the coast. The 26.4 sigma-t surface is at a depth of about 105 m 75 km offshore and rises to a minimum depth of about 25 m near the coast. The 33.75‰ isohaline rises from 100 m to less than 10 m. The very fresh water at the surface (salinity less than

32.0‰) is due to dilution by the Columbia River plume which extends southward along the coast during summer (Ball, 1970). The temperature distribution shows a warm downward intrusion about 10 km off the coast; the intrusion is parallel to isohalines and likely corresponds to the temperature inversion discussed by Mooers et al. (1973), and described earlier by Pak et al. (1970). There is a core of cool (< 7.3 C), relatively fresh (< 33‰) water centered at about 20 m, 20 km off the coast. The deepest observations at about 15 to 20 km offshore are both colder and saltier than those somewhat further offshore in deeper water.

The wind began to blow northward late on 7 July, and its effect on the hydrography is apparent from the section on 9 July. Fresher, warmer water is observed at the surface. The isopycnals have become less steeply inclined near shore, but offshore they are relatively unchanged. The warm intrusion appears to be more nearly horizontal and is still locally parallel to the isohalines. The cool, relatively fresh water persists, but the two branches observed on 6 July have merged; its center is now about 30 km offshore. The coldest water on the shelf is both less cold and less salty than earlier. Vertical sections of the low passed current observations were contoured to correspond to this section and the subsequent hydrographic sections (Figure 5). On 9 July, the poleward undercurrent observed inshore of NH-15 is only in water saltier than 33.75‰, or with sigma-t higher

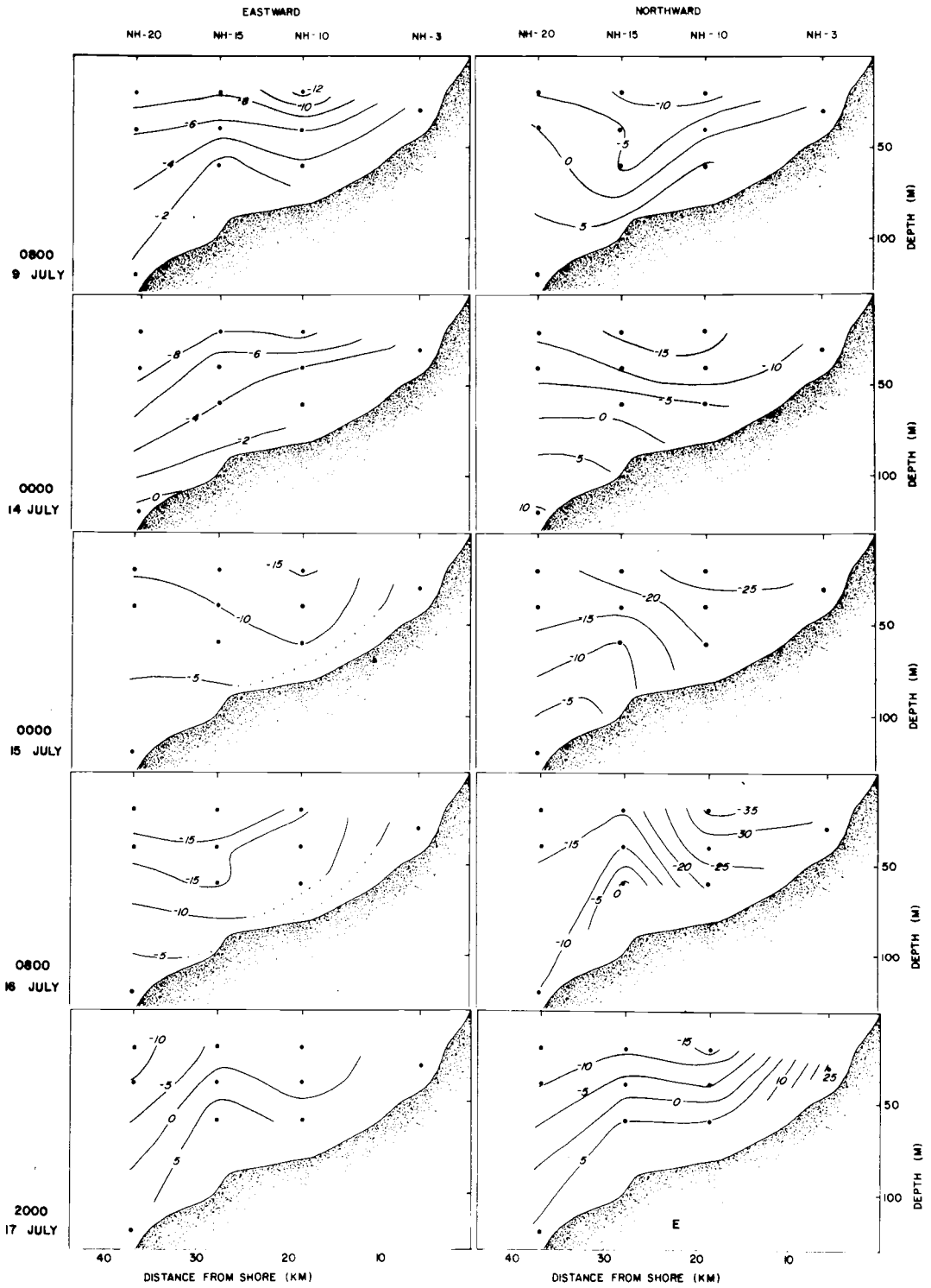

Figure 5. Vertical distributions of the eastward and northward components of the low passed current observations along 44°40'N.

than 26.4. Further offshore, the undercurrent is observed at shallower depths, and in less dense water. A jet-like structure is apparent in both the eastward and northward components of the currents; the section is not perpendicular to the mean flow. Currents appear to be westward in the entire section; however, we cannot rule out eastward flow beneath the deepest current meters and, in particular, along the bottom.

The wind continued to blow northward until 13 July, except for a brief calm period on 10 July. The vertical temperature distribution on 13-14 July shows very warm (> 14 C) and very fresh (< 30‰) water at the surface. Near surface isohalines are all nearly horizontal. Near the coast, the isohalines are even sloping downwards. The cool core persists. The volume of water with salinity greater than 33.75‰ is very large - it is greater than on either 7 or 9 July. Much of this water is now flowing south; only the current meter at 120 m, NH-20 still shows northward flow. It seems likely that the increased volume of cold, salty water is associated with the reversal in the direction of its flow; Stonewall Bank, which is south of this line, would act as a barrier to southward flow.

The wind continued to blow southward until after the last hydrographic section. At midnight of 14-15 July, only twenty-four hours after the previous section, the nearshore isohalines and isopycnals are again sloping upward toward the coast. The structure of the cool

core is more complex. It appears that a warm intrusion is again present; it is again locally parallel to the isohalines. The fresh water associated with the Columbia River plume has apparently moved offshore. The volume of cold, salty water at the bottom is reduced as the deep currents are now flowing rapidly southward. The surface jet is apparent in both northward and eastward current components. The southward component is about 10 cm sec^{-1} stronger than a day earlier.

On 16 July, the isopycnals and isohalines inshore of 35 km are strongly sloped. Upwelling is apparently stronger than it had been on 6 July; the surface salinity was higher than 33.75‰ from the coast to 8 km offshore. The coldest, saltiest water on the shelf again appears at about 15 km offshore. This water is moving southward more rapidly than is the deep water observed further offshore at NH-20. A surface jet is still present in the southward component of the current. The distribution of the westward component shows a subsurface maximum centered roughly along the 33.2‰ isohaline or the 26.0 isopycnal. The current is relatively constant within the cool core.

On 17 July, the isohalines and isopycnals are very steeply sloped inshore but nearly level between 15 and 25 km offshore (slopes $> 10^{-2}$ and $< 2 \times 10^{-3}$ respectively). The effect of surface heating penetrates to the bottom to about 5 km offshore. The warm downward intrusion is about 10 km wide. The surface jet coincides well with the position of both the warm intrusion and the largest horizontal salinity gradient.

Poleward flow at depth has resumed and all of the water saltier than 33.75‰ is flowing northward again. For the first time, we observe an eastward component at all of the deepest current meters.

DISCUSSION

The Hydrographic Regime

The main features of the hydrographic regime changed little during this sequence of observations. The isopycnals and isohalines generally rose and converged toward the coast, and each of the sections was consistent with the general description of the hydrographic regime during the upwelling season given by Mooers et al. (1973).

A core of relatively cool, fresh water persisted throughout the period of observation. Its minimum temperature and its shape varied during the period, but these changes were apparently not related to variations in the wind or currents. The presence of this cool, fresh water cannot easily be explained in terms of the two dimensional distributions; it was apparently advected southward across the line of stations. Variations in the core could be due to variations at the source of the water, or to variations in the rates of advection and mixing.

The similarity between the hydrographic sections was limited to the interior of each section. Marked changes occurred in what appear

to be boundary layers near the surface, the shore and the bottom. Changes in the surface layer were limited to the upper 20 m. Heating of the surface layer occurs through surface heat flux which is positive in July (Lane, 1965); cooling and increase in salinity can occur through wind mixing; and advection can cause either warmer, fresher water or cooler, saltier water to be present. Between 6 and 13 July the surface layer became both warmer and fresher. The relatively warm, fresh Columbia River plume moved shoreward during the period of predominantly northward winds. It appears that this onshore motion was restricted to a layer of water shallower than 20 m as the position of the shallow cold core was not greatly affected. This is consistent with the direct current observations; all of the 20 m current meters show a westward component to the flow during this period.

After the wind began to blow southward, the surface layer became cooler and saltier. The observed distributions (Figure 3) strongly suggest that the Columbia River plume moved offshore without much mixing. This motion apparently penetrated to depths greater than 20 m; each of the 20 m current meters showed an increase in the westward component of the flow on 15 July.

Changes in the nearshore area were limited to the region less than 10 km from the coast, and seemed to be closely related to the changes in the surface layer. The isograms of both temperature and salinity diverged toward the shore in this boundary layer; this may be

explained by the increased turbulence and mixing near shore. Changes in the distributions of properties within this region can occur through the surface heat flux which produces warming only; by advection, and by mixing throughout the entire water column, which can only produce increased divergence of the isograms. Between 6 and 13 July the vertical gradients of both temperature and salinity increased in the near shore region; this could only be caused by advection. At the most inshore station, the 33.75‰ isohaline was observed at the surface on 7 July and at 24 m on 13 July, implying that there was a net downward velocity in the near shore region. Between 13 and 14 July the near-shore slopes of the deep isograms changed sign, and they converged and sloped upward toward the coast on 14 July. This too could only occur through advection, with upward velocity in the nearshore region. This upward component to the advection persisted through the last hydrographic section on 17 July.

The remaining region where large variations were observed was near the bottom. Mixing would cause the bottom water to become less stratified, while advection could increase or decrease stratification. It appears that the upward or downward flow in the nearshore region was not simply balanced by a uniform onshore or offshore flow in the bottom layer: such a flow regime in the bottom layer is not consistent with the observation of extrema of temperature and salinity at about 15 or 20 km offshore. Extreme values of temperature and salinity

occurred for both southward and northward flow. Examination of the topography leads us to believe that the occurrence of the extrema is due to the presence of Stonewall Bank. Figure 6 shows a series of east-west bottom profiles in the vicinity of the bank. Comparison of these bottom profiles with the temperature and salinity distributions in Figure 4 shows that the coldest and saltiest bottom water on the shelf was north of the trough between Stonewall Bank and the coast. We conclude that the near bottom temperature and salinity are determined largely by the longshore flow, and that this flow is deflected around both sides of Stonewall Bank.

The largest volume of very dense water (sigma-t > 26.4) was observed over the shelf during the section of 13-14 July, soon after the time the deep current changed direction from northward to southward. This section shows no evidence of the wind reversal to southward. Increased isopycnal slopes were observed on 14-15 July, and we conclude that upwelling occurred between the two occupations of the line. Yet if we examine the depth of a particular isogram, such as the 33.75‰ isohaline, to determine the vertical velocity, we conclude that downwelling had occurred; it is necessary to exercise considerable caution when computing vertical velocities from displacement of isograms. It seems likely that the large volume of dense water observed during 13-14 July was due to the current reversal in the deep water with Stonewall Bank acting as a barrier to southward flow. When the

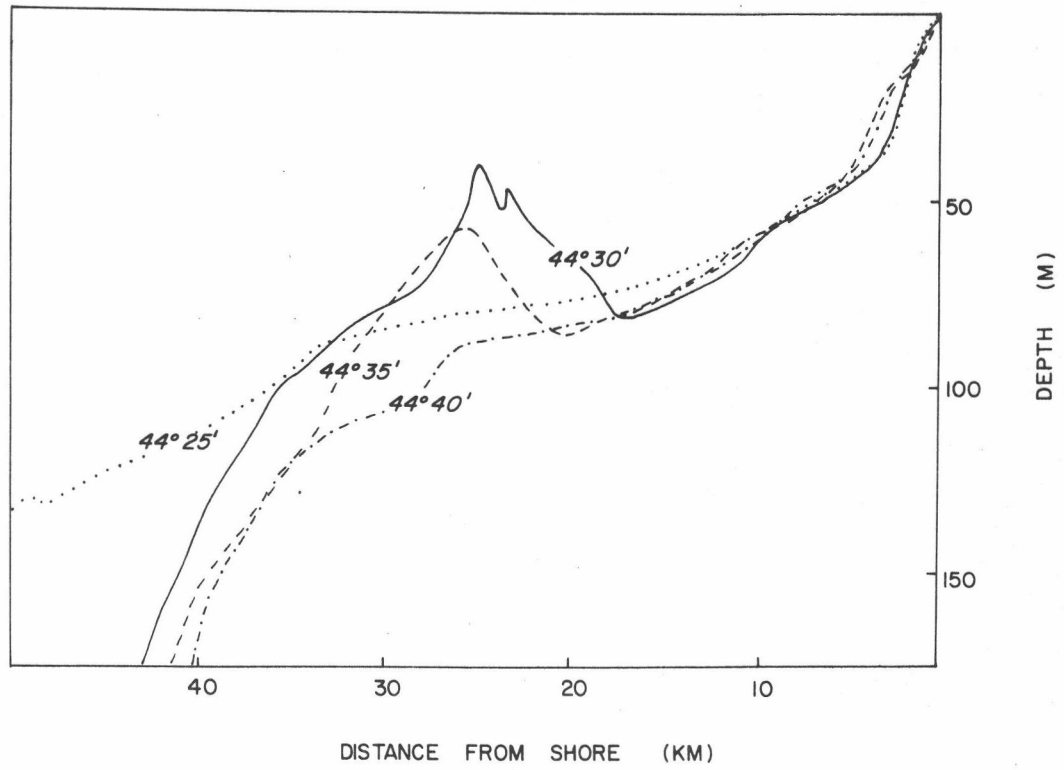

Figure 6. Bottom profiles in the vicinity of Stonewall Bank, between 44°25' and 44°40'N.

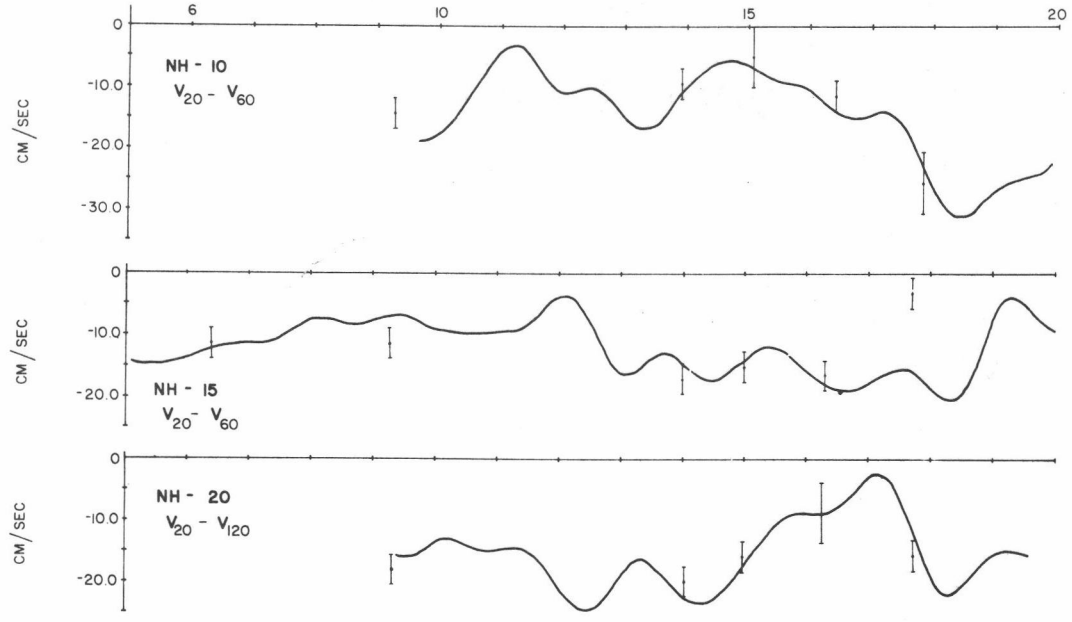

Figure 7. Comparison between observed and geostrophic differences in the northward component of the current between the top and bottom current meters at NH-10, NH-15, and NH-20.

deep southward current became well established, the volume of very dense water behind the bank was reduced.

Currents

From theoretical and numerical models of coastal upwelling (e.g., Allen, 1973; O'Brien and Hurlburt, 1972) we expected the observed currents to be mainly geostrophic. To test this hypothesis, we computed the northward component of the relative velocity both from the observed density distributions and from the direct current observations, i.e., we tested the validity of the "thermal wind" relation which holds if the currents are geostrophic.

Hydrographic stations normally used for computing the currents at NH-10 were located at 124°12' and 124°24'W; for NH-15, at 124°18' and 124°30'W; and for NH-20, at 124°24' and 124°36'W. When the isopycnal slopes between these pairs of stations were clearly non-linear, we also used closer spaced stations if these were available. The dynamic height anomalies were calculated using data from all observed depths. The geostrophic relation was then used to compute the northward component of the 30 m current relative to 60 m and 120 m. On one occasion during each of the YAQUINA cruises, several CTD casts were made at the same location during a period of a few hours (Y7207A, Stns. 79-84; Y7207B, Stns. 35-38). On each occasion, the difference in dynamic height between 20 and 60 m varied by ± 0.2 dynamic cm.

If the isopycnals are linear, and for a station spacing of 16 km, this causes an uncertainty in the calculated northward velocity of about $\pm$ 2 cm sec^{-1}. For non-linear isopycnals or smaller station spacing, the error could be much larger.

The time series of the differences between the northward components of the low-passed observed currents at the top and bottom current meters at NH-10, NH-15, and NH-20 are shown in Figure 7. Estimates of the geostrophic velocity computed from the hydrographic observations are shown for each of the sections with error bars indicating the approximate error for each of the values. The larger error bars are associated with estimates based on stations 8 km (6' of longitude) apart; other estimates are based on stations 16 km apart. The geostrophic relative velocities do not appear to be significantly different from the observed relative velocities except on one occasion. At NH-15, on 17 July, the geostrophic difference is much smaller than the observed difference; this is associated with the almost level isopycnals in the vicinity of this array. We conclude that the observed currents were mainly geostrophic during the period from 5 to 20 July, even though the winds were variable.

Current meters at different depths and locations appear to show similar fluctuations (Figure 2). This is especially true for the instruments at NH-3, NH-10, and DB-7. At both NH-10 and DB-7, this similarity could be enhanced by using a coordinate system rotated

somewhat clockwise from the east-north system to alignment with local bathymetry. Rotation of axes would also increase the similarity of the fluctuations at NH-20, and probably at DB-13, although this record is really too short for comparisons of this kind. The data from NH-15 are not as closely related to the others, but rotation of axes would again enhance the similarity. It appears that the magnitude of the fluctuations is determined by a common influence, but that the orientation of the major axis of the fluctuations is determined by conditions of a very local nature such as the bottom topography. There is some suggestion that the fluctuations at NH-15 are qualitatively different from those observed elsewhere. It may be that the currents at this location are disturbed by the flow around Stonewall Bank.

Clearly the change in wind from strong northward to southward on 13 July is associated with a barotropic response in the currents (Figure 2): the fluctuations in the currents are very similar to the fluctuations in sea level. The ratio of the amplitudes of fluctuations in the northward component of current and the sea level is about 2 sec^{-1}. The ratio is approximately the same for NH-3 and DB-7. At NH-20, it is reduced to about 1.5 (Figure 2). The depression in sea level and the maximum southward velocity occurs on 15-16 July. Before the wind changes significantly, the sea level rises and the current reverses with a maximum northward velocity on 18 July. During this period the currents rotated clockwise, as seen most clearly in the deep

current at DB-7 (Figure 4). These observations are consistent with the presence of a first mode barotropic continental shelf wave (Cutchin and Smith, 1973). It may be that a free shelf wave was generated by the rapid change in the wind from northward to southward on 13 July.

A poleward undercurrent has been observed in many upwelling regions, and Mooers et al. (1973) included it as an essential feature of the upwelling regime off the Oregon coast. Our observations show that there was frequently a poleward flow near the bottom. With the barotropic response in the currents on 13 July, flow at depth became equatorward instead of poleward. However, the vertical shear persisted, and it may be that flow at depth is normally poleward during upwelling in this region.

The vertical distributions of the currents show the jet-like structure of the alongshore current. To examine this in greater detail, we estimated the surface velocity for each array off Yaquina Head (Figure 8) using the thermal wind relation to extrapolate the 20 m current observations to the surface. A jet-like structure was observed on each occasion, although there were a variety of shapes. The structure of the jet would be modified by currents existing seaward of the jet; by currents, such as those associated with continental shelf waves, which exist independent of the presence of the jet; and by the scale of the lateral friction which brings the velocity to zero at the coast.

Mooers et al. (1973) estimated the width scale of coastal

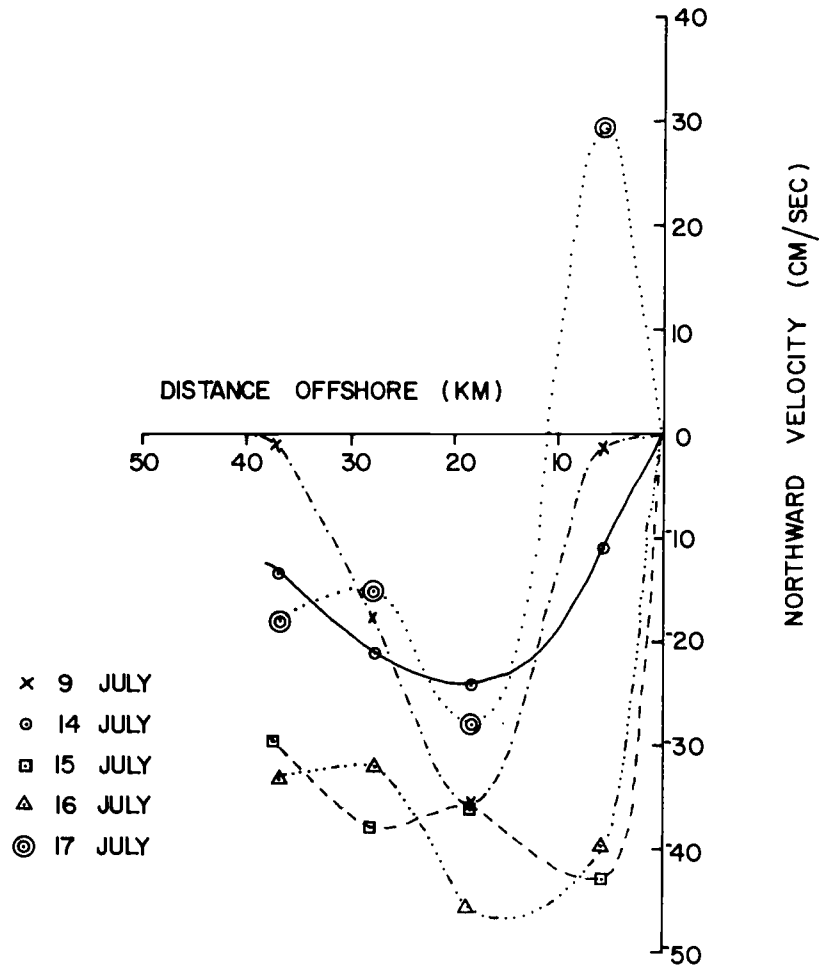

Figure 8. Northward component of the surface current versus distance offshore.

Table II. Estimates of minimum Richardson number, 5-20 July 1972.

	NH-10		NH-15		NH-20
	20-40 m	40-60 m	20-40 m	40-60 m	20-40 m
6 July			1.9	2.6	
9 July	0.7	0.4	2.8	2.8	0.7
12 July			2.1	1.8	
14 July	0.6	0.5	2.7	1.2	0.8
15 July	1.9	1.3	1.9	2.9	5.9
16 July	1.9	0.7	2.0	1.4	0.8
17 July	0.5	0.8	0.5	0.8	1.5
18 July	0.4	0.3			

upwelling (the baroclinic radius of deformation) for a two layer model of coastal upwelling to be 20 km for the continental shelf off Oregon. This follows from the assumption of geostrophic balance and the conservation of potential vorticity and implies the existence of a near-surface, near-shore southward jet (cf., Stommel, 1965, p. 111, and McNider and O'Brien, 1973).

We attempted to estimate the width of the jet to compare the results with the models. The width is taken to be the distance between the point of maximum velocity and the point at which the velocity is reduced to e^{-1} of the maximum. On 9 July, the jet was well defined, with the maximum occurring at 18 km offshore. The width of the jet then was 12 km. Assuming the offshore surface velocity on 14 July to be $-10\ \mathrm{cm\ sec^{-1}}$, the width of the jet was 17 km. On 15, 16 and 17 July the structure of the jet was very complex, and without observations from further offshore it is impossible to estimate its width. On 17 July, the current at NH-3 was northward. This was due to the barotropic current reversal, and the jet appears to be superimposed on it. In spite of these complexities, the jet-like structure continues to exist, and we conclude the observations are consistent with the models.

Stability

Mooers et al. (1973) have suggested that instability could occur in this region by the combination of weak vertical density gradients and

a large vertical velocity shear because of the internal semi-diurnal tide. According to Phillips (1966, p. 186) a sufficient condition for stability in an arbitrary shear flow is that the gradient Richardson number is everywhere greater than 1/4. The gradient Richardson number may be approximated by

$$Ri = \frac{\delta \sigma_t}{\delta z} / \left(\left(\frac{\delta u}{\delta z} \right)^2 + \left(\frac{\delta v}{\delta z} \right)^2 \right)$$

where u and v are eastward and northward components of the velocity. We used current meters separated in depth by 20 m at NH-10, NH-15, and NH-20 and the corresponding hydrographic observations to estimate this ratio. For each pair of current meters, we computed hourly values of vertical shear from current time series which had not been filtered to remove tidal and inertial oscillations. For each date on which a hydrographic station was made at that location, we chose the maximum value of the shear. We then used the observed difference in sigma-t to estimate the minimum Richardson number. Results are shown in Table II. On any day, the smallest value of the Richardson number was one or two orders of magnitude smaller than the largest value. The estimates in Table II correspond to only a very brief period of each day, and are the smallest values that occurred, if we assume the velocity shear and density gradient to be linear between pairs of current meters. This is an unlikely assumption, and for part of the water column the Richardson number was probably smaller than

the estimates in Table II. It seems likely that the Richardson number was less than 1/4 for brief periods at NH-10 on 9, 14, 17 and 18 July, and at NH-15 on 17 July. Such periods of instability may have allowed the formation of the downward warm intrusion in the vicinity of NH-10. Also, the flattening of the isopycnals in the vicinity of NH-15 between 16 and 17 July may have been the result of an instability of this nature. This could perhaps explain why the observed velocity at that time and location did not agree well with the calculated geostrophic velocity.

CONCLUSIONS

Variable winds over the upwelling regime off Oregon caused related variations in sea level, currents and the hydrographic regime. The relatively slow variations in the wind from 5 July to 12 July did not affect the alongshore current directly, but a response was apparent in the hydrographic regime. A sudden change to southward winds on 13 July was associated with a rapid drop in sea level and a barotropic response in the currents. The highly correlated variations in sea level and current suggest the generation of a barotropic first mode continental shelf wave. The barotropic impulse did not affect the hydrographic regime. The structure of the alongshore jet is modified, and poleward flow at depth ceased temporarily.

The vertical shear and a jet-like structure of the alongshore current persisted throughout the period. The observed currents were

mainly geostrophic.

The response to the wind in the hydrographic regime was observed mostly in the surface layer, the nearshore region and near the bottom. The Columbia River plume moved rapidly offshore during southward winds. The properties of the interior were largely unchanged by the variable wind.

It appears that the topography has a significant effect on both the current and the hydrographic regimes. Current fluctuations tend to be oriented along the local bottom contours. The hydrographic observations suggest that the current may be deflected around Stonewall Bank and that Stonewall Bank may act as a barrier to flow in the deep water. Current reversals increase the complexity of topographic effects.

Two-dimensional representations of the current and hydrographic fields do not suffice to explain the observed features. Three-dimensional effects are not only due to local variations in the bottom topography, but also due to advection through the region, as shown by the core of relatively cool, fresh water.

Estimates of the minimum Richardson number suggest that instabilities are important in this region. The presence of a warm downward intrusion in the vicinity of NH-10 could be due to the increased mixing that results from shear instability occurring there for a brief period each day. The flattening of isopycnals and isohalines in the interior observed on 17 July and the departure of the current at NH-15 from geostrophy could be due to a shear instability.

III. A SUBSURFACE RIBBON OF COOL WATER OVER THE CONTINENTAL SHELF OFF OREGON

Detailed hydrographic observations in a small area off the Oregon coast made as part of CUE-I showed the existence of a subsurface ribbon of relatively cool (<7.8C) water at a depth of about 25-50 m roughly parallel to the coast. The purpose of this section is to present the evidence for the existence of the ribbon, to describe its properties and to present hypotheses concerning its relation to the upwelling process.

THE OBSERVATIONS

A grid of hydrographic stations adjacent to the coast of Oregon was surveyed five times by R/V YAQUINA between the middle of May and the end of August 1972 (Table III). Stations were along six lines between 44°35'N and 45°00'N (Figure 9). Station separation was no greater than 8 km along each line. Observations were made with a Geodyne conductivity-temperature-depth (CTD) system. Usually at least one set of values was obtained for every two or three meter depth interval. The data have been reported (Anon., 1972a, b, d; 1973a, b).

Each grid survey was completed in about two days. Usually one line in the grid was occupied more than once during the survey.

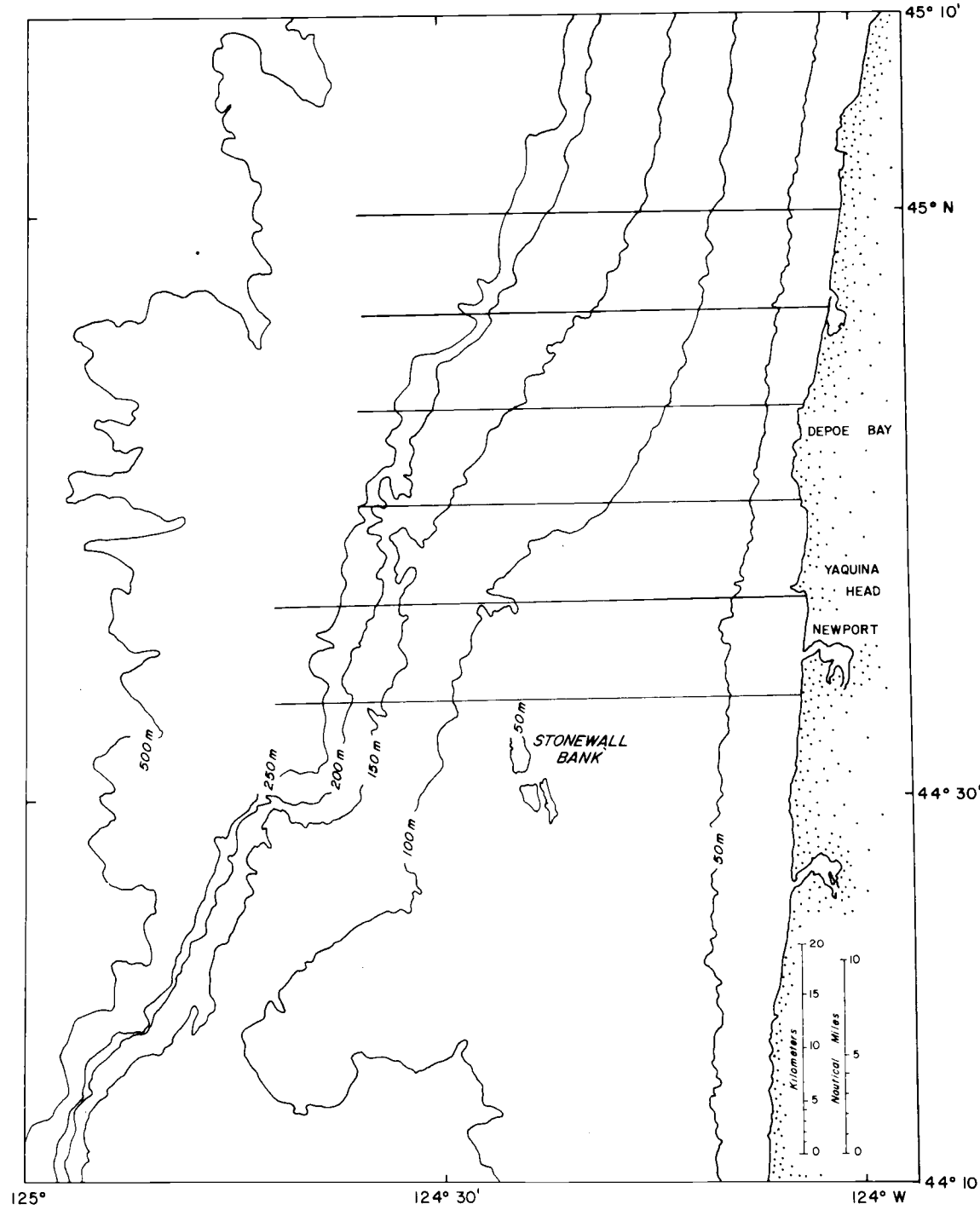

Figure 9. Location of the grid surveyed by YAQUINA, summer 1972. Lines show the position and length of sections occupied several times during the summer.

Table III. Dates of hydrographic surveys by R/V YAQUINA of the grid adjacent to the Oregon coast, 1972.

Date	Cruise Number	Station Numbers
18 - 21 May	Y7205A	5 - 46
21 - 22 June	Y7206C	8 - 45
5 - 7 July	Y7207A	1 - 59
31 July - 2 August	Y7207E	1 - 63
27 - 30 August	Y7208E	14 - 63, 80 - 86

Although significant differences were observed in such repeated sections, the major features were still present.

As an early step in analyzing the hydrographic data from the Coastal Upwelling Experiment, vertical distributions of the temperature, salinity and sigma-t were drawn for every offshore line of stations occupied by YAQUINA (Huyer, 1973). Temperature inversions were common, but salinity inversions were rare; sigma-t always increased with depth. In contouring the temperature distributions we initially assumed a two-dimensional interpretation of the temperature inversion (Pak et al., 1970; Mooers et al., 1973) as a guide; i.e., we assumed local formation of an anomalously warm, salty water mass which sinks approximately along the 26.0 sigma-t surface. However, it was not possible to draw all sections to be consistent with this interpretation. By increasing the station density inshore, thereby decreasing the ambiguity in contouring, we found a different interpretation that was more consistent with the data.

RESULTS

Sections from three lines observed during the June cruise are shown in Figure 10. The temperature distribution along 44°40'N appears to be consistent with the two-dimensional interpretation: the water warmer than 7.8C could reflect an intrusion of a warm, salty water mass generated locally. However, the sections along 44°50'N and 45°00'N show that, in the two-dimensional plane, the relatively cool, shallow water is isolated from its surroundings; it is restricted to a rather narrow zone over the continental shelf. When the evidence from the three lines is combined, we see that there is a ribbon of shallow cool water roughly parallel to the coast.

Surveys of the grid in May and early July showed similar results (Huyer, 1973). The hydrographic regime appeared to be more complex during the early and late August surveys (Huyer, 1973; p. 38-55); at many stations, there was more than one temperature inversion. Typical vertical temperature distributions from these surveys are shown in Figure 11.

During the three earlier surveys, the ribbon was relatively well defined, and it was possible to map its thickness, depth, temperature and salinity (Figure 12). The thickness of the ribbon was defined as the difference between the depth of the relative temperature maximum beneath the minimum and the depth at which the same temperature was

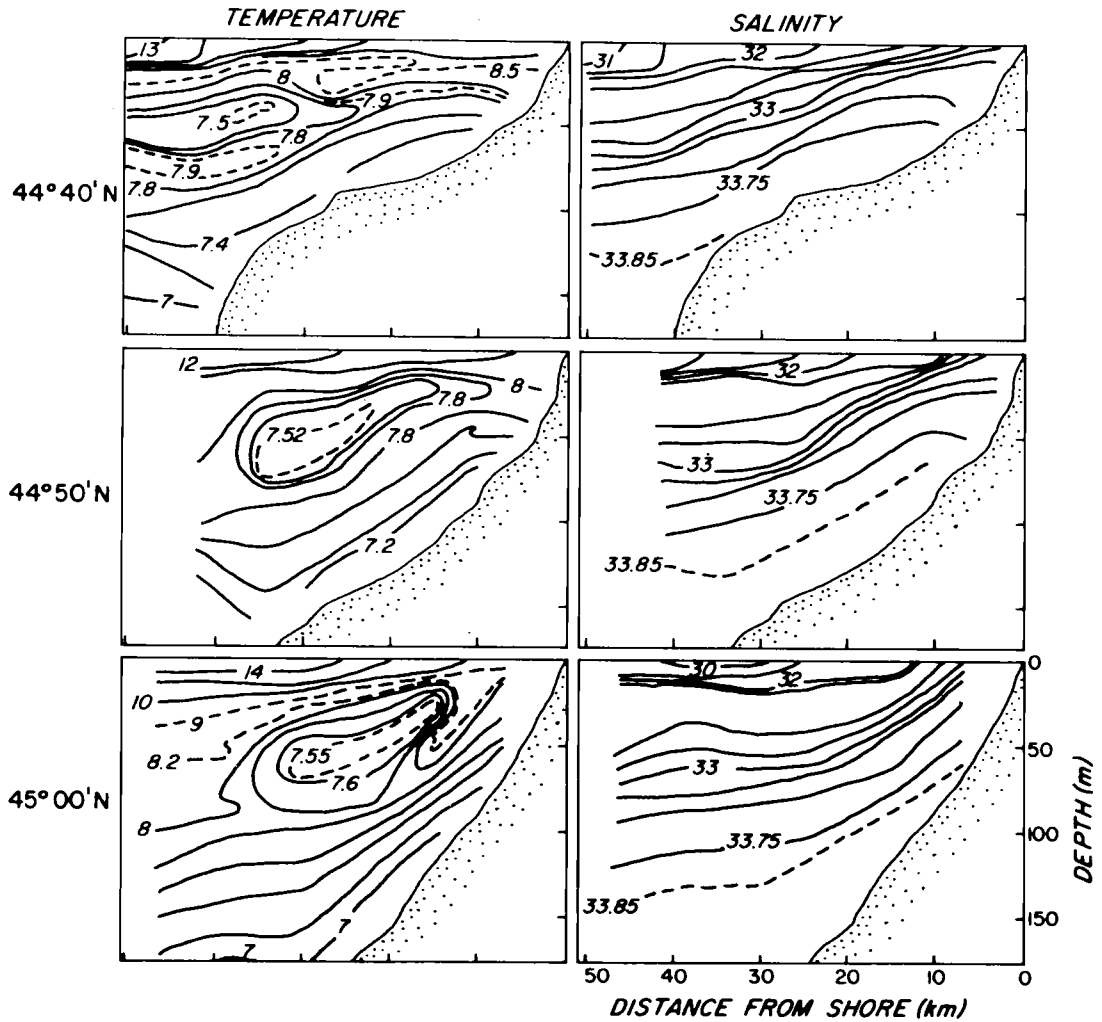

Figure 10. Vertical distributions of temperature and salinity during the YAQUINA survey of 21-22 June, along 44°40'N, 44°50'N, and 45°00'N.

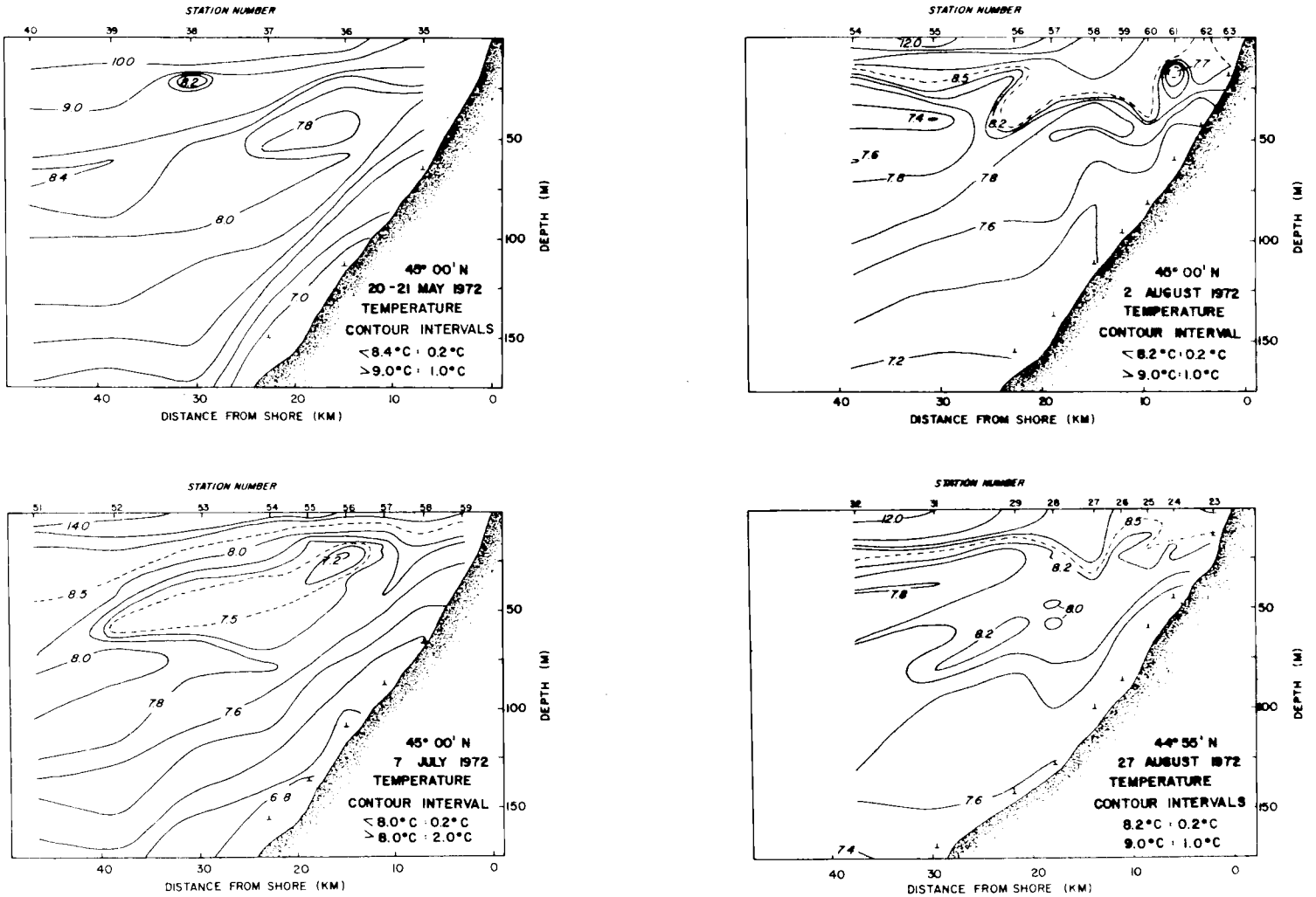

Figure 11. Vertical distributions of temperature at 45°00'N, 20-21 May, 7 July and 2 August 1972, and at 44°55'N, 27 August 1972.

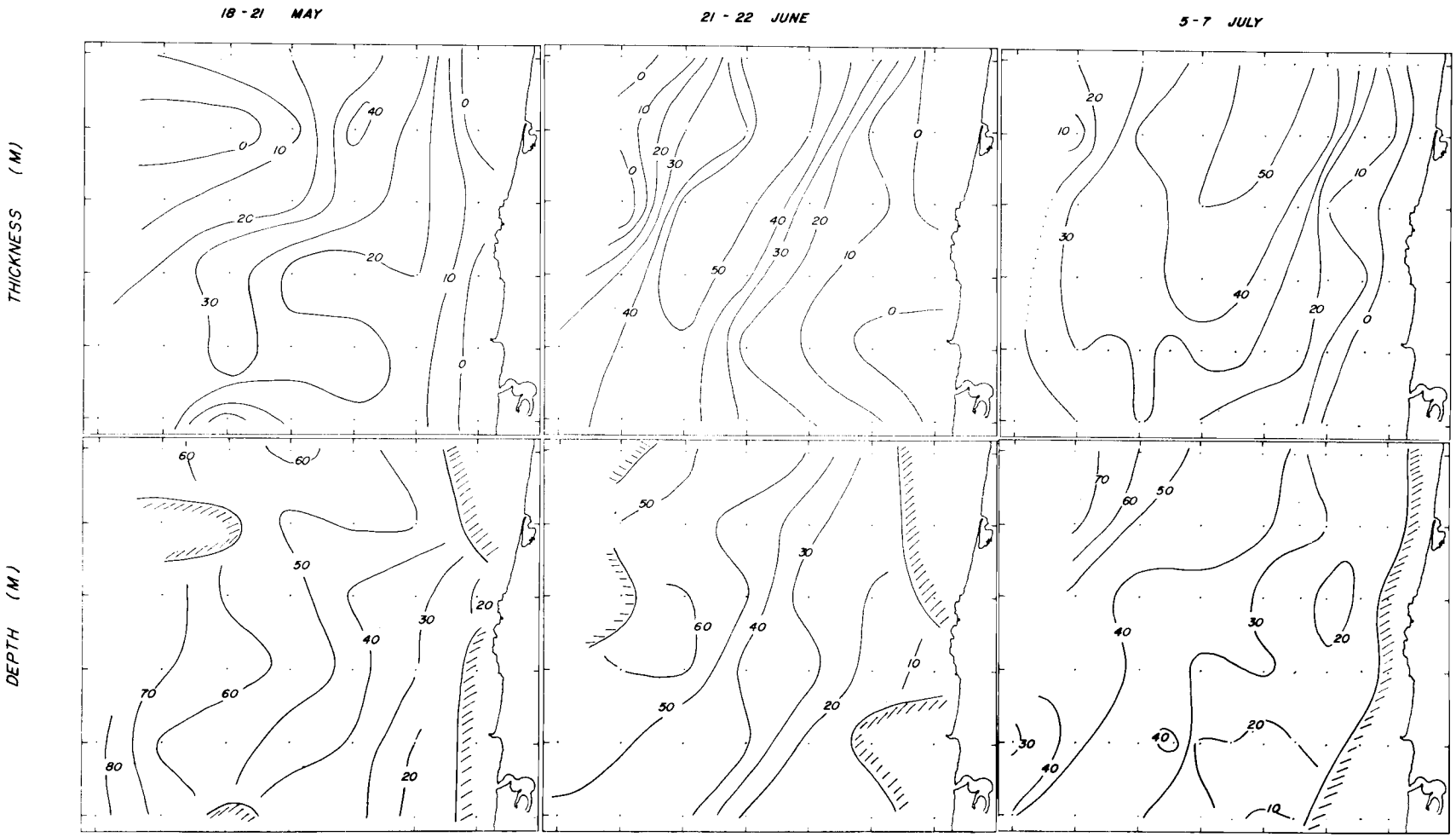

Figure 12(a). Thickness and depth of the cool ribbon observed during surveys in May, June and early July 1972.

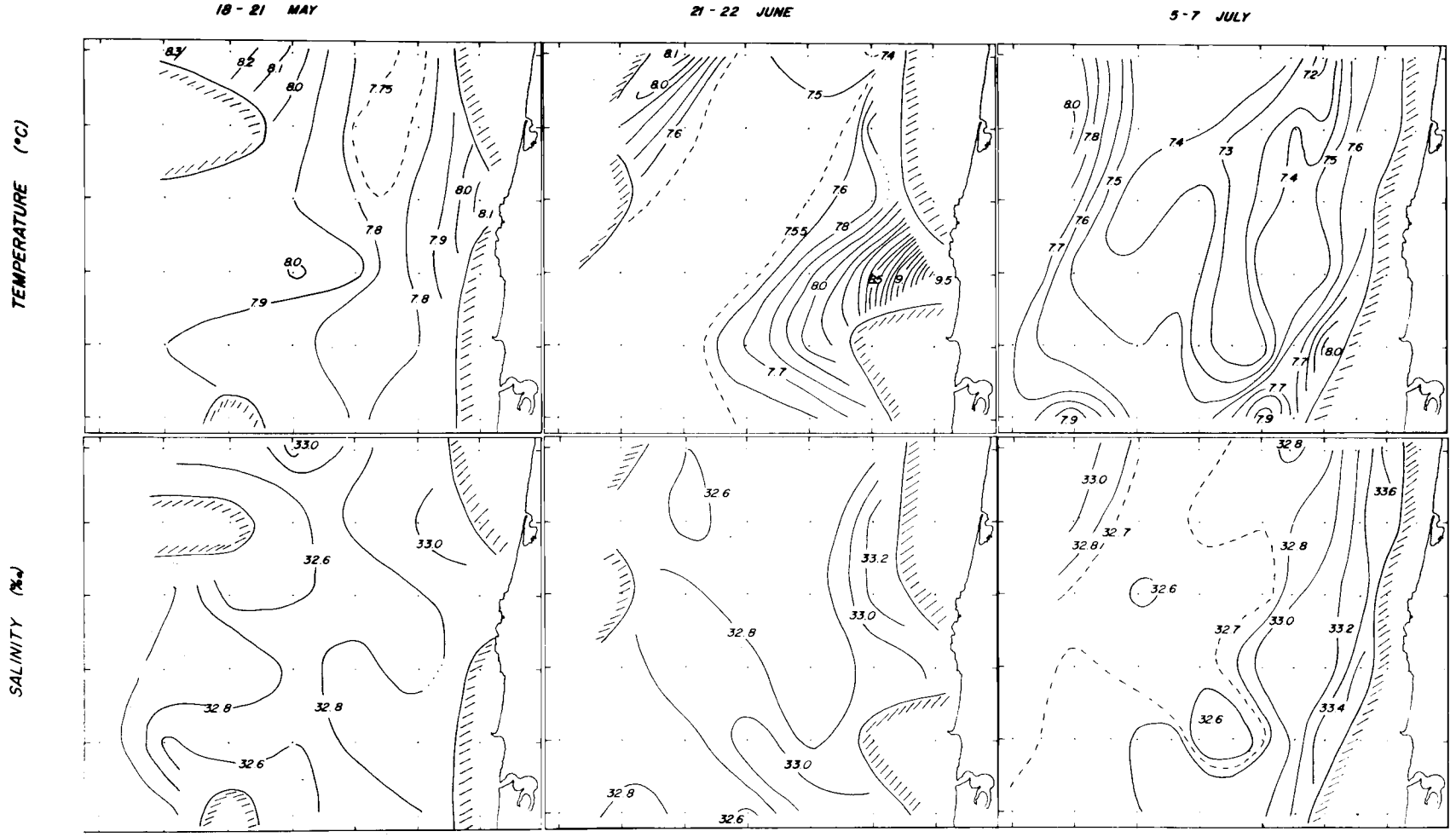

Figure 12(b). Temperature and salinity of the cool ribbon observed during surveys in May, June and early July 1972.

observed above the minimum. The depth, temperature and salinity of the ribbon were defined as being those at the relative temperature minimum. For the two later surveys, when there was often more than one temperature inversion, it was more difficult to map the properties of the ribbon. Thickness especially would have to be defined very arbitrarily. It was possible to map the depth, temperature and salinity at one or another of the relative temperature minima. The deepest minimum was mapped for the early August survey, and the shallowest minimum was mapped for the later survey (Figure 13).

The maximum thickness of the ribbon appears to be about 50 m. The direction of its axis is roughly parallel to the local bottom contours. The total width of the ribbon is of the same order as the offshore extent of the grid, about 50 km. The width of the thicker part of the ribbon (over 20 m) increases between the May and July surveys from about 20 km to about 40 km.

The ribbon is sloped upward toward the coast. Its greatest depth is less than 100 m, and its shallowest is less than 20 m. The slope is most uniform during the June survey, and least uniform during the early August survey. The slope appears to be greatest during the May and June surveys.

Lateral temperature gradients in the ribbon were usually strongest at the shoreward and seaward edges. During the three earlier surveys, when the ribbon was well defined, temperature

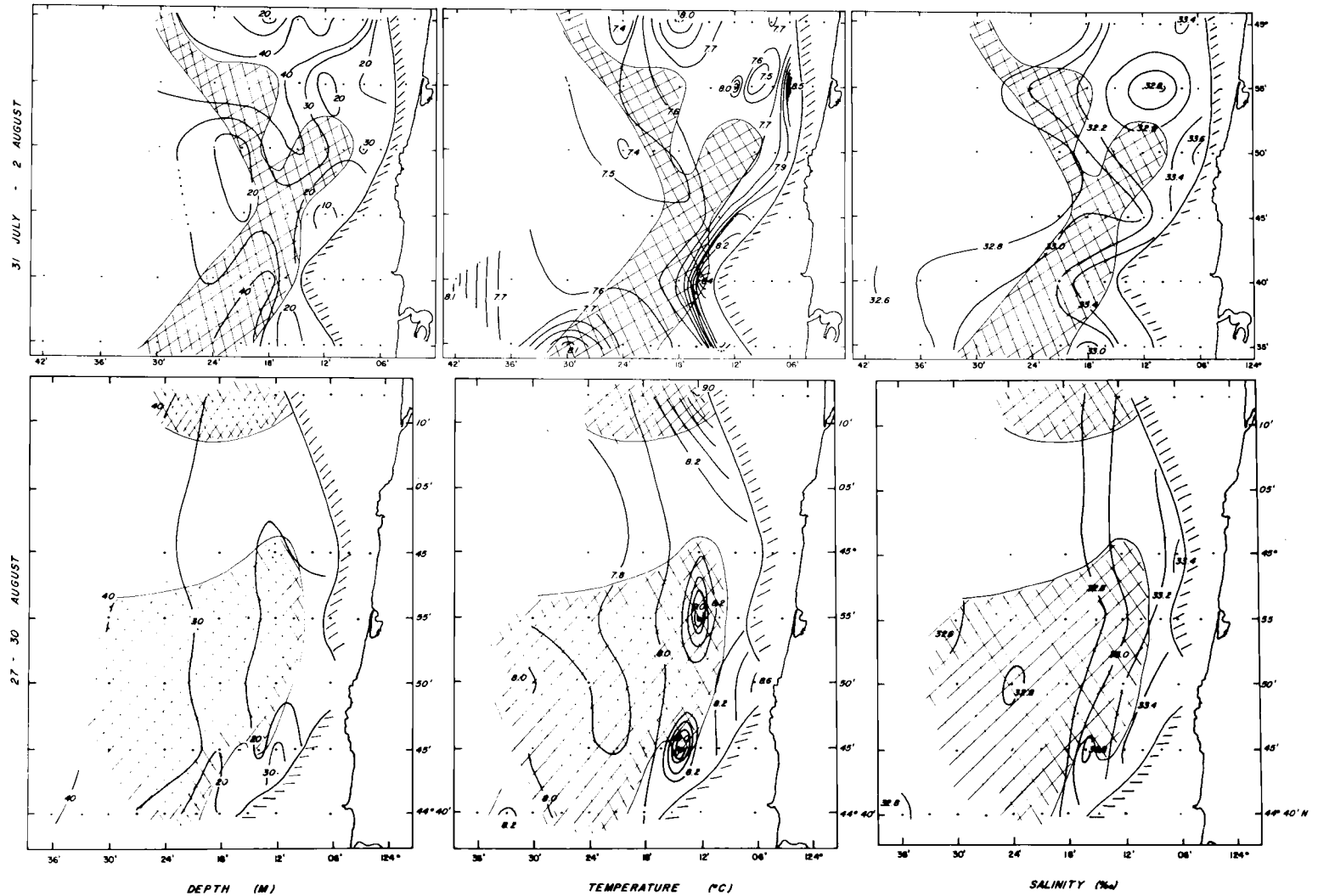

Figure 13. Properties of a relative temperature minimum layer during surveys in August. Areas where more than one relative minimum were observed are shaded.

increased almost monotonically from the axis to the edges of the ribbon. Patchiness in the temperature distribution appeared in the early July survey and was a prominent feature in the early August survey. Warm patches are shown for the late August survey, but these may be connected, and part of a longer band of warm water.

The lowest temperatures (7.2C) were observed in early July. The lowest temperature observed in early August (7.4C) was about the same as in June. However, most of the core had a very uniform temperature (7.5C) during the June survey. The coolest temperatures observed in May and late August were very similar (7.7C) but the highest temperatures observed in late August (9.0C) were much warmer than those in May (8.3C). Only the early July survey showed some evidence of a north-south temperature gradient within the ribbon.

Most of the water in the ribbon has salinity between 32.6 and 32.8‰. Salinities along the edges are higher, especially along the shoreward edge, where salinities exceeded 33.6‰ during the early July and early August surveys. During each survey, some of the water was fresher than 32.6‰.

Direct current measurements obtained as part of the experiment made it possible to examine the vertical distribution of the current along 44°40'N. Comparison of the vertical distribution of the temperature and the northward component of the current shows that the ribbon is within the southward surface flow rather than in the northward

undercurrent frequently observed on the Oregon continental shelf (Huyer, Smith and Pillsbury, 1973).

DISCUSSION

Seasonal Evolution of the Ribbon

The properties of the cool ribbon (Figures 12 and 13) suggest that there may be a systematic evolution in its development. The ribbon was best developed during the June and early July surveys and seemed to decay between the early July and late August surveys. The June and early July surveys showed very smooth distributions of ribbon thickness and depth. There is a suggestion that the thickness of the ribbon is greatest during these surveys. The temperature distributions observed during these cruises are much smoother than during the later surveys. The minimum temperature decreases from its May value until early July; later surveys show warmer temperatures. The property distributions also suggest that typical length scales were greater during the June and early July surveys than during the two later surveys.

There is some evidence to link the evolution of the ribbon to the seasonal progression of the upwelling season. A monthly index of upwelling, the offshore Ekman transport based on the mean atmospheric pressure distribution, shows that in 1972 the upwelling began in April,

reached a maximum in June, remained at that intensity until August, and was weaker but still occurring during September and October (Bakun, 1972). We note that the ribbon was both best-defined (in June) and had its lowest temperatures (in early July) relatively early in the upwelling season. Continued upwelling may lead to instabilities (Mooers et al., 1973; Huyer, et al., 1973) which limit the growth and intensity of large scale features in the regime.

Spatial Extent of the Ribbon

We attempted to estimate the length scales of the ribbon from the 1972 observations by computing the correlation between stations in each survey. To compute the correlations, we considered temperature to be a function of salinity rather than of depth. This eliminated the effect of vertical excursions due to internal waves and tides, and to some extent the effect of sloping isograms due to upwelling. For each station we determined the temperature at intervals of 0.1‰ over a common salinity range (e.g. 32.0‰ to 33.8‰). Then for a pair of stations, we computed the correlation between the temperature over this salinity range as follows:

$$C = \frac{\sum_{i=1}^{n} (T_{1i} - \overline{T}_1)(T_{2i} - \overline{T}_2)}{\left(\sum_{i=1}^{n} (T_{1i} - \overline{T}_1)^2 \sum_{i=1}^{n} (T_{2i} - \overline{T}_2)^2\right)^{1/2}}$$

where T_{1i} and T_{2i} are the temperature values at the ith salinity values for the first and second station respectively; $\overline{T}_1$ and $\overline{T}_2$ are the average temperatures over the entire salinity range, i.e.:

$$T_1 = \frac{1}{n} \sum_{i=1}^{n} T_{1i} \quad ;$$

n is the number of salinity values over which the comparison is made; and C is the correlation coefficient for the particular pair of stations. Temperature was almost always a single valued function of salinity; no comparison was made when it was not.

Because of the upwelling process, surface salinities are highest at the near shore stations, and a comparison between all stations can be made over only a very small salinity range. Estimates of the correlation are more reliable over a larger salinity range. We compromised by using the range 32.4‰ to 33.7‰ (i.e. 14 temperature values for each station) for the June and early July surveys. During both the early and late August surveys, surface salinities exceeded 32.5‰, and the common salinity range between all stations was too small for meaningful estimates of the correlations. During the May survey, the maximum salinity was frequently less than 33.7‰ and we used a salinity range of 32.4‰ to 33.6‰. For each survey, we chose one reference station and compared all other stations to it. The reference station

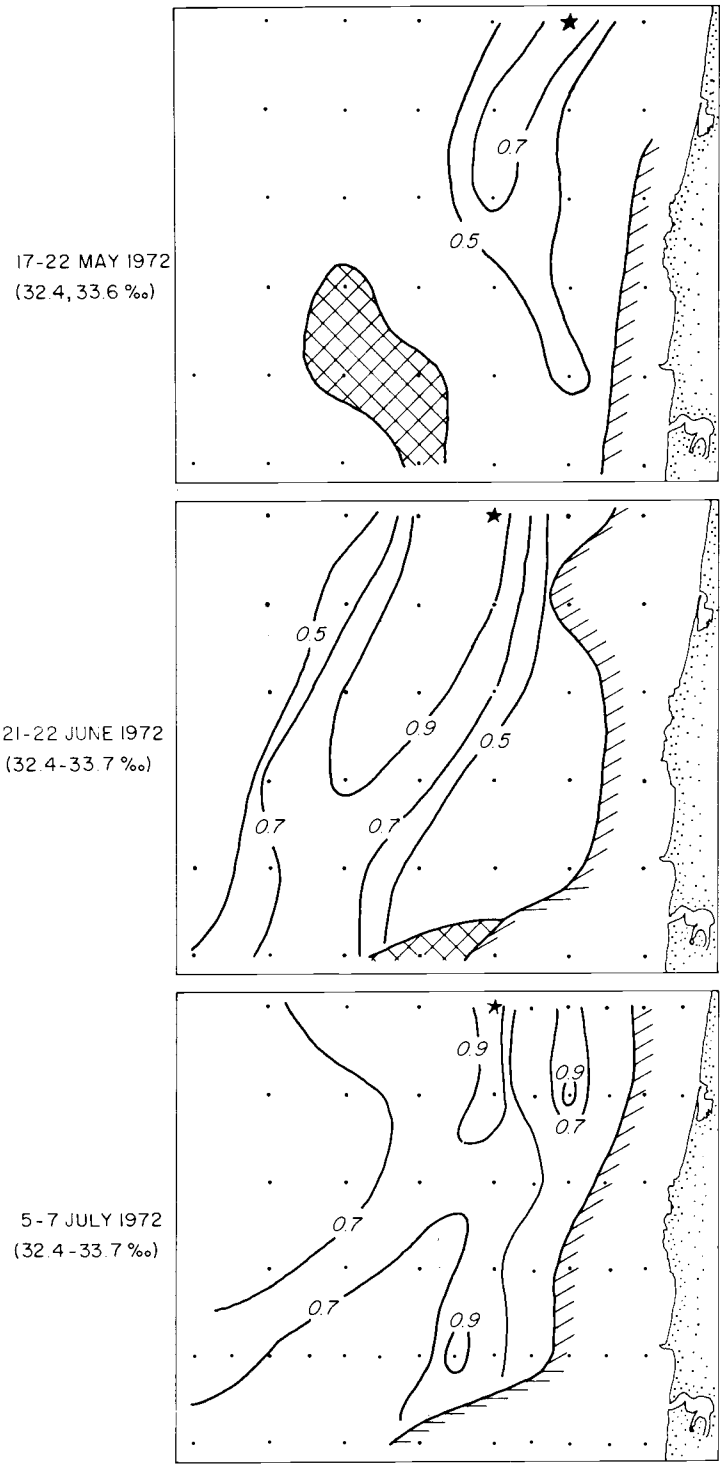

Figure 14. Distribution of the correlation between a reference station (*) and each other station of the May, June and early July surveys. Cross-hatched areas show regions where the maximum salinity was too small to compute the correlation. The nearshore area had minimum salinities too large to compute the correlation.

was chosen to be near the axis of the ribbon at 45°00'N. Distributions of the correlation are shown in Figure 14. From these distributions it is obvious that the alongshore length scale greatly exceeds the offshore length scale. If we arbitrarily define the length scale to be the distance at which the correlation drops through 0.7, the width scale is of the order of 20 km in June and early July, and the length scale exceeds 50 km.

Data from earlier years were examined to see if more information about the ribbon was available. One YAQUINA cruise, in June 1968 (Barstow, Gilbert and Wyatt, 1969b), was particularly useful: it covered a much greater area, i.e., from 46°21'N to 43°20'N and from the coast to 127°00'W (Figure 15), and offshore sections showed evidence of the ribbon (Figure 16). This cruise indicates that the ribbon is at least 300 km long (from 46°N to 43°20'N), and that it may be much longer. There is some suggestion that the ribbon does not extend much further north but there is no evidence that its southern limit was approached. The width of the ribbon during this cruise appeared to be of the same order as during the 1972 surveys, about 30 km (Figure 16).

The Ribbon as a Permanent Feature of the Upwelling Regime

Bakun (1973) has computed values of the upwelling index for each month from 1946 to 1971. Hydrographic observations have been made

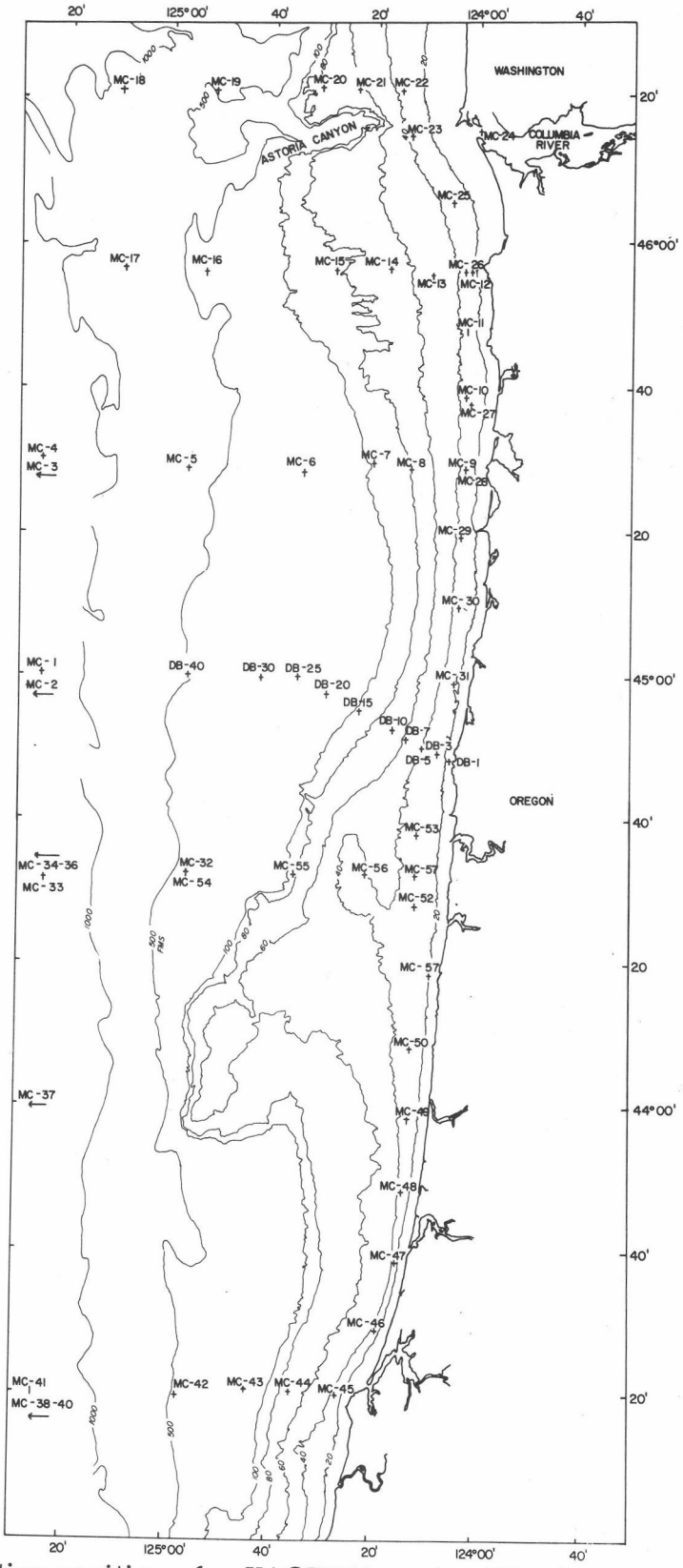

Figure 15. Station positions for YAQUINA cruise Y6806C, 24 June-3 July 1968.

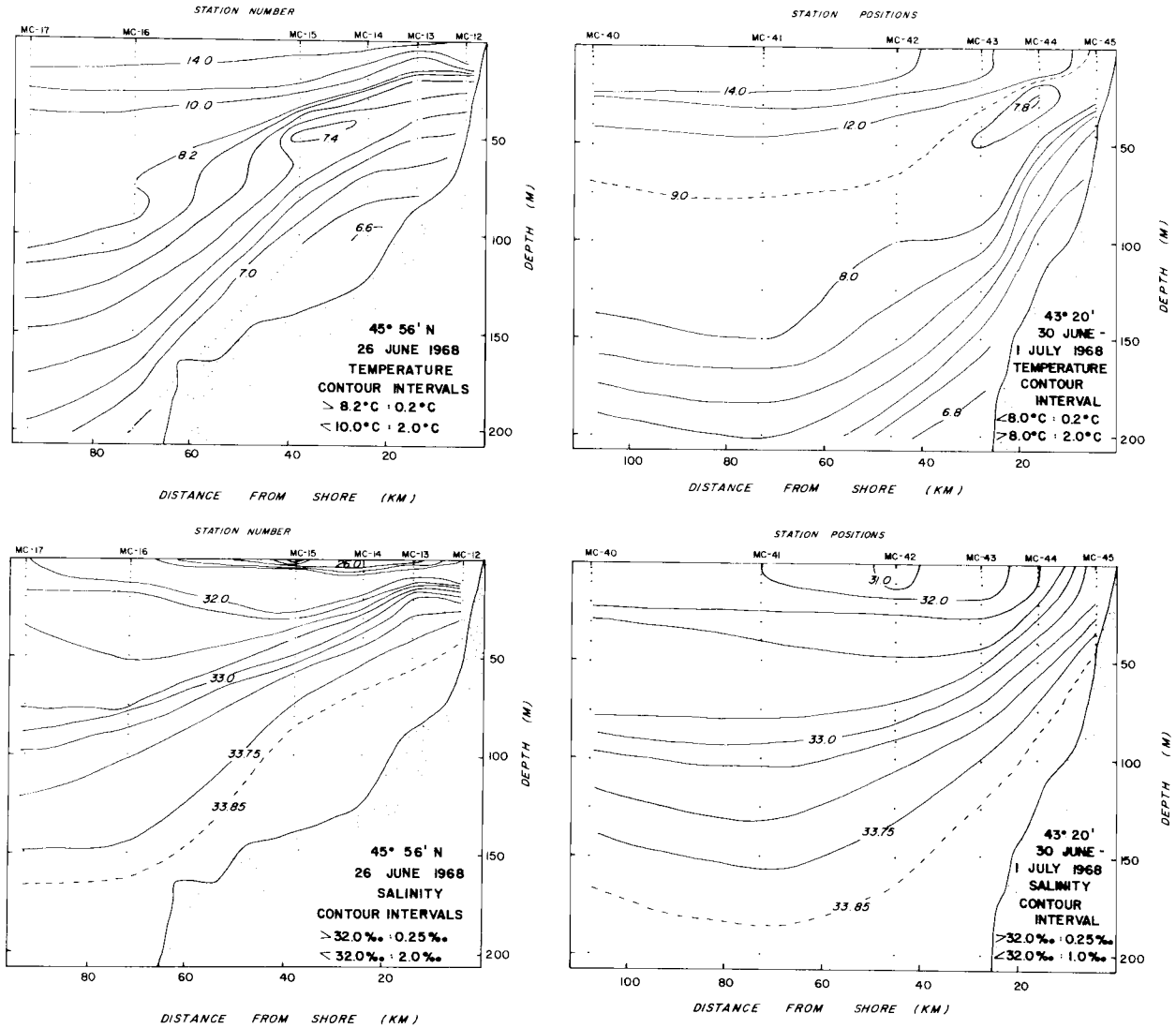

Figure 16. Vertical distributions of temperature and salinity for two sections of YAQUINA cruise Y6806C.

frequently off the coast of Oregon by Oregon State University since 1961. Data from all cruises during the upwelling season were examined for evidence of the ribbon. On most cruises, station spacing was not close enough to examine the details of the ribbon; a relative temperature minimum at salinities between 32.5‰ and 33.2‰ that did not extend offshore was taken to be evidence of the ribbon. If the inversion was very small, and observed at only one depth at only one station, it was not judged to be evidence of the ribbon. Both the results of this data survey and the values of the upwelling index at 45°N, 125°W are shown in Table IV. While a (*) in Table IV indicates evidence for the presence of the ribbon, a (°) does not indicate evidence for its absence; station spacing on some of the cruises was of the same order as the width of the ribbon. In spite of this and other limitations in the data set, Table IV shows that the ribbon was observed at some time during the upwelling season of all but two years between 1961 and 1971. The ribbon was observed only once in April, twice in May and frequently in June. It is usually observed in July and August, and part of the time in September.

Table IV shows that, in general, the ribbon was observed when the upwelling index was high, and it was not observed when the index was small. There are, however, a number of exceptions to this rule. The ribbon was observed in conjunction with low values of the index in September 1966, August 1968, May 1969, and September 1969. In

Table IV. Values of the upwelling index at 45°N, 125°W, and observations of the presence of the cool ribbon during the upwelling season off Oregon, 1961-1971. A (*) indicates the ribbon was observed; a (°) indicates observations were made but there was no evidence of the ribbon. Units of the upwelling index are $m^3/sec/100$ m.

	April	May	June	July	Aug.	Sept.	Reference for Hydrographic Observations
1961	11°	1°	21°	51°	33°	42	Wyatt and Kujala (1962; 1963)
1962	-7°	42°	29°	107*	21	11	Wyatt and Gilbert (1967)
1963	-9	8°	72°	38°	35	-5°	Wyatt and Gilbert (1967)
1964	57*	45	32*	51*	40	32	Wyatt and Gilbert (1967)
1965	5°	84	103*	99*	48	75	Wyatt et al. (1967)
1966	43°	101	20°	80*	110	6	Barstow et al. (1968)
1967	11°	88°	135*	134*	93*	15	Barstow, Gilbert and Wyatt (1969a)
1968	47°	33*	59*	104*	21*	18°	Barstow, Gilbert and Wyatt (1969b)
1969	-21°	13*	61*	106	46*	6*	Wyatt et al. (1970)
1970	25	33*	46*	71	73	11	Wyatt et al. (1971)
1971	-2°	66	13*	65	24*	8	Wyatt et al. (1972)

three of these cases, the value of the index was high in the previous month. In May 1969, although the upwelling index was small, the hydrographic section off Newport obviously reflected the effects of upwelling - the near shore surface salinity was greater than 33.7‰. Relatively high values of the upwelling index without evidence of the ribbon also occurred on a number of occasions: July 1961, May 1962, June 1963, May 1967, and April 1968. However, each of these occurrences was preceded by a month with a low upwelling index.

The conclusion is that the cool ribbon is a permanent feature of the upwelling regime off Oregon. It develops within about a month after the mean wind becomes favorable for upwelling and it may persist about a month after the mean wind becomes unfavorable.

Source of the Ribbon

A relative temperature minimum is normally observed at the bottom of the thermocline in summer in the Subarctic Pacific (Uda, 1963). The temperature at the relative minimum increases eastward from less than 1.0C in the western Subarctic to over 6.0C off British Columbia and over 7.0C along the coast of Washington. No relative temperature minimum exists south of the Subarctic Boundary (Uda, 1963). The relative minimum is usually observed at the top of the halocline, i.e. at about 32.6‰, and occurs at depths between 100 and 150 m in the eastern Subarctic Pacific (Bennett, 1959). The relative

temperature minimum is believed to be due to winter surface cooling which causes the winter mixed layer temperatures to be lower than the temperatures in the permanent halocline; summer heating does not usually penetrate to the permanent halocline in the Subarctic Pacific (Uda, 1963).

Hydrographic observations between Cobb Seamount, Cape Flattery and Vancouver Island in September and October 1972 (Reed and Halpern, 1973) showed the presence of a relative temperature minimum. The salinity at the relative minimum is about 32.6‰. Its depth decreases from over 100 m near Cobb Seamount to less than 50 m near Cape Flattery. The temperature at the relative minimum increases from west to east, and is less than 7.0C near Cobb Seamount. The relative temperature minimum observed in this region seems to be part of the larger feature described by Bennett (1959) and Uda (1963).

The temperature structure observed in the CUE-I area is very similar to that observed by Reed and Halpern except that the minimum is slightly warmer off Oregon. It seems very likely that the relative temperature minimum observed off Oregon is the result of southward advection of Subarctic water.

Southward flow off Oregon occurs as a result of both the California Current and the "coastal jet" associated with upwelling. Maximum velocities in the California Current

at the surface varies between 5 and 15 cm sec^{-1}, with highest velocities north of Pt. Conception occurring during winter (Pavlova, 1966). The California Current is broad, and its maximum is at a distance of several hundred kilometers from the coast. The "coastal jet" is described in Sections II and IV. Its maximum velocities at 20 m depth often exceed 20 cm sec^{-1} (see Figure 35). Higher velocities are achieved at the surface. Its width is of the order of 20 or 30 km (see Figures 8 and 35). The relatively high speed and the narrowness of the coastal jet apparently enhance the southward advection of Subarctic water in a narrow band along the Oregon coast, resulting in the observation of the ribbon. Figure 17 shows the vertical distributions of temperature and of the northward component of velocity for a particular date; the positions of the ribbon and the coastal jet appear to agree rather well. Observations made in the summer of 1973 (Cue-II) may provide further insight into the relation between the cool ribbon and the coastal jet.

Other Temperature Inversions in the Region

Temperature inversions are very common in the Northeast Pacific, and they have a variety of causes (Roden, 1964). In the Subarctic Pacific, inversions are often the result of winter cooling above the permanent halocline and subsequent summer heating; subtropical temperature inversions off Baja California appear to be due to

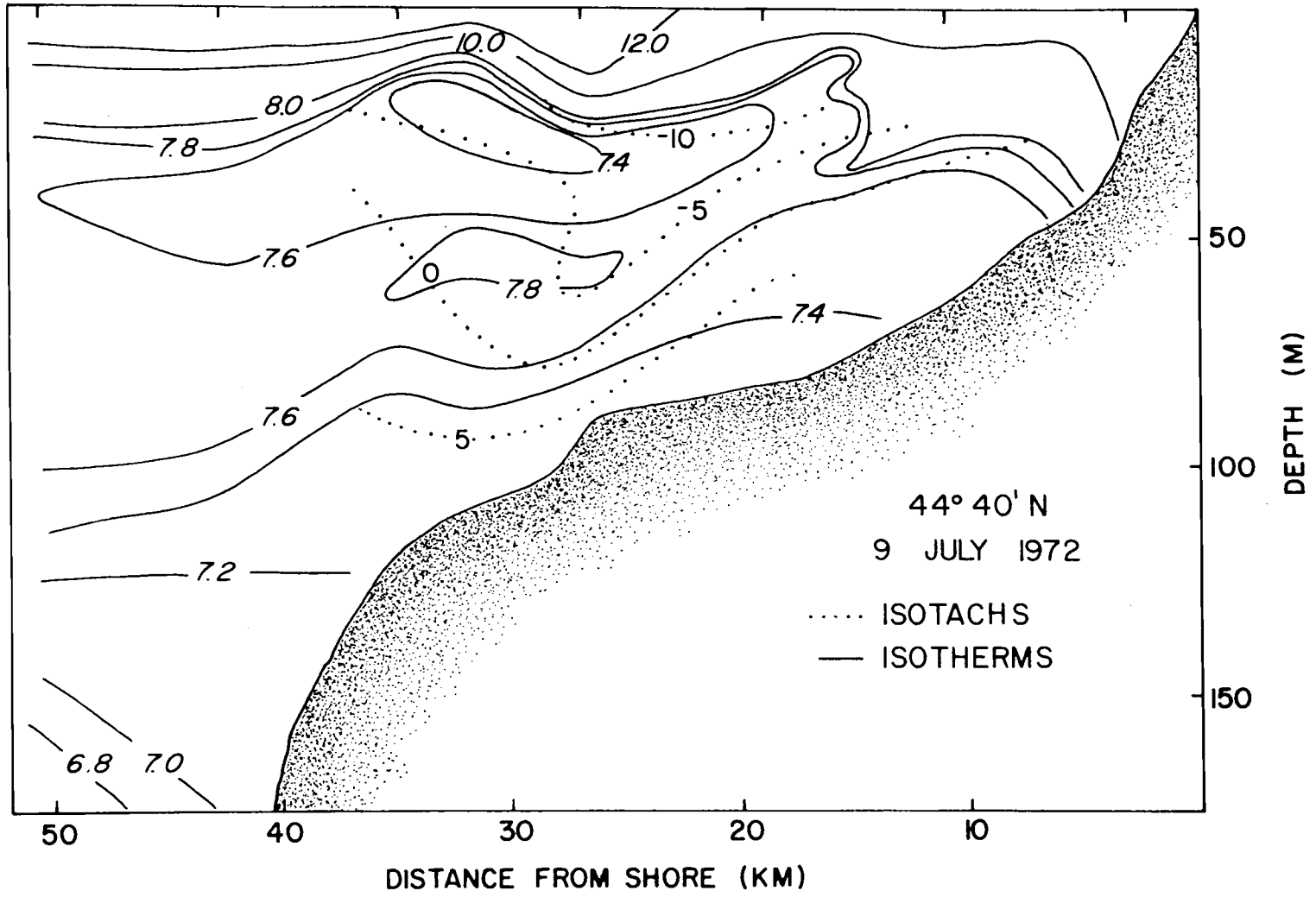

Figure 17. The vertical distributions of both temperature and the northward component of velocity at 44°40'N, 9 July 1972.

the differential advection of water masses of different temperatures. Roden (1964) shows that relatively few temperature inversions have been observed off Washington, Oregon and northern California, i.e., in the transition region between the Subarctic and the Subtropic. Southward advection occurs not only in the coastal jet associated with upwelling, but also in the California Current, and we would expect to observe water with Subarctic properties, i.e. with a temperature inversion, offshore in the California Current as well as in the upwelling region. Temperature-salinity characteristics at stations both offshore and within the cool ribbon during the June 1968 cruise (Figure 18) do show similarities. Examining bathythermographs as well as the discrete samples showed that temperature inversions occurred at MC-3, 36 and 37. However, in the salinity range 32.5 to 33.0‰, temperatures in the cool ribbon were about 1C cooler than at the corresponding salinities offshore. The temperature difference is attributed to the slowness of the California Current compared to the coastal jet; early in the upwelling season mixing rates are probably not much larger nearer shore than offshore, except in the boundary region about 10 km wide.

All of the 1972 observations were inshore of 125°W, almost all of the stations were within the cool ribbon, and it is not possible to make a comparison between characteristics within the upwelling region and those within the California Current. Two stations (nos. 28

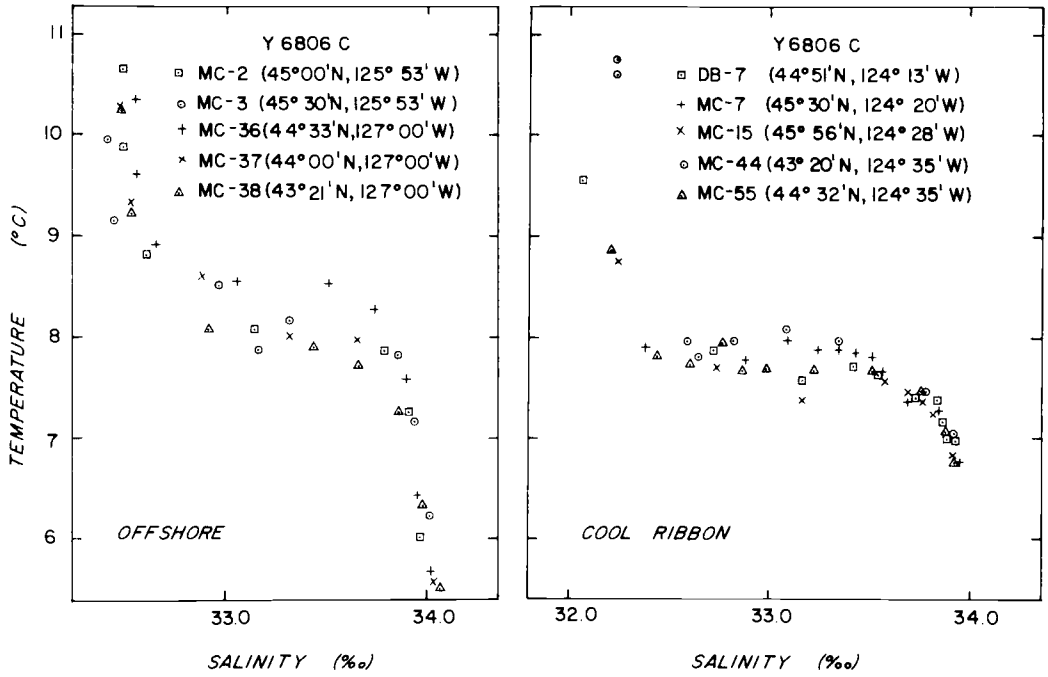

Figure 18. Temperature-salinity characteristics both offshore and along the cool ribbon, June 1968.

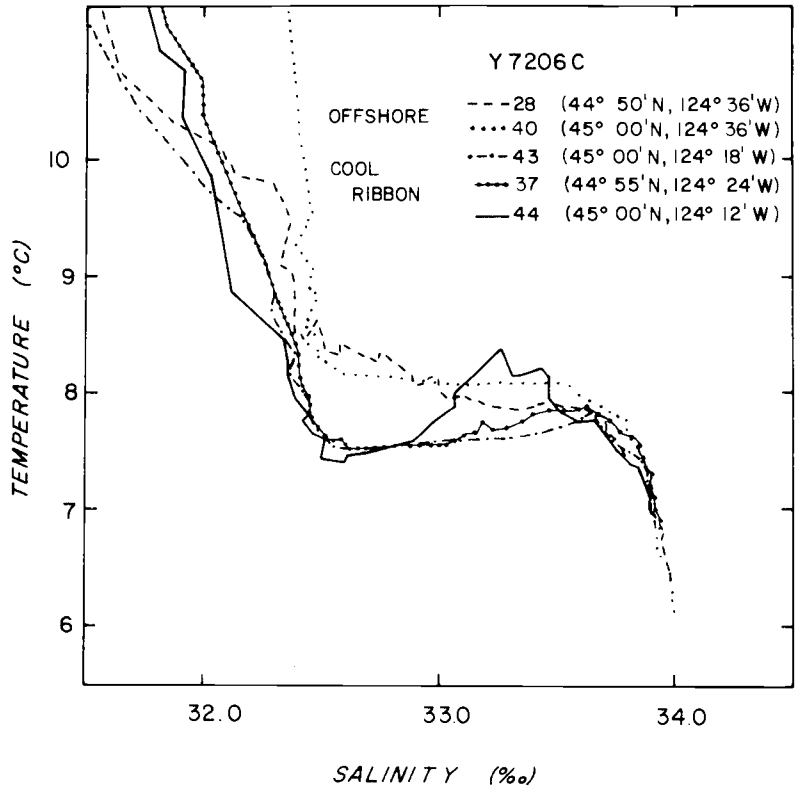

Figure 19. Temperature-salinity curves for selected stations from the June 1972 grid survey.

and 40) of the June 1972 cruise appeared to lie seaward of the cool ribbon; their T-S curves are compared to stations near the axis of the ribbon (Figure 19). Again, it is apparent that water within the ribbon is cooler over a wide salinity range including 32.5 to 33‰. The two stations (28 and 40) are probably between the coastal jet and the California Current. It would be interesting to do some closely spaced hydrographic sections extending from the coast to the seaward edge of the California Current, both to determine the seaward extent of the cool ribbon and to see whether a similar feature is associated with the California Current.

There is another kind of temperature inversion within the upwelling region which should not be confused with the cool ribbon. It is observed inshore of the ribbon. Although the cool ribbon has been overlooked in past studies, the warm inversion has received a great deal of attention. Pak et al. (1970) have shown that the anomalously warm water of this inversion was associated with high turbidity. Their mechanism for the generation of the warm anomaly seems essentially correct: cold saline water is brought to the surface by intense upwelling, is then subject to solar heating and is carried offshore by the Ekman transport. When it approaches lighter surface water (usually lighter because of lower salinity) it tends to sink and to be mixed with the surrounding water. The warm temperature anomaly results from the onshore-offshore component of the flow.

The resulting warm tongue does not appear to extend seaward of the axis of the cool ribbon. The section at 45°00'N on June 22 (Figure 10) is a clear example of the presence of both the cool ribbon and the warm temperature anomaly. The T-S curve for the station with the warm anomaly (no. 44) is shown with those in the ribbon and further offshore in Figure 19; the anomalously warm water occurs at salinities between 33.0 and 33.5‰. Later in the 1972 upwelling season (September), the intensity of this anomaly exceeds 1C and is associated with a salinity inversion (Anon., 1973c).

The warm temperature anomaly resulting from the local heating of highly saline upwelled water frequently has a complex structure (for examples, see Huyer, 1973). It appears that the exact location of the sinking of relatively warm water is sensitive to changes in very local surface conditions, so that a particular section may show evidence of two or more downward intrusions of anomalously warm water, for example on 16 July and 13 September 1972 (Huyer, 1973, p. 35, 57). When this occurs, it may modify the structure of the subsurface cool ribbon. The ribbon can also be modified if the warm intrusion is not at the inshore edge of the ribbon, but instead intersects it; this apparently occurred on 2 August 1972 (Figure 11). Such interactions between the warm temperature anomaly which is determined mainly by the onshore-offshore component of the flow, and the cool ribbon which is determined by the alongshore flow, likely contributed to the

frequent observation of more than one relative temperature minimum.

In spite of these other temperature inversions, both inshore and seaward of the ribbon, the cool ribbon can be distinguished when stations are taken at fairly close spacing (less than ten miles apart) across the upwelling region.

CONCLUSIONS

An alongshore, subsurface ribbon of relatively cool water was observed to be an integral part of the upwelling regime off Oregon during 1972. The ribbon was observed during each of five grid surveys by YAQUINA during the upwelling season of 1972. The ribbon was of the order of 50 km wide, and 50 m thick. It was relatively shallow, and was observed to be within the southward surface flow associated with the upwelling regime. The temperature of the ribbon was a few tenths of a Celsius degree colder than water beside and below it. Its salinity was between 32.5 and 33.0‰.

There appeared to be a seasonal evolution of the ribbon. Its minimum temperature was observed fairly early in the upwelling season (July), and it appeared to be most clearly defined early in the season (June). The axis of the ribbon appeared to move offshore as the season progressed. There was some suggestion that it widened, but observations were not made far enough from the coast to define the seaward edge during the later surveys.

Data from a June 1968 survey indicated the ribbon is at least 300 km long. Observations from other years also indicated the presence of the ribbon. Comparisons of the observations with an upwelling index showed that evidence for the ribbon was generally found when the upwelling index was high. There is some suggestion that there is a lag of about a month between the upwelling index and the presence of the ribbon.

The ribbon can be accounted for by southward advection of Subarctic water due to the coastal jet associated with the upwelling regime. We expect a similar temperature minimum to exist in the California Current, although southward advection is slower there. A warm temperature anomaly due to the sinking of modified upwelled water is frequently observed inshore of the cool ribbon. These different temperature inversions can be distinguished by close station spacing and to some extent by their T-S characteristics.

IV. SEASONAL EVOLUTION OF THE UPWELLING REGIME OFF OREGON, 1972

Off Oregon, coastal upwelling is a seasonal phenomenon, governed by the seasonal variations in the wind. Upwelling is observed in summer when the winds are predominantly southward, but not in winter when winds are mostly eastward or northeastward. The evolution of the oceanographic regime during the upwelling season is not well understood. Pillsbury (1972) has examined variations in the mean upwelling regime, but sufficient observations have not previously been available to study the evolution of the regime during a single year.

It is the purpose of this section to determine whether there was any systematic development of the regime during the 1972 upwelling season, and to describe it in as much detail as possible. The study is limited to phenomena of relatively low frequencies - inertial, tidal and higher frequency oscillations are neglected.

THE OBSERVATIONS

The observations obtained as part of the 1972 Coastal Upwelling Experiment consisted primarily of detailed hydrographic observations from two ships and current and temperature data from a moored current meter array. Wind, atmospheric pressure and sea level

observations were also available.

Current meters were successfully moored at eight locations (Figure 20). Observations were obtained at most locations during July and August and at a few locations until late October (Figure 21). Gaps in the records due to servicing of the moorings were filled by a time series whose spectral characteristics were determined from the end of the previous record and the beginning of the following record. The wind and atmospheric pressure were measured at Newport, Oregon. Sea level was measured at Newport and Depoe Bay. The hourly wind, sea level, atmospheric pressure and current data were filtered to suppress tidal and inertial oscillations. We used a symmetrical cosine filter spanning 121 hours with a half power point of 40 hours. This filtering method was the main reason for filling in short gaps in the current data: smoothing results in truncating the series by 2 1/2 days at each end. The resulting low passed series is not very sensitive to the artificial data inserted in the gaps.

Repeated hydrographic surveys of a small grid of stations, consisting of six lines extending about 50 km from the coast (Figure 9), were made by R/V YAQUINA and R/V OCEANOGRAPHER. Since surveys by the two ships overlapped rather than alternated in time (Table V) only the observations from YAQUINA are discussed here. The observations were made with a Geodyne conductivity-temperature-depth (CTD) unit lowered at a rate that ensured at least one data set

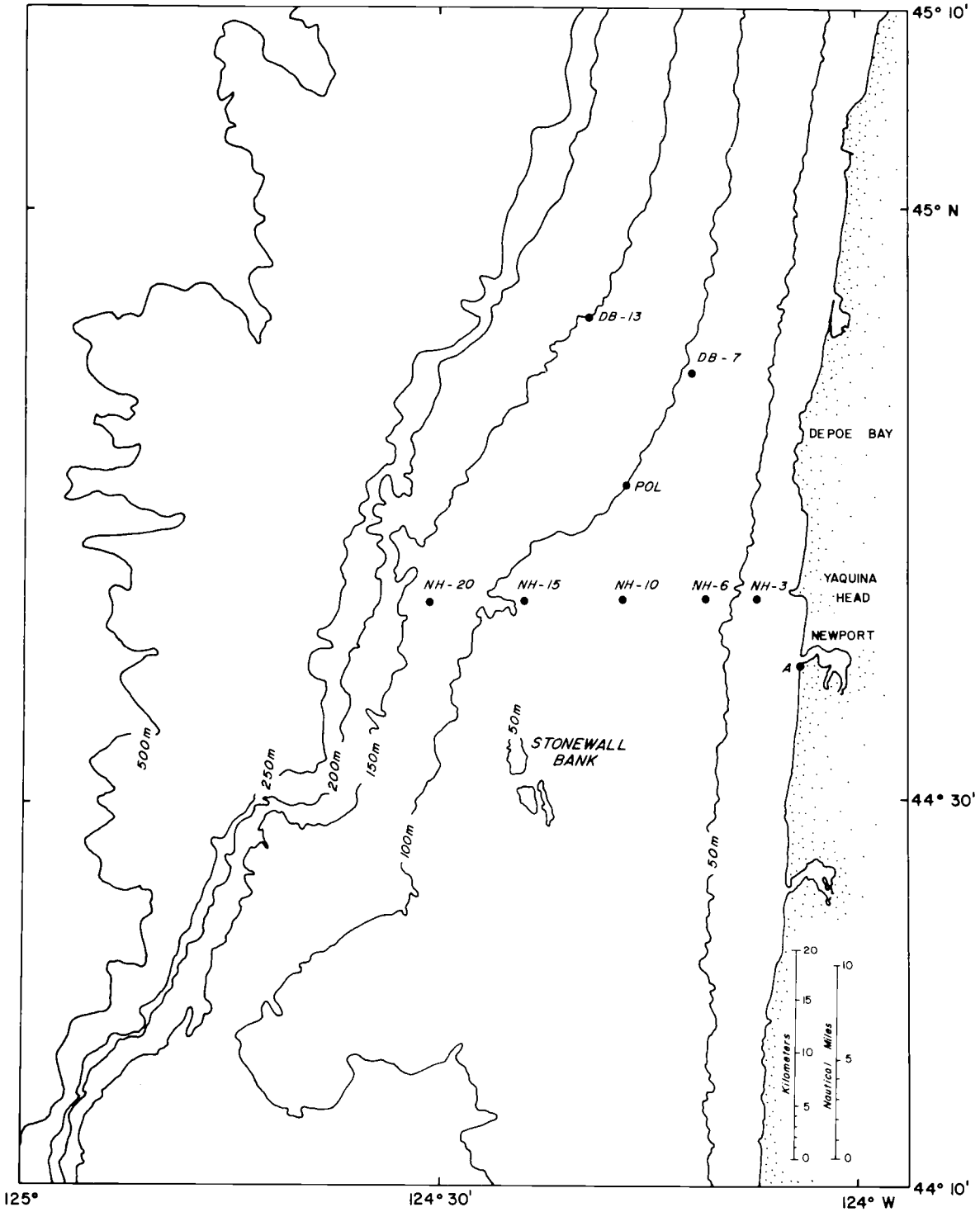

Figure 20. Positions of the moored current meter arrays, April to October 1972.

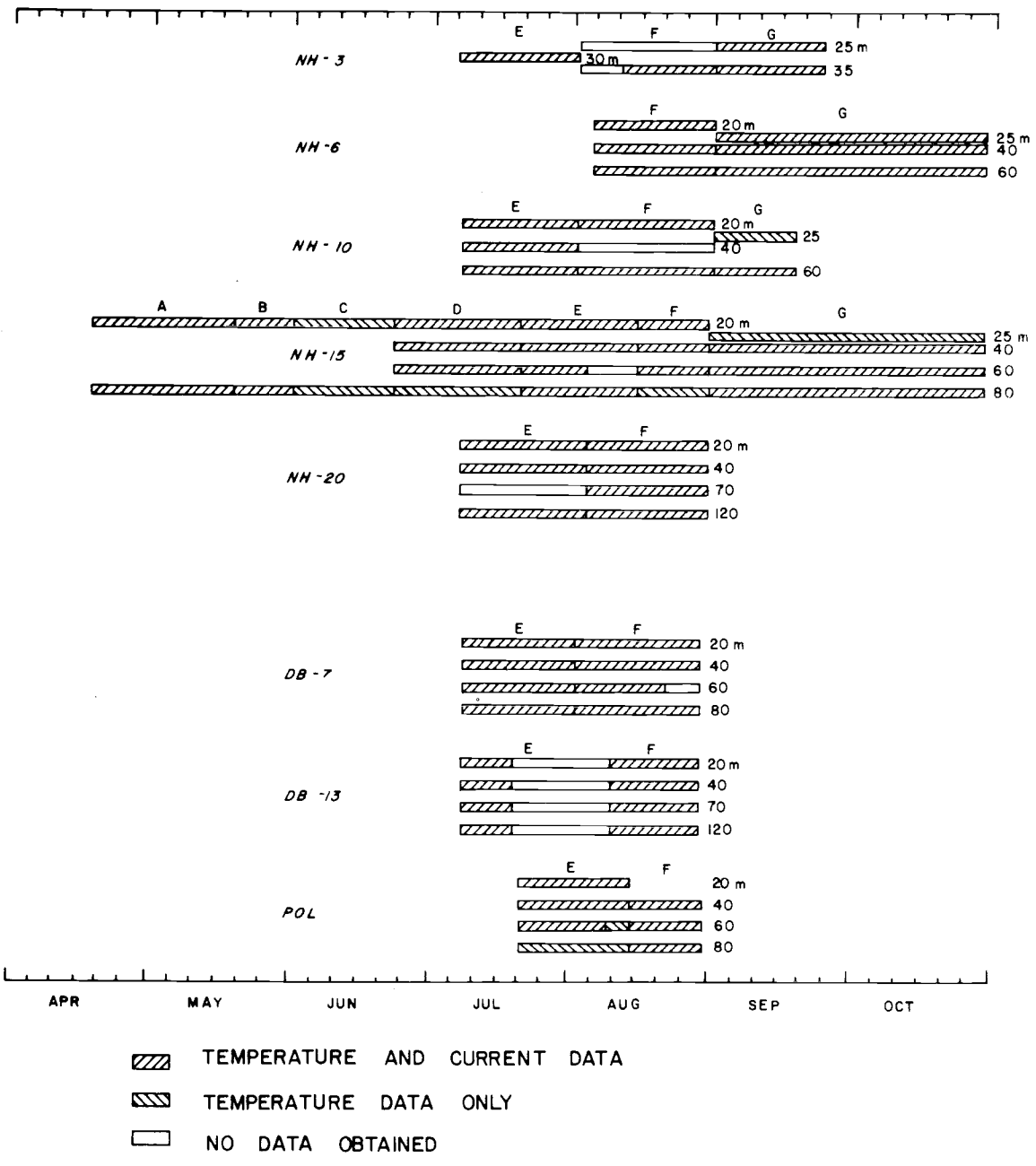

Figure 21. Periods of moored current meter operation off Oregon, April to October, 1972.

Table V. Dates of hydrographic surveys off the coast of Oregon, 1972.

Date	Ship	Cruise and Station Numbers
17-22 May	YAQUINA	Y7205A, 1 - 63
19-23 June	YAQUINA	Y7206C, 1 - 69
5-9 July	YAQUINA	Y7207A, 1 - 103
10-18 July	YAQUINA	Y7207B, 1 - 103
8-14 July	OCEANOGRAPHER	Oc-001 to Oc-158
30 July, 6 August	OCEANOGRAPHER	Oc-159 to Oc-349
31 July, 7 August	YAQUINA	Y7207E, 1 - 117
19-31 August	OCEANOGRAPHER	Oc-350 to Oc-721
22-23 August	YAQUINA	Y7208C, 1 - 26
26-30 August	YAQUINA	Y7208E, 1 - 86
11-13 September	YAQUINA	Y7209A, 1 - 33
28-30 October	YAQUINA	Y7210B, 1 - 24

for every 2 or 3 m depth interval; the data have been reported (Anon. 1972a-e; 1973a-c). Vertical distributions of temperature, salinity and sigma-t have been prepared for each line occupied (Huyer, 1973).

RESULTS

The low passed time series of the wind, currents and sea level are shown in Figures 22 and 23. Figure 23 shows rather high visual correlation between the currents at different depths and locations. The northward component of the currents seem to be well correlated with sea level, and less so with the northward component of the wind. Figure 22 shows the currents measured west of Yaquina Head. There appears to be good correlation between some of the currents but rather less between others. Currents measured at NH-15 seem to differ

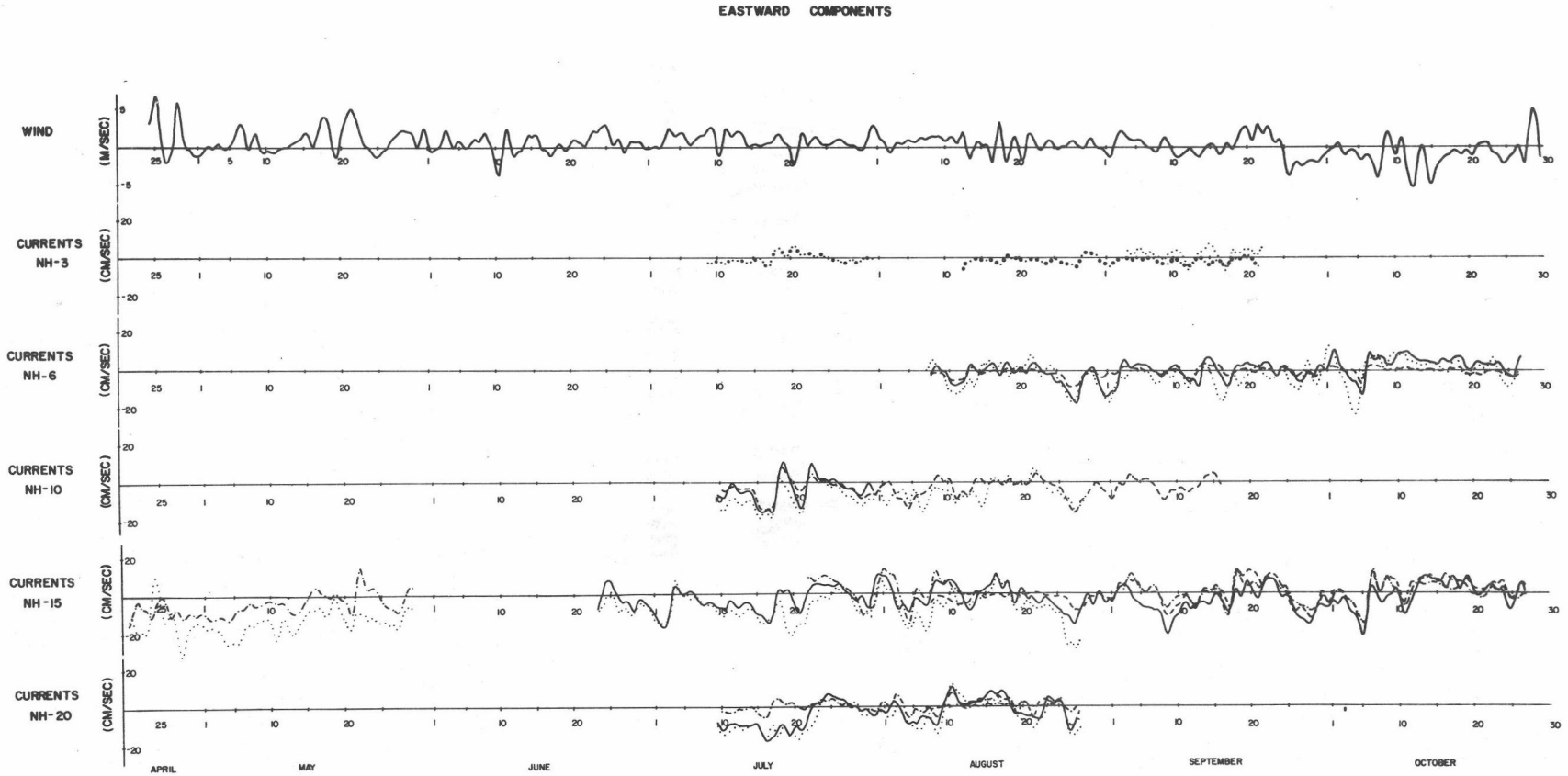

Figure 22(a). Low passed time series of the eastward component of wind and currents measured at locations off Yaquina Head, April to October 1972.

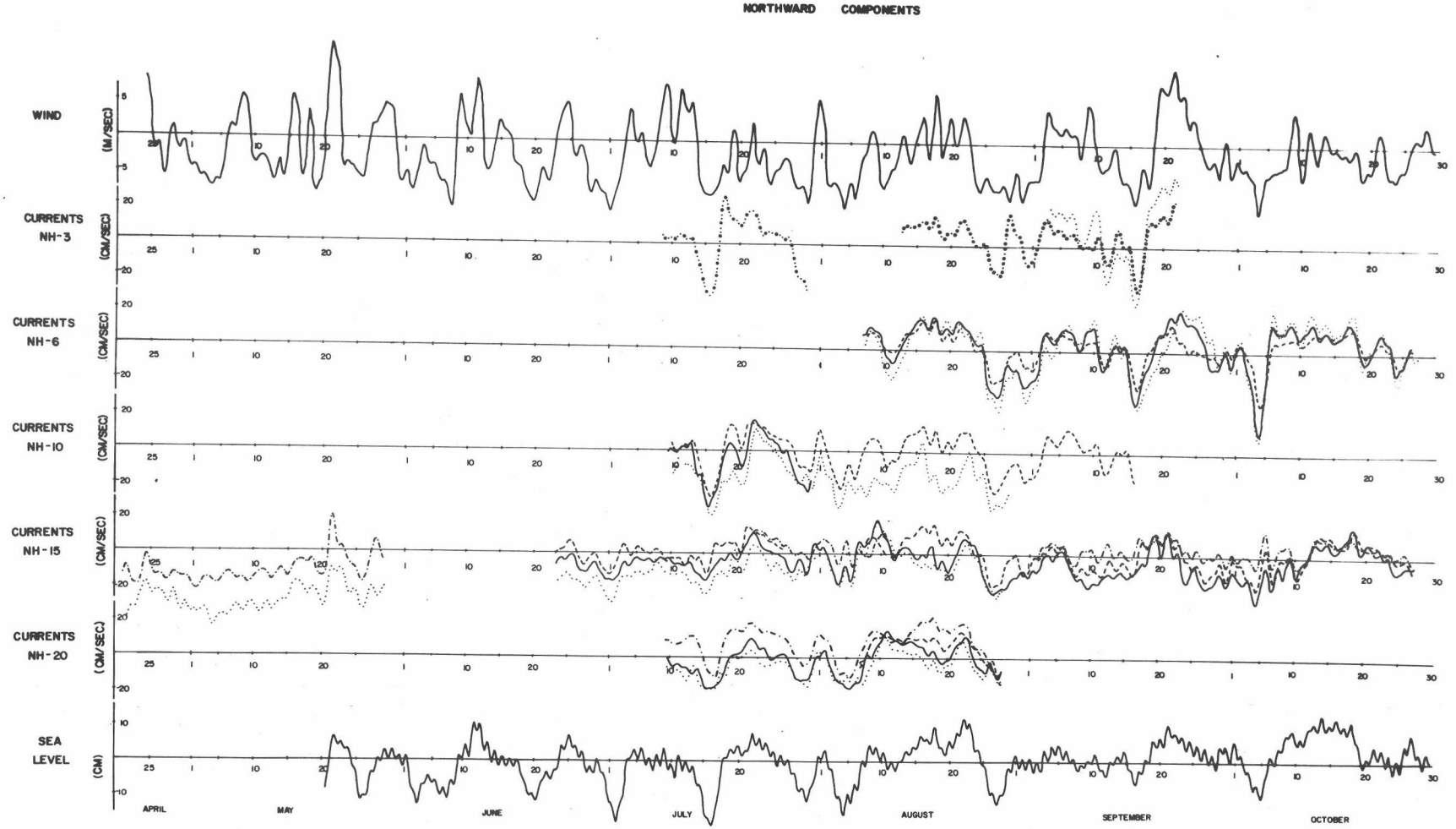

Figure 22(b). Low passed time series of the northward component of the wind and currents measured at locations off Yaquina Head, April to October 1972, and sea level at Depoe Bay.

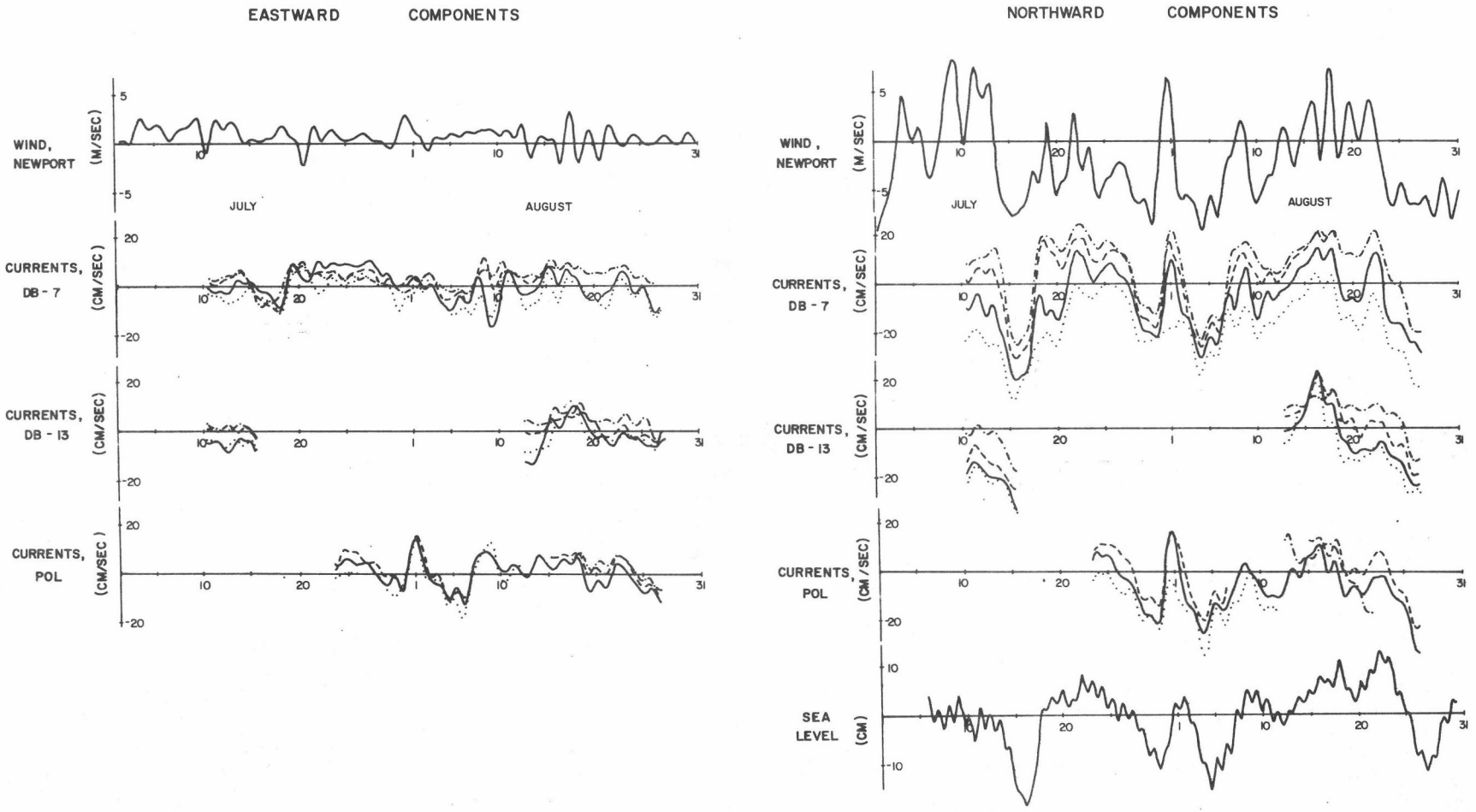

Figure 23. Low passed time series of the currents measured off Depoe Bay, July and August, 1972. Wind and sea level are repeated from Figure 22.

most from the others.

A vertical current shear was already present when the earliest current observations were made in April; usually during winter no vertical shear is observed (Collins and Pattullo, 1970). The deeper current meter shows southward flow at this time. A vertical current shear is maintained throughout the season at most locations. The shear varies less than the current at a particular location (Smith, 1973). The array at NH-6, which was installed relatively late in the season, shows no mean vertical shear. The deepest current meter at NH-6 was within a few meters of the bottom; at this depth, there seems to be a smaller amplitude in current oscillations, but no mean difference from the shallower current meters.

Figure 24 shows repeated hydrographic sections from the line along 44°55'N. Steepest isograms and lowest temperatures were observed in early July. Temperatures and near surface salinities were lower in May than in October. In May and June, water at salinity 33.75‰ was cooler than 7.5C; by October, it was warmer than 8C. A ribbon of relatively cool water about 50 m deep increased in width from May to July, and then either moved further offshore or disappeared. A tongue of relatively warm water extending downward and offshore from the surface grew in size and intensity from early August to the middle of September. The depth and shape of the band between 25.5 and 26.0 sigma-t changed little between May and September; it

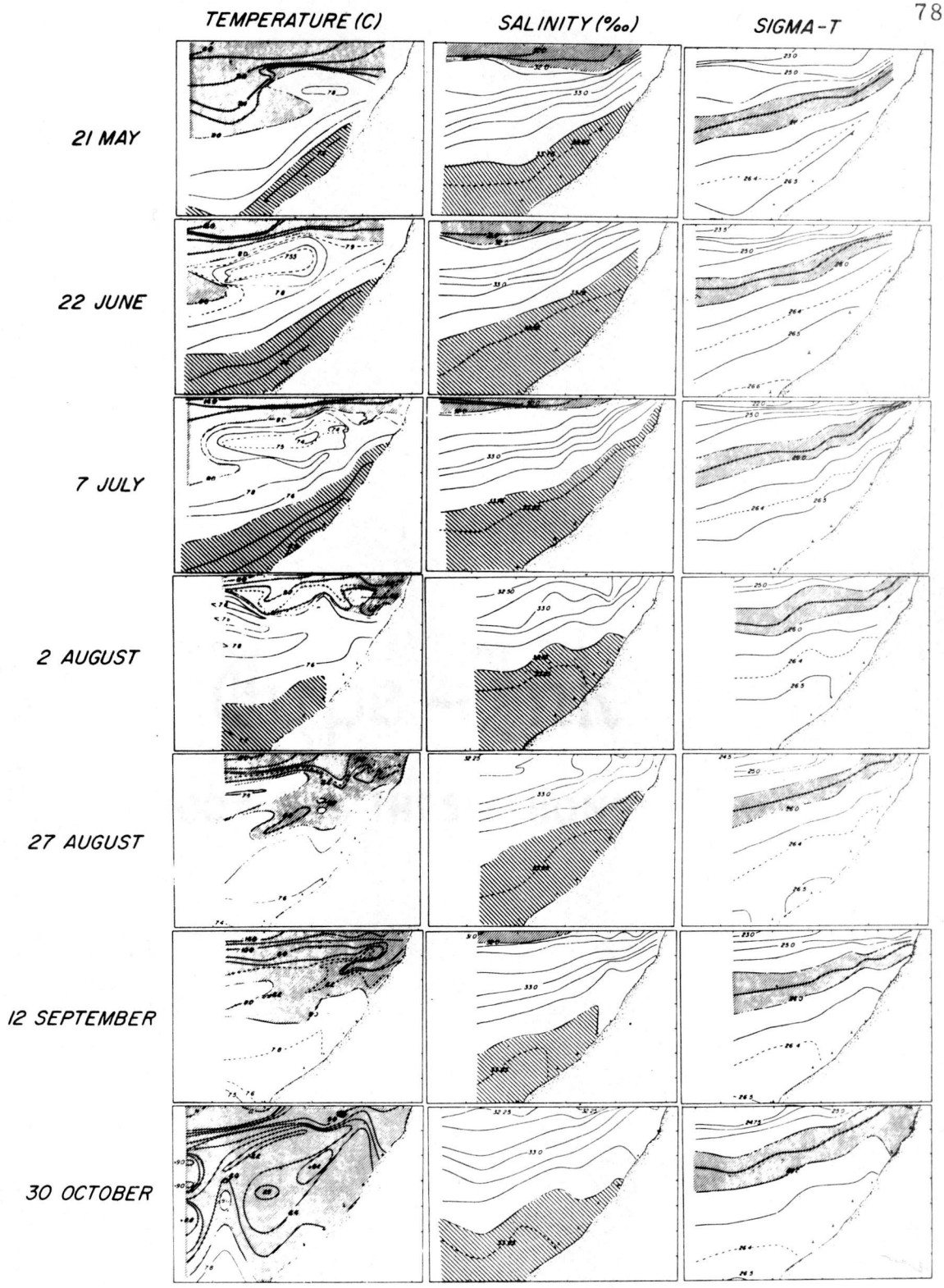

Figure 24. Hydrographic sections along 44°55'N showing vertical distributions of temperature, salinity and sigma-t.

thickened considerably by the end of October.

Low passed time series of the temperature observations at the deepest current meters of each array are shown in Figure 25. Each of these records shows that the minimum temperature was attained about the middle of July. Coherence between the temperature at the different locations appears to be good.

DISCUSSION

Wind

Both local wind observations and the geostrophic wind computed from synoptic atmospheric pressure charts have been used to study upwelling off Oregon. It is still not known which is of greater importance to the upwelling process, and both were studied in CUE-I. Bakun (personal communication) used the synoptic pressure charts to compute six-hourly values of the wind stress and hence the Ekman transport at 45°N, 125°W. The zonal component is shown in Figure 26; it is westward almost the whole season from late April to the end of October. Notable exceptions occur about 23-25 April, 8-12 June, 8-13 July, and 19-23 September, with eastward Ekman transport, and presumably convergence at the coast. There are also a few extended periods of very low zonal Ekman transport: 8-13 May, 16-23 August, and 12-18 October. From this figure we would conclude that conditions

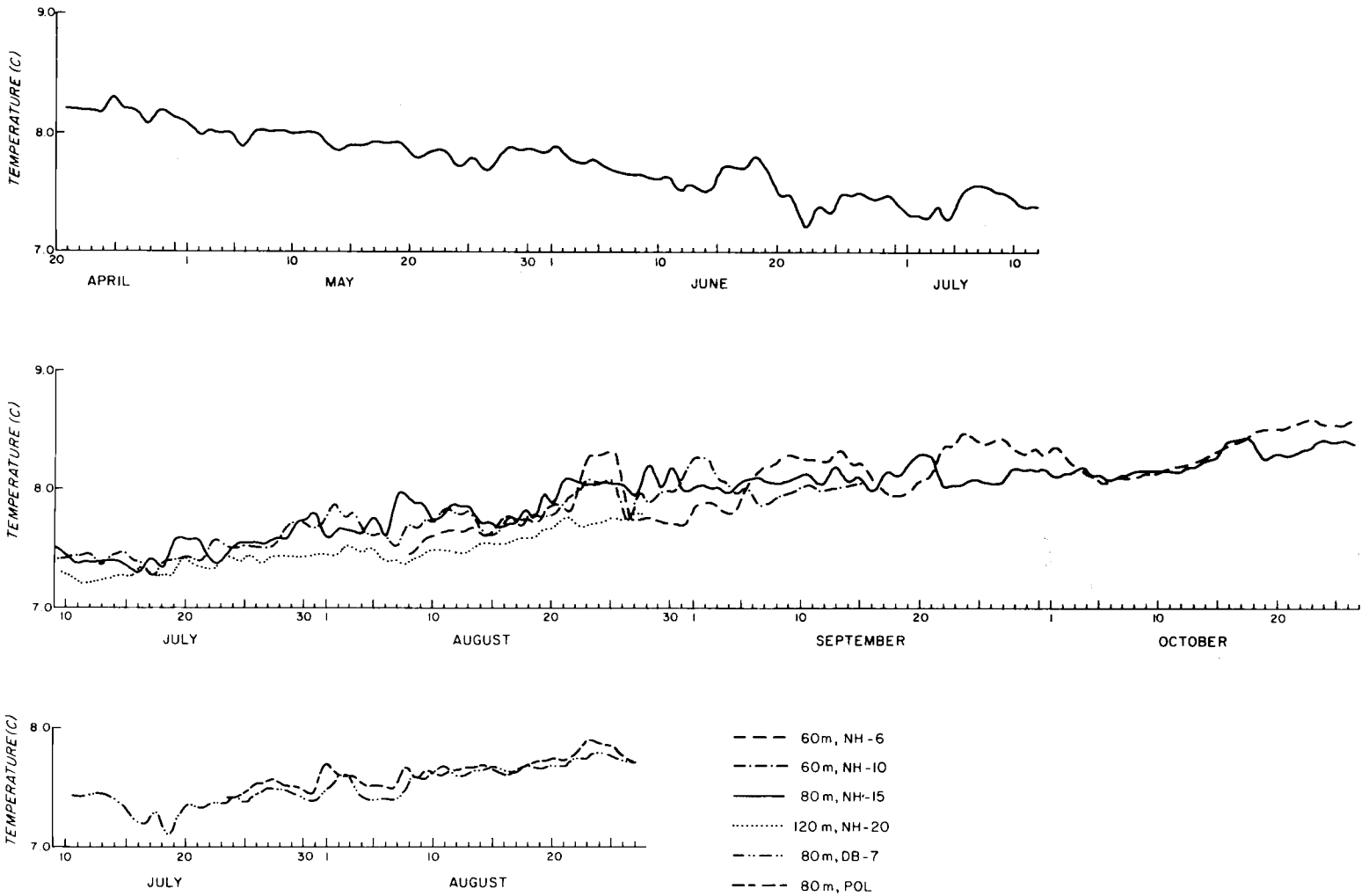

Figure 25. Low passed time series of temperature from the deepest current meter at each moored array except NH-3.

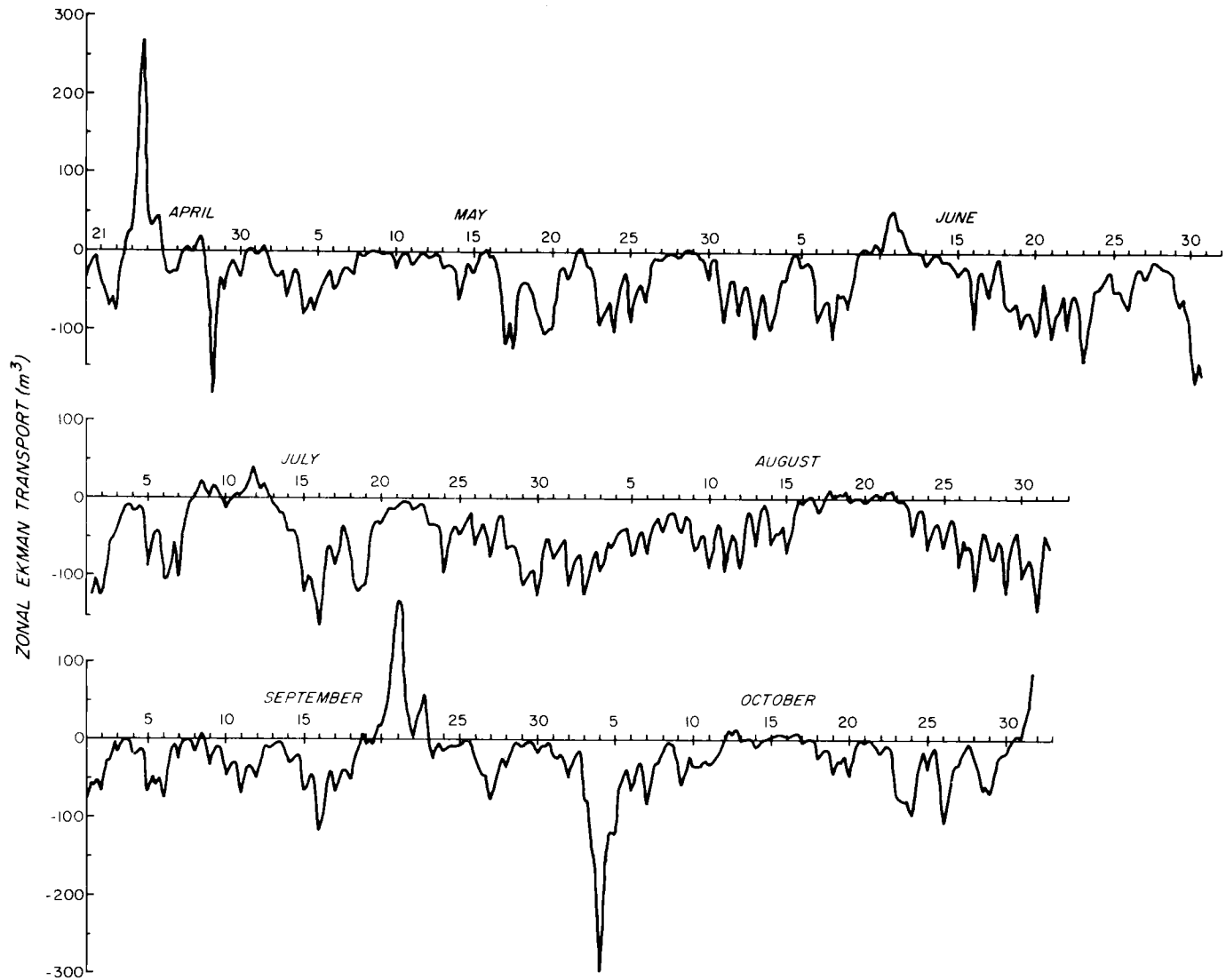

Figure 26. Zonal Ekman transport per 100 m of coastline, in the vicinity of 45°N, 125°W.

were favorable for upwelling during the whole season except these brief periods.

The direct wind observations from the south jetty at Newport (Figure 22) indicates the local wind was frequently northward, and that locally favorable conditions for upwelling (a southward component to the wind) were not nearly as frequent or as constant as we would infer from the computed zonal Ekman transport.

Bakun (1972) also computed the mean monthly offshore transport, the upwelling index, for the 1972 upwelling season and compared it to the 20-year mean monthly values at 45°N, 125°W (Figure 27). The 20-year mean monthly upwelling index clearly shows the seasonal cycle, with the transition between positive and negative values normally occurring in April and September. In 1972, the monthly upwelling index remained positive from April through October, i.e. during the entire period when observations were made. Monthly means and standard deviations of the northward component of the low passed wind measured at Newport were computed for May through October 1972 (Figure 28); as expected from the 1972 upwelling indices, no seasonal trend is apparent.

The wind stress was estimated both from the local wind and from Bakun's values of the Ekman transport. The local wind stress was computed from the hourly wind observations and the series decimated to six-hourly values. Means for the period 22 April to 31 October and

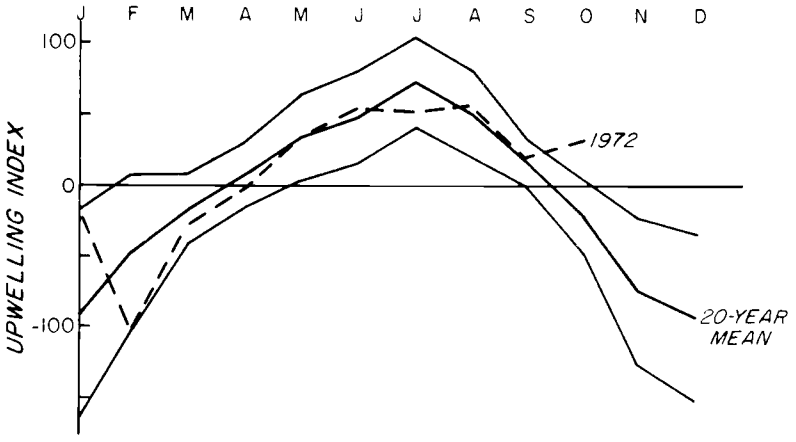

Figure 27. Monthly mean values of the upwelling index at 45°N, 125°W, from Bakun (1972). Heavy solid line indicates the twenty-year mean; lighter lines show the standard deviation. The dashed line shows the 1972 values.

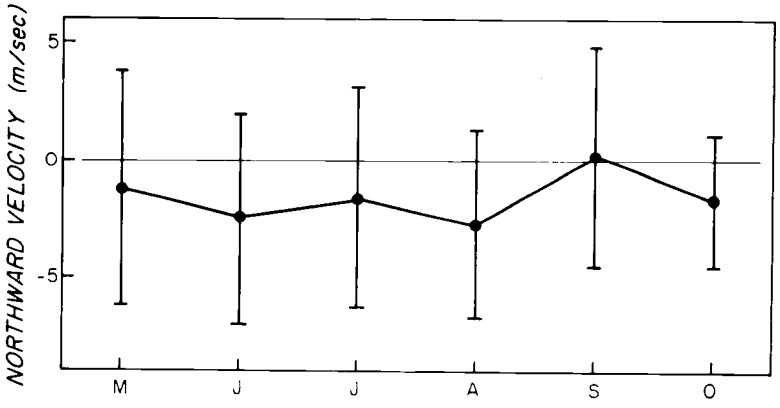

Figure 28. Monthly means and standard deviations of the low passed wind measured at Newport, May to October 1972.

the monthly means for both series of the wind stress are shown in Table VI. In each case, the meridional component is greater for the stress based on the synoptic pressure charts than for the local wind stress. In almost every case, the zonal component of the stress is larger for the local wind than for the geostrophic wind. The difference between the estimates could reflect real differences in the local and the larger scale winds. Offshore winds are generally believed to be stronger, while coastal winds often have a stronger onshore-offshore component because of the sea-breeze.

The two series of wind stress were also compared by computing their spectra and cross-spectrum. The rotary-component method of computing the spectrum of a vector, described by Gonella (1972), results in statistical coefficients that are independent of the coordinate system. The rotary auto-spectra and coherence-squared spectrum

Table VI. Comparison of means of local wind stress and wind stress computed from Bakun's values of Ekman transport.

	Mean Wind Stress (dynes cm^{-2})			
	Local		Bakun	
	τ_x	τ_y	τ_x	τ_y
22-30 April	0.219	-0.010	0.351	0.038
1-31 May	0.177	-0.096	0.099	-0.304
1-30 June	0.102	-0.341	0.079	-0.442
1-31 July	0.125	-0.270	0.026	-0.452
1-31 August	0.072	-0.359	0.009	-0.428
1-30 September	0.093	-0.112	0.135	-0.175
1-31 October	-0.053	-0.194	-0.186	-0.319
22 April-31 October	0.091	-0.183	0.041	-0.335

are shown in Figure 29. Negative frequencies correspond to the clockwise rotary component, while positive frequencies represent the counterclockwise component. The wind stress computed from Bakun's Ekman transport values has highest energy at very low frequencies; except for a peak at the diurnal period, the energy drops off with increasing frequency. The local wind stress also has greatest energy at the lowest frequency and peaks at the diurnal frequency. However, its energy is roughly independent of frequency in the band between 0.4 and 1.2 cpd, except at 1.0 cpd. The coherence-squared spectrum shows high coherence at low frequencies. Except at the diurnal frequency, coherence is not significant at the 99% level for counterclockwise frequencies higher than 0.4 cpd, and for clockwise frequencies higher than 0.6 cpd.

Hydrography

A single section of detailed hydrographic observations is available along 44°45'N for early January 1973 (Figure 30), i.e., two months after the CUE-I observations presented earlier. This section is typical of the winter hydrography in the region, with isopycnals roughly level or sloping downward toward the coast, low salinity water at the surface very near shore and temperatures near 10C down to 100 m. All temperatures above 175 m are warmer in winter than at any time during the upwelling season, except in the very near surface layer. The difference between this winter section and any of the sections during

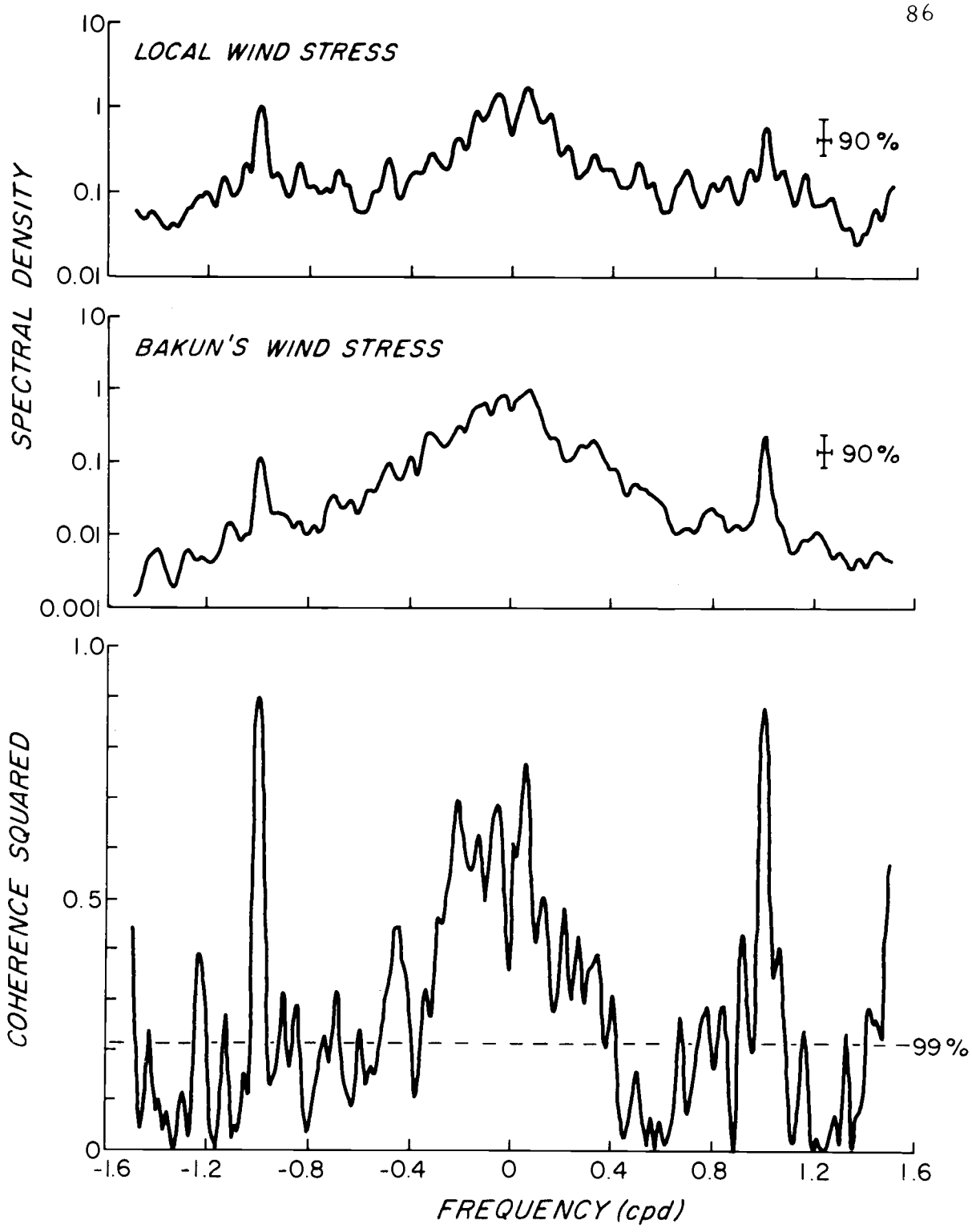

Figure 29. Autospectra and the coherence-squared spectrum for the local wind stress and the wind stress computed from Bakun's values of the Ekman transport, 22 April to 31 October 1972. The dashed line shows the 99% significance level for coherence squared.

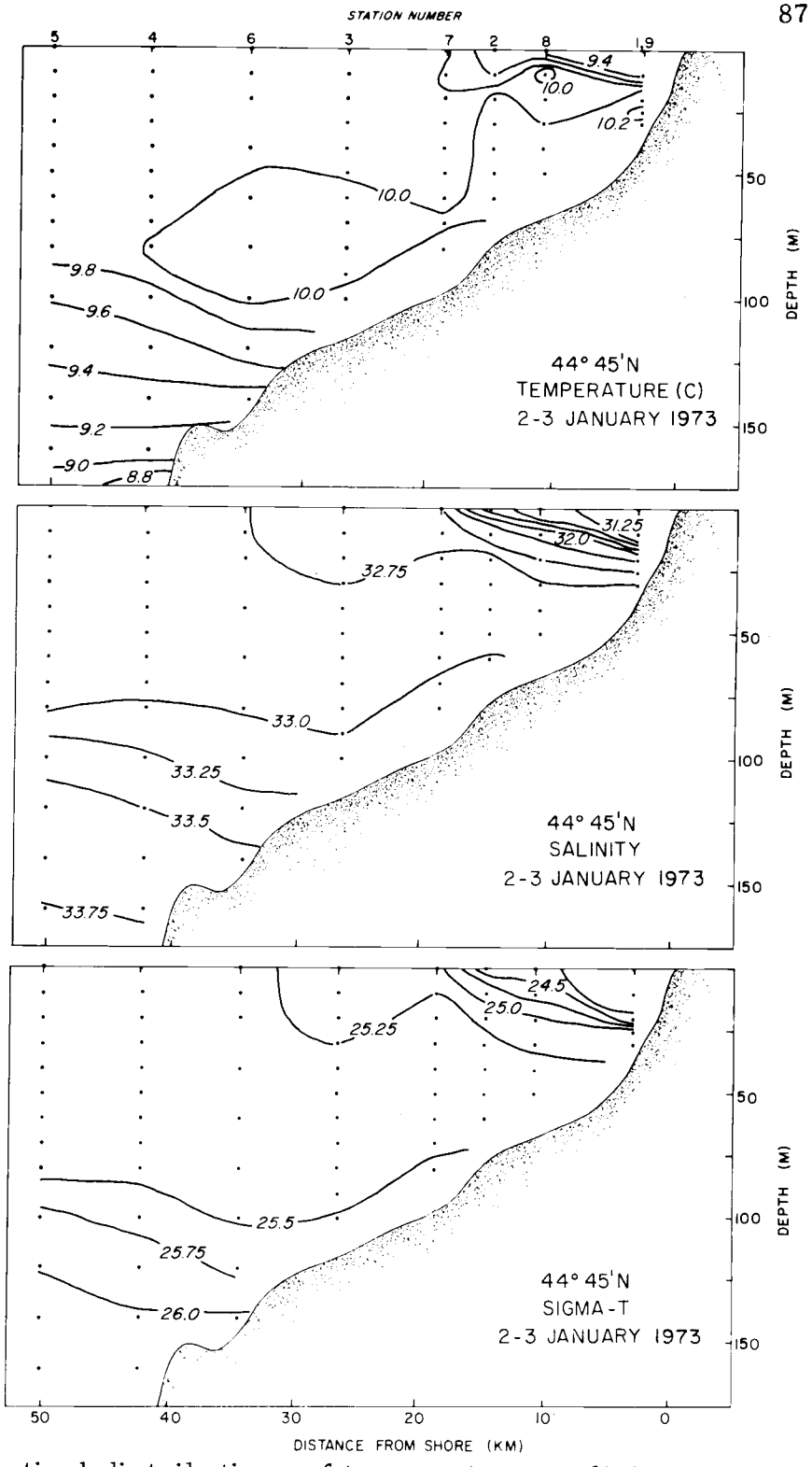

Figure 30. Vertical distributions of temperature, salinity and sigma-t along 44°45'N, 2-3 January 1973.

the upwelling season is much greater than between any two of the sections taken during the upwelling season (Figure 24).

The sequence of hydrographic sections during the upwelling season (Figure 24) showed variations in the depths and slopes of isograms with time, and also indicated temperature changes of water at the same salinity. Figure 31 shows these observations plotted on a distance vs. time diagram; the depth and temperature are shown for four values of salinity. Hatched boundaries indicate regions where the bottom salinity is less than the particular value of salinity. The depth of the isohalines generally increased with distance from the shore (at approximately 124° 00'W). The depth of each of the isohalines was observed to be shallower in summer, not only at the nearshore end of the section but over its entire length. The slopes of the isohalines are greater between May and early August than later in the season, i.e. contours of constant depth are closer together early in the season. Isohalines are shallowest in early August. In regions where the isohaline depth is very shallow (less than 30 m), the temperature contours tend to parallel the depth contours, i.e. temperature is a function mainly of depth. Highest temperatures are observed nearest the surface. At isohaline depths exceeding 80 m, the temperature contours tend to parallel the distance axis, indicating temperature is mainly a function of time; the temperature of the 33.75‰ isohaline decreases until early in July, and then begins to increase.

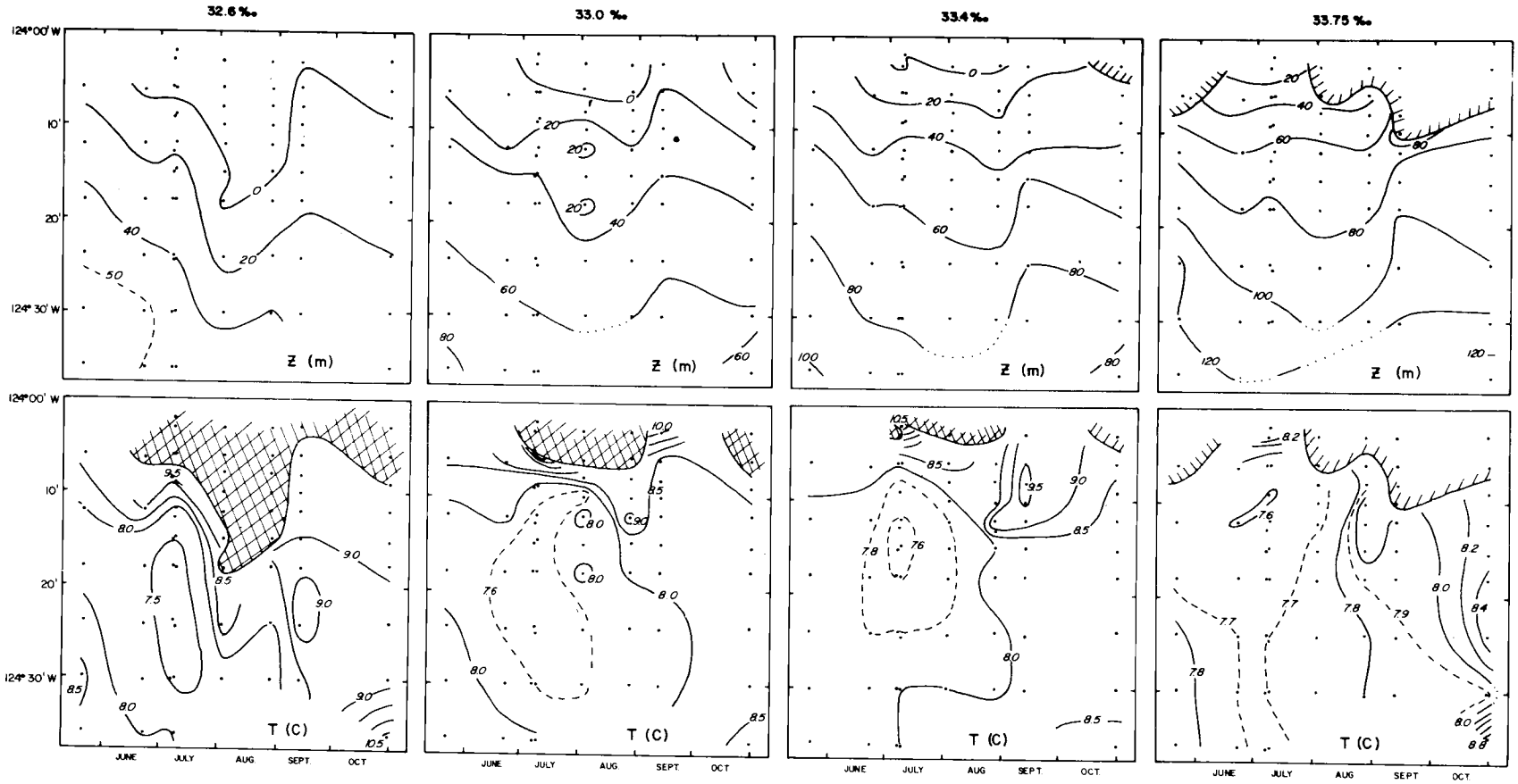

Figure 31. Distance vs. time plots of the depth and temperature of isohalines at 44°55'N, May to October 1972.

The cool water (<7.5C) observed at 32.6‰ in early July is part of the cool ribbon described in Section III. Its influence is also apparent on the 33.0‰ and 33.4‰ isohalines. The cool ribbon is seen to move offshore between May and August; it is not observed in September and October. The water at 33.75‰ is also coolest in early July.

The section along 44°55'N was chosen to demonstrate the seasonal variation because of the combination of rather good temporal coverage and the relatively narrow shelf width there; the seaward extremity of the line approaches the seaward boundary of the upwelling region more closely than do the lines further south. However, the line at 44°55'N was not occupied repeatedly at intervals of a few days, and the data cannot be used to determine whether the trends noted from Figure 31 are due to aliasing of phenomena with a period of a few days. Distance vs. time plots of isohaline properties at 44°40'N are shown for a twelve day period in early July (Figure 32). Comparable depth and temperature contours are observed to be further from shore for this section; we attribute this to the increased width of the continental shelf. At depths greater than 20 m, most of the contours are roughly parallel to the time axis, indicating that the aliasing problem is not serious, in spite of the large changes in winds and currents during this period (Figures 2 and 22).

The low passed time series of the temperature at the deepest current meters on the moorings at NH-6, 10, 15, 20 and DB-7 and

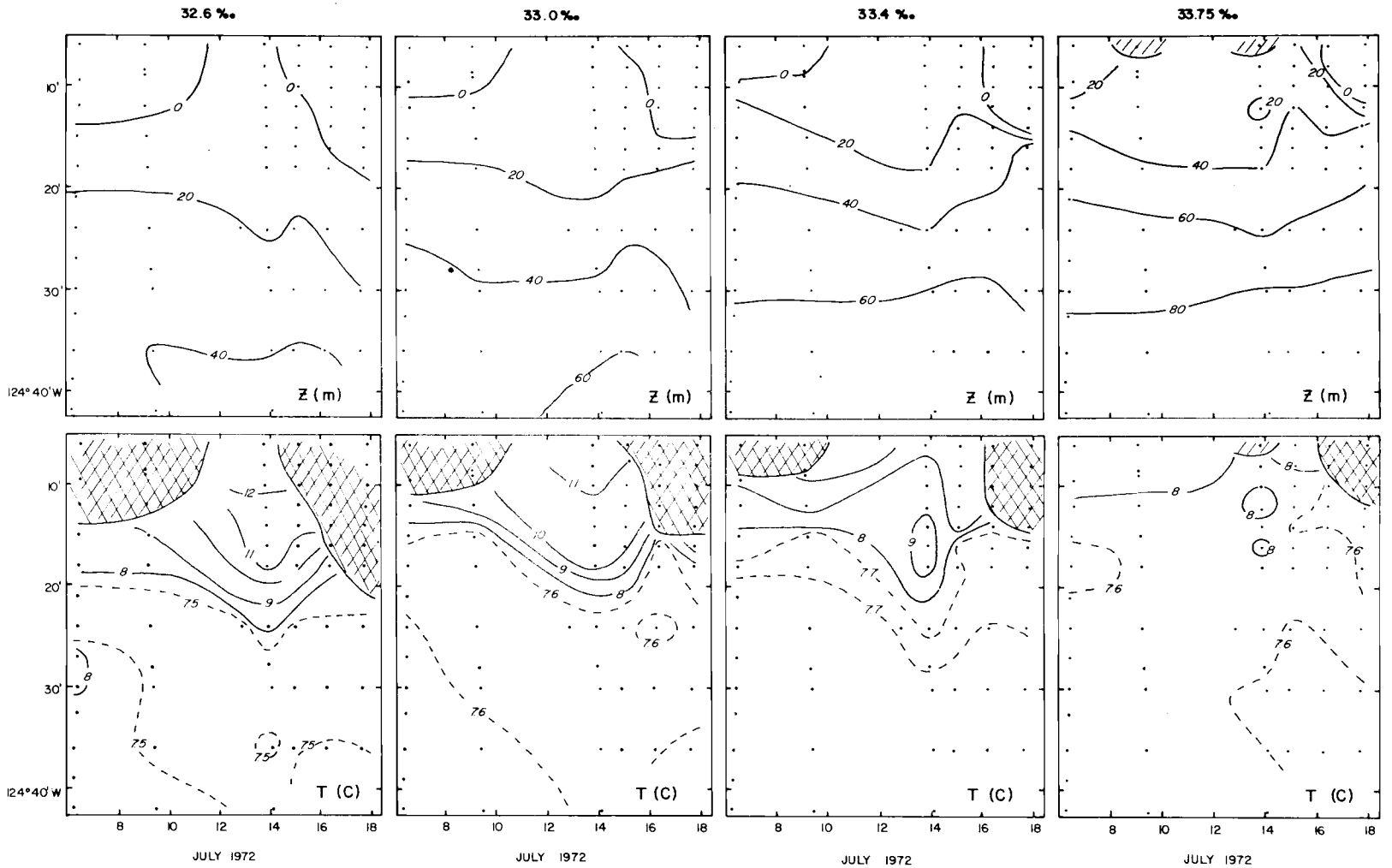

Figure 32. Distance vs. time plots of the depth and temperature of isohalines at 44°40'N, 6-18 July 1972.

POL (Figure 25) show the same trend as the 33.75‰ isohaline (Figure 31), with temperature decreasing until nearly the end of June, and increasing from about the middle of July. From Figure 22, it appears that flow in the deeper layer was predominantly southward until early July and became predominantly northward about the middle of July (see also Figure 38 and discussion of the undercurrent). The deep temperature minimum in early July may result from the cessation of equatorward advection of cooler water and the onset of poleward advection of warmer water. The amplitude of the seasonal oscillation exceeds 2.0C; this is much greater than the amplitude associated with the variations with periods of a few days. Pillsbury (1972) shows that the mean monthly temperature near the bottom at NH-25 is lowest in July; in this respect, 1972 is a normal year.

Both the deep temperature time series (Figure 25) and the overall hydrography (Figures 24 and 30) seem to have a stronger seasonal signal than does the local wind (Figures 22 and 28). The occurrence of a temperature minimum in early July, both in the deep water and at salinities as low as 32.6‰, does not seem to coincide with maximum offshore Ekman transport (Figure 26) or with maximum southward wind at Newport (Figure 22).

We expected that the temperature, even in relatively deep water, would be related to the wind which drives upwelling. We compared the wind and a deep temperature record by computing their rotary spectra

and cross-spectra (Figure 33). Coherence squared is significantly different from zero at the 99% level if it exceeds .21. There is some coherence between wind and temperature at periods of several days, but it is not significant at the 99% level. Smith (1973) found very high coherence between wind, sea level and currents at periods of several days. The relatively low coherence between temperature and wind at these frequencies supports the idea that current fluctuations at these frequencies are mainly barotropic.

Fisher (1970) found that near surface temperatures ($\simeq$ 20 m) were well correlated with the wind. We computed the cross-spectra between wind and temperature for two of the shallow temperature records, 20 m at DB-7, and 20 m at NH-20, for the period 10 July to 26 August 1972. These coherence-squared spectra are shown with the coherence squared spectrum between the temperature at 80 m, NH-15 for the same period (Figure 34). None of the temperature records show coherence with the wind at periods of several days at the 99% significance level; the coherence at these frequencies is barely significant at the 99% level. Both shallow records show significant coherence at very low frequencies, although the deep temperature record does not. The hydrographic observations suggest that at depths shallower than 20 m or water inshore of 10 km, the temperature reflects wind variations with periods of several days. At present, no shallow or very near shore temperature record is available for analysis. It seems likely

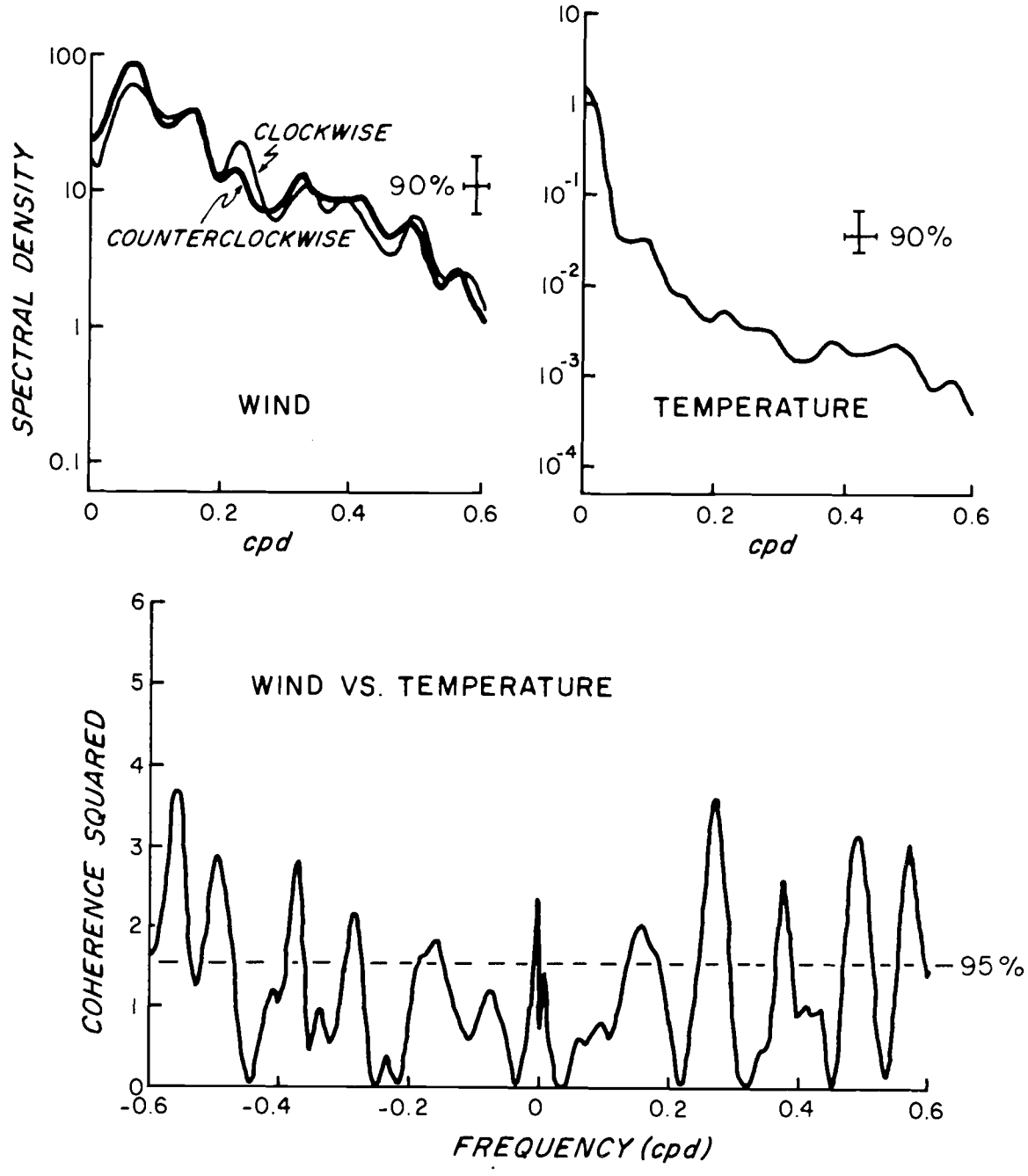

Figure 33. Autospectra and the coherence squared spectrum of the wind at Newport and the temperature at 80 m, NH-15, 24 April to 26 October 1972. The dashed line shows coherence squared significantly different from zero at the 95% level.

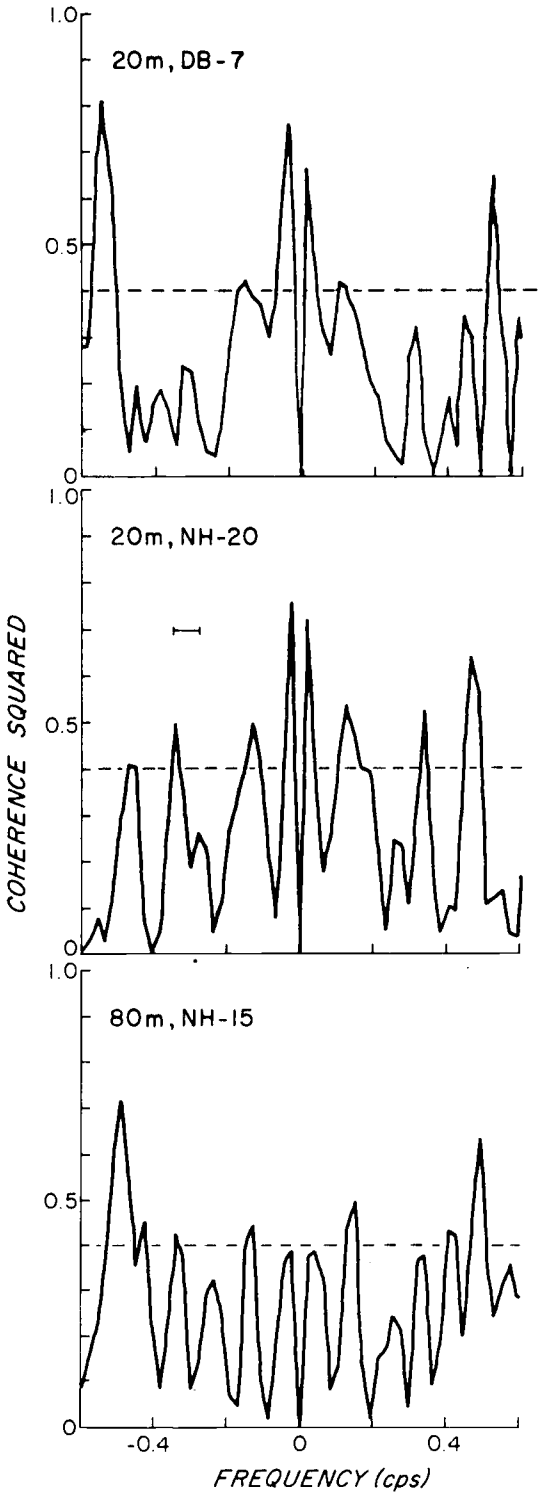

Figure 34. Coherence squared spectra between the wind at Newport and three temperature records at 20 m, DB-7; 20 m, NH-20; and 80 m, NH-15, 10 July-26 August 1973. The dashed line shows coherence squared significantly different from zero at the 95% level.

that in the very near surface water the temperature would be very coherent with the wind at periods of a few days.

The relatively low coherence between the temperature of subsurface water and the wind at periods of several days is very intriguing. It does indicate that current fluctuations with periods of several days, which are highly coherent with the wind, are barotropic rather than baroclinic. Also, the temperature at a given time and location depends on the previous history of the water, for instance whether the water has been advected from warmer or colder regions; the temperature spectrum indicates that most of its energy is at very low frequencies. Presumably the wind and temperature are coherent at the annual period; since the records are less than seven months long, the spectra cannot show this.

Currents

Figures 22 and 23 evoke a single natural reaction about the currents in the upwelling regime - they appear to be highly variable and confused. Closer examination of the data shows a surprising degree of simplicity. Previous studies of the currents in the region led us to expect:

(1) a "baroclinic surface jet" during the upwelling season, i.e., a nearshore maximum in the southward surface flow because of the sloped isopycnals associated with upwelling (Mooers et al., 1973);

(2) a poleward undercurrent during the upwelling season (Mooers et al., 1973);

(3) the alongshore flow to be mainly geostrophic (Mooers et al., 1973); and

(4) a high degree of correlation between variations in the current and variations in the wind (Huyer and Pattullo, 1972).

The 1972 current data were analyzed to determine whether these features existed and whether they exhibited any seasonal trends.

(1) The Surface Jet

Near surface current observations at more than three positions along the line off Yaquina Head are available only for July and August. These observations suffice to determine whether or not the jet existed, but not to study its seasonal variations. The data were examined in detail for two periods: 10-29 July and 13-27 August. The northward component of the currents were computer contoured on distance vs. time plots (Figure 35). The distance scale of the plots is not uniform. For the earlier period, data for NH-6 was interpolated linearly from the NH-3 and NH-10 data. Many of the contours are parallel to the distance axis, implying that there is a large component of the current independent of distance offshore. The surface currents relative to NH-3 are also shown in Figure 35; this approximates the baroclinic part of the surface current. This procedure enhances the relative

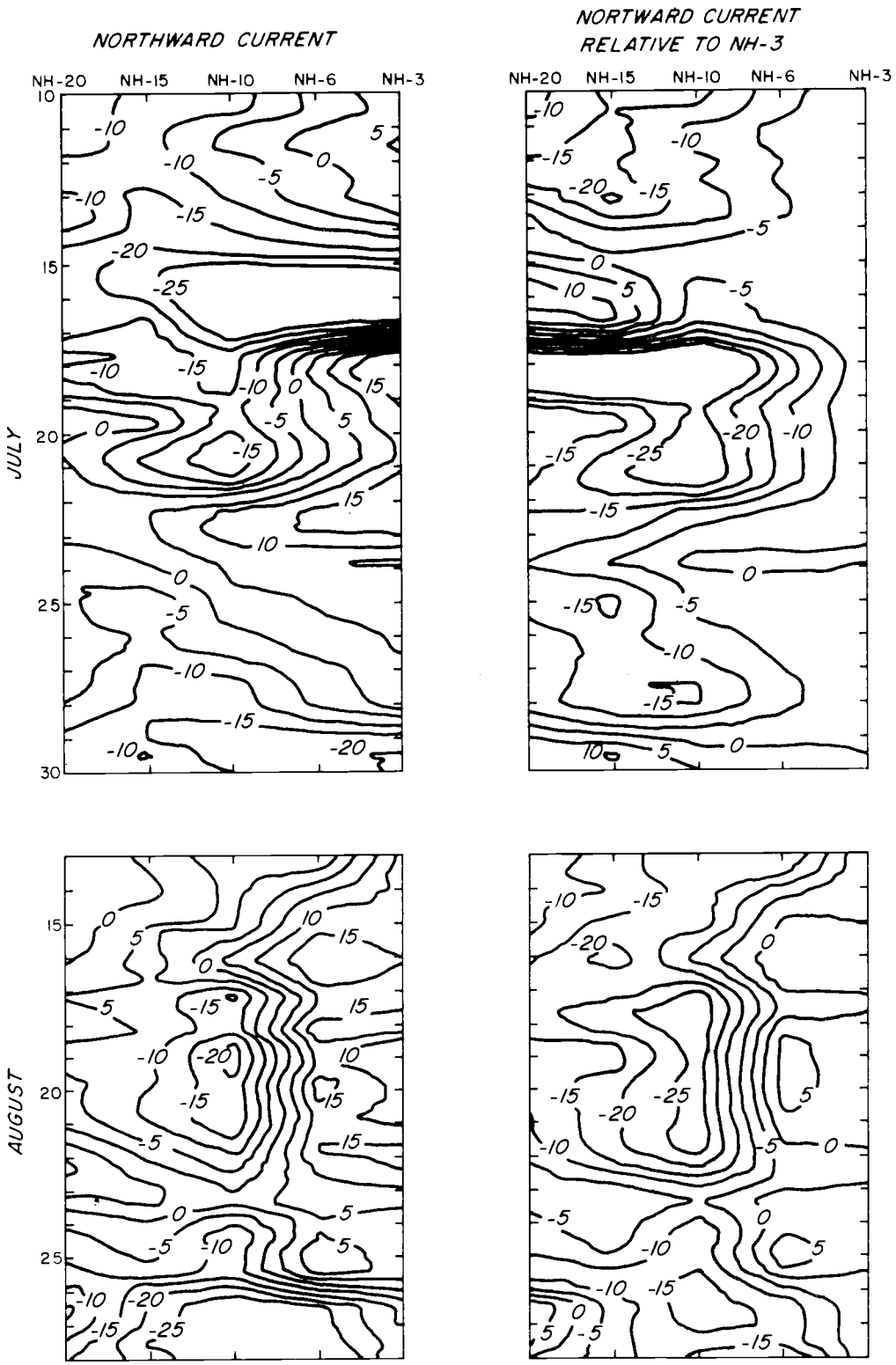

Figure 35. Time vs. distance plots of the northward component of velocity along 44°40'N, 10-29 July and 13-27 August 1972.

maximum which is observed. The intensity of the maximum varies from less than 5 cm sec^{-1} (14-16 July, and 23 August) to over 25 cm sec^{-1} (18-21 July and 17-22 August). The location at the velocity maximum is usually at NH-10, but it is observed to occur further offshore at NH-15 during two periods (10-15 July and 15-17 August); there is some suggestion that it is at about NH-20 from 22-24 July.

From the simple theory of a baroclinic coastal jet, we expect the intensity of the jet to depend on the isopycnal slopes. The isopycnal slopes also influence the surface density distribution, so that we can expect a relationship between the offshore density gradient and the intensity of the southward flow. Figure 36 shows both the 20 m southward current and the 20 m value of sigma-t vs. distance offshore for dates when hydrographic observations were made. It is not clear that a definite relationship exists between the offshore density gradient and the intensity of the southward flow. This can be partly attributed to the nonlinear relationship between the 20 m sigma-t and the slopes of the isopycnals. However, isopycnal slopes are small on 22 and 24 August (Huyer, 1973, p. 47; Halpern et al., 1973, p. 133), but a jet-like structure is observed on these dates. We conclude that baroclinicity is not the only cause of a maximum in the southward flow.

(2) The Poleward Undercurrent

Inherent in the notion of a poleward undercurrent is not only the

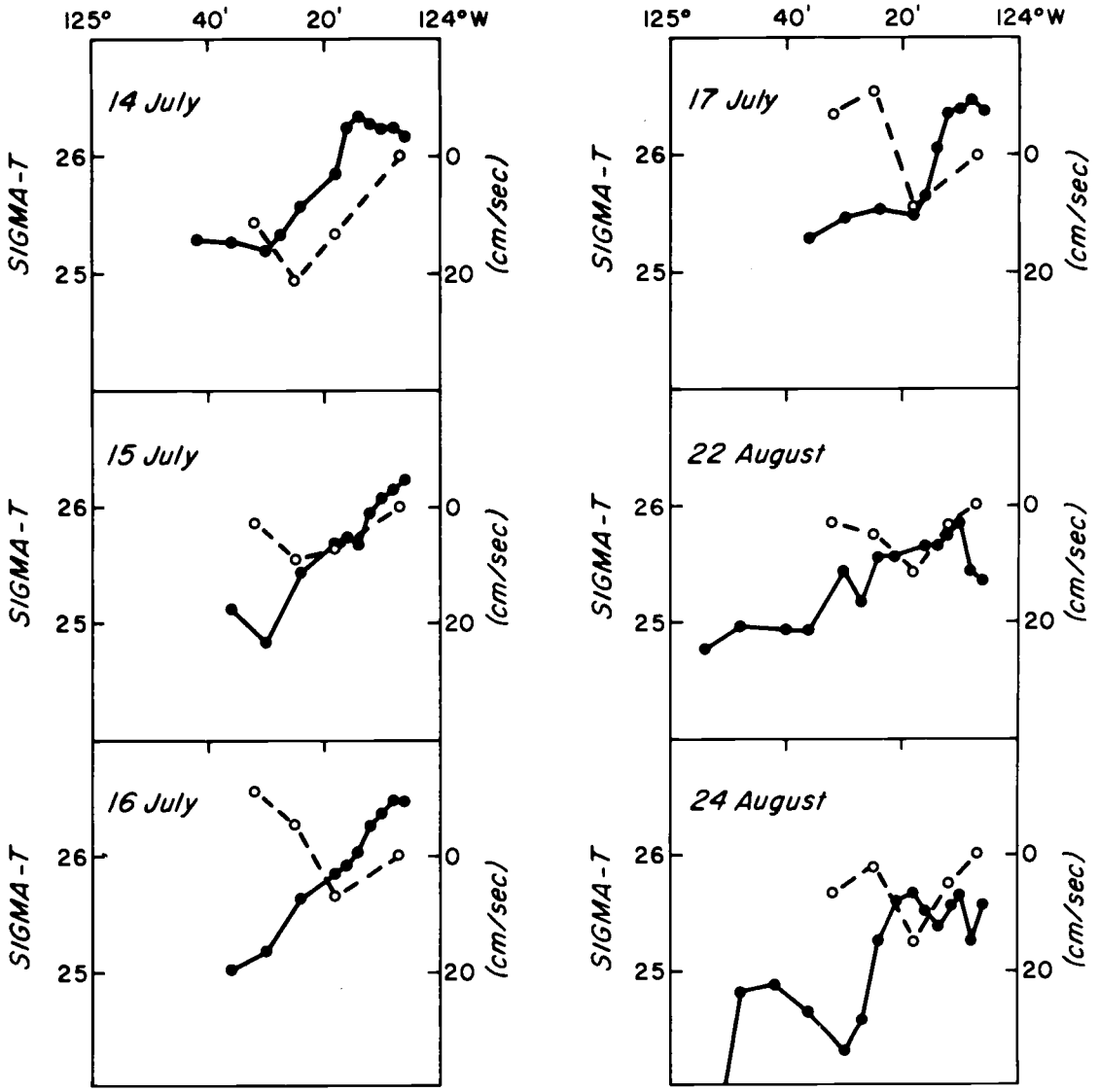

Figure 36. Northward velocity and sigma-t at 20 m, along 44°40'N, vs. distance offshore.

idea that there exists a vertical current shear, but also the idea that the mean flow at some depth is poleward while the surface flow is equatorward. Poleward undercurrents are believed to be a common feature of most upwelling regimes; they are frequently observed at some intermediate depth away from the bottom. Off Oregon, the poleward undercurrent has been observed near the bottom over the continental shelf; its offshore extent and its depth over the continental slope can only be inferred from very meager observations. Mooers et al. (1973) have speculated that the undercurrent "forms a jet under the steepest portion of the inclined frontal layer". They have also estimated its speed (10 cm sec^{-1}), width (50 km), thickness (200 m) and the poleward mass transport (10^6 m^3 sec^{-1}), though they do not attempt to justify these estimates. Pillsbury (1972) who summarized all the direct current observations off Oregon from 1965 to 1969, shows that there is frequently poleward flow at intermediate and near bottom depths during August and September, although southward flow is also observed at these depths during both August and September. For the 1972 data, we attempt to answer the two questions separately: first, whether there is a persistent vertical shear in the alongshore current; and second, whether there is a layer in which the mean flow is poleward.

For each location, we computed the northward component of the relative current between the shallowest and the deepest current meter.

We calculated its mean and standard deviation for the total record length, and also by month. No attempt was made to adjust the monthly means for the time of occurrence of the record segment. The results (Figure 37) indicate that the existence of vertical shear is a function of location as well as of time. This is also apparent from Figure 22. Because of the failure of the shallowest current meter at NH-15 during September and October, no comparison between the deepest and shallowest current meters at a single location extends over the whole period from April to October. However, there are indications from Figure 37, supported by the more detailed data in Figure 22, that the vertical shear decreases during the later part of the upwelling season. Data is scarce early in the season (April to July) but the shear seems to be relatively constant during this period. No net vertical shear is observed at NH-6, but observations there did not begin until early August. The lack of mean shear late in the upwelling season at NH-6 can be attributed to the relatively low density gradients there. At NH-15 the vertical shear became zero about 10 October 1972; it was also near zero during brief periods of northward wind in September (2-7 and 18-22 September 1972).

We conclude that there is a persistent vertical shear in the alongshore current during the upwelling season, with flow in the deep layers always being northward relative to the surface. The mean alongshore current becomes more northward with increasing depth (except

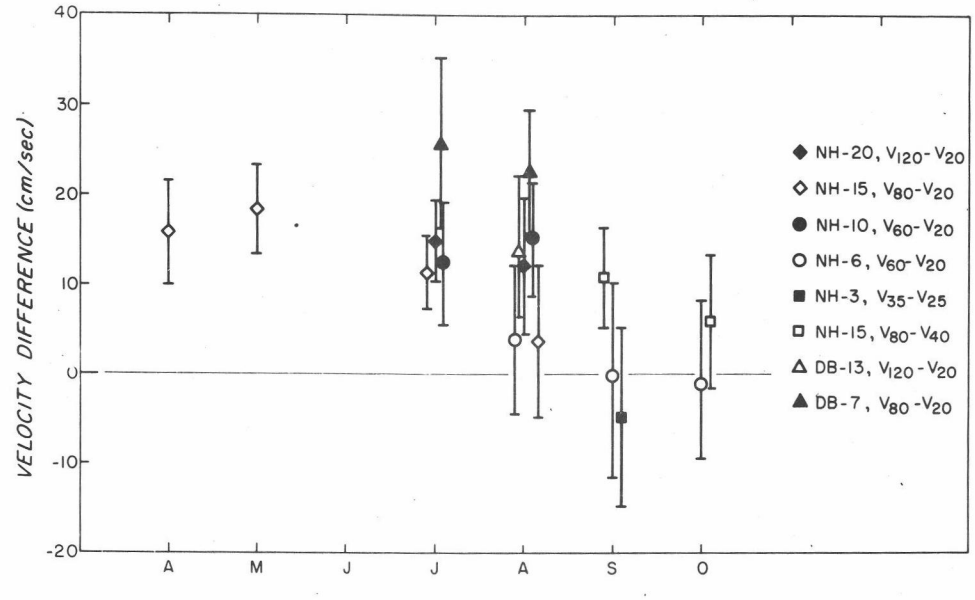

Figure 37. Monthly mean values of the northward component of the relative velocity between the deepest and shallowest current meter at each location, April to October 1972.

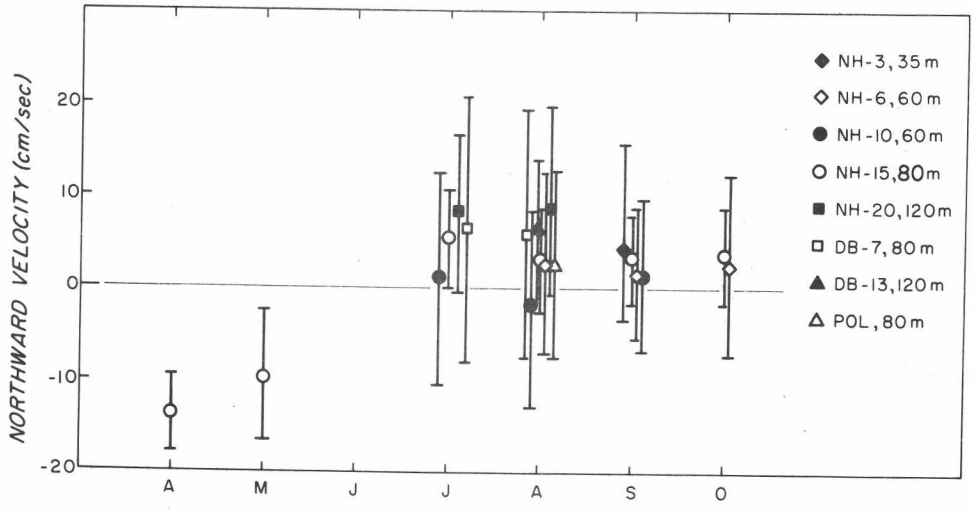

Figure 38. Monthly mean values of the northward component of the current at the deepest current meter of each array, April to October 1972.

presumably in some bottom boundary layer) at all locations where direct current observations were made. The intensity of the velocity shear varies with location and time.

Since the mean currents become more northward with increasing depth, the poleward undercurrent, if it was observed at all, would have been observed at the deepest current meters. Monthly mean values of the current at the deepest instruments were calculated in the same way as the means for Figure 37; the results are shown in Figure 38. The magnitude and direction of the alongshore flow at depth are a function of location as well as time. At NH-3, NH-6 and NH-10 no net flow was observed that was significantly different from zero. At NH-15, first southward flow and then northward flow was observed. Poleward flow appears to be significant, although barely so, during July and August at DB-7, DB-13, NH-15, and NH-20. From the NH-15 data, it appears that no poleward undercurrent is present early in the upwelling season; it is observed in the middle of the season (July and August in 1972) and diminishes late in the season. There is no evidence from the 1972 data that the poleward undercurrent has a jet-like structure - its strength does not decrease with distance offshore.

The presence of the poleward undercurrent is clearly not dependent solely on the baroclinic shear associated with upwelling. The baroclinic shear is a necessary but not a sufficient condition for the poleward undercurrent to exist.

Comparing these observations to the summary by Pillsbury (1972), we see a similar pattern for the deep flow, but a different pattern for the vertical shear. Pillsbury showed the shear to be maximum in June and July, and near zero in April and September; the 1972 data suggest a relatively constant shear from April to August, decreasing from August through October. No poleward undercurrent is observed early in the upwelling season; the 1972 data suggest it is strongest during July and August, while Pillsbury found it to be greatest in September.

(3) Geostrophy of the Alongshore Flow

Mooers et al. (1973) found the alongshore flow to be mainly geostrophic, and used absolute geostrophic velocities to infer their schematic of the alongshore flow. The validity of this hypothesis during a period of variable wind was tested in Section II; comparison of geostrophic and measured relative velocities showed good agreement except in one case (see Figure 7). The one exception during the period may have been due to shear instability.

The hydrographic sections along 44°40'N were used to compare relative geostrophic velocities to the direct current observations throughout the season (Figure 39). We used the most widely separated pair of current meters at each location in order to minimize the error of the estimates. The error in the geostrophic relative velocities is

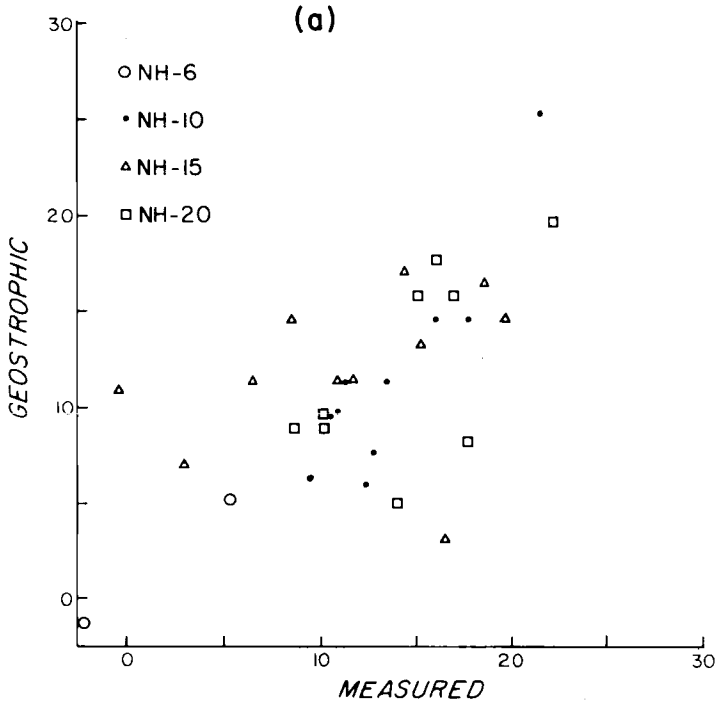

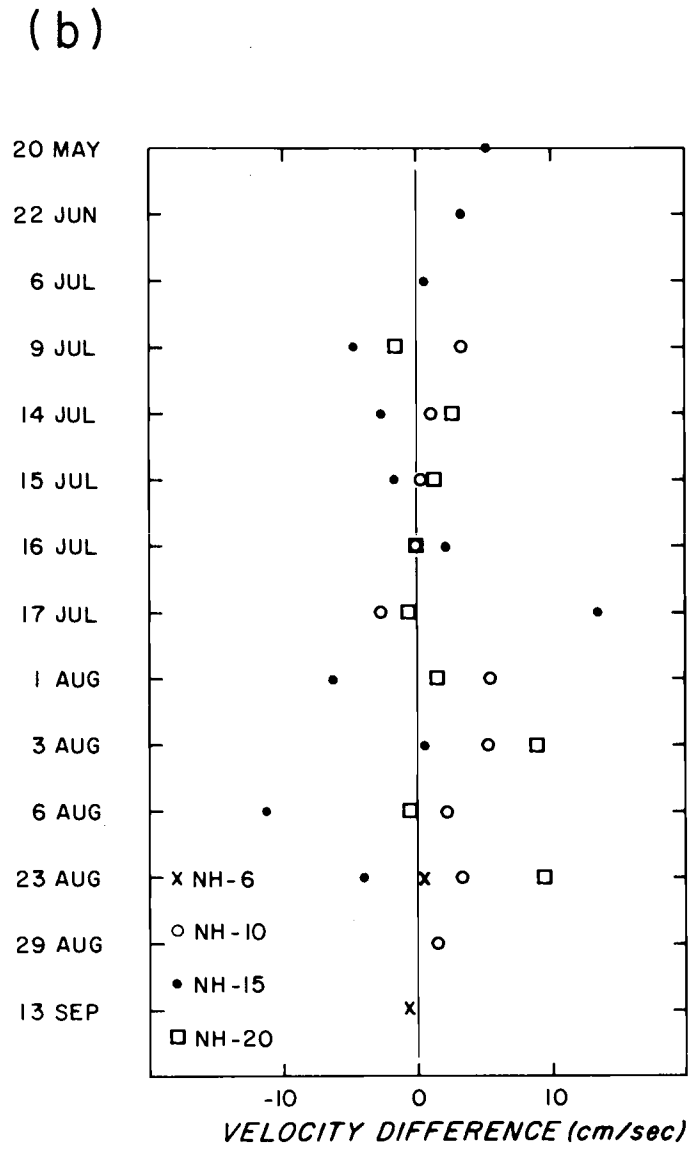

Figure 39. Comparison between measured and geostrophic relative velocities: (a) geostrophic vs. measured relative velocity; (b) difference between measured and geostrophic relative velocity for each date.

about ± 3 cm sec^{-1}. Figure 39 (a) shows the geostrophic relative velocity plotted versus the measured relative velocity. The correlation between the geostrophic and measured relative velocities is 0.61; this is significantly different from zero at the 99% level. The least squares fit by a line of the form $y = m x$ has a slope of 0.89; the geostrophic velocities are less than the measured velocities at high speeds. Figure 39 (b) shows the difference between observed and geostrophic relative velocities for each date when data were available. Good agreement is apparent during the July period of variable winds. Larger differences are observed in August. There is a hint that agreement is good at the end of August and during September, but the data are not sufficient to be very certain. Agreement also seems to be good in May and June. Smith (1973) found agreement between measured and geostrophic relative velocities at DB-7.

We conclude that the alongshore flow is mainly geostrophic both early and late in the upwelling season, but that there can be significant departures from geostrophy.

(4) Comparison Between Wind and Current

Smith (1973) has investigated the relation between wind, current and sea level using the current observations at DB-7. This relationship is further examined here to see if his results are generally applicable to the area. Simultaneous current records are available for

60 m, NH-10; 40 m, NH-15; and 40 m, NH-20. These are analyzed by the same method used by Smith - i.e. by computing the rotary cross-spectra between the wind and each current record. The coherence squared spectra for the four locations are shown in Figure 40. Values of coherence squared greater than .55 are significantly different from zero at the 99% level. All spectra show high coherence in the clockwise frequency band between 0.1 and 0.2 cpd; except at NH-15, the coherence is higher in this band than in any other, and exceeds 0.8. The currents also show high coherence at the 0.1 to 0.2 counterclockwise frequency band. High coherence at very low frequencies is observed at NH-15 and NH-20.

The current fluctuations appear to be mainly barotropic, not only at DB-7 (Smith, 1973), but also at the other locations (Figures 22 and 23). The current variations with frequencies about 0.15 cpd, especially those rotating clockwise, are highly coherent with the wind. There is some suggestion that these current oscillations are manifestations of continental shelf waves generated by the wind, but the evidence is not conclusive (Smith, 1973).

Comparing the longest current record (40 m, NH-15) to the wind shows there is no significant coherence at low frequencies over the longer period (Figure 41). We conclude that wind and current are closely related, but that this correlation is limited mainly to frequencies between about 0.1 and 0.2 cpd, and that it is strongest for the

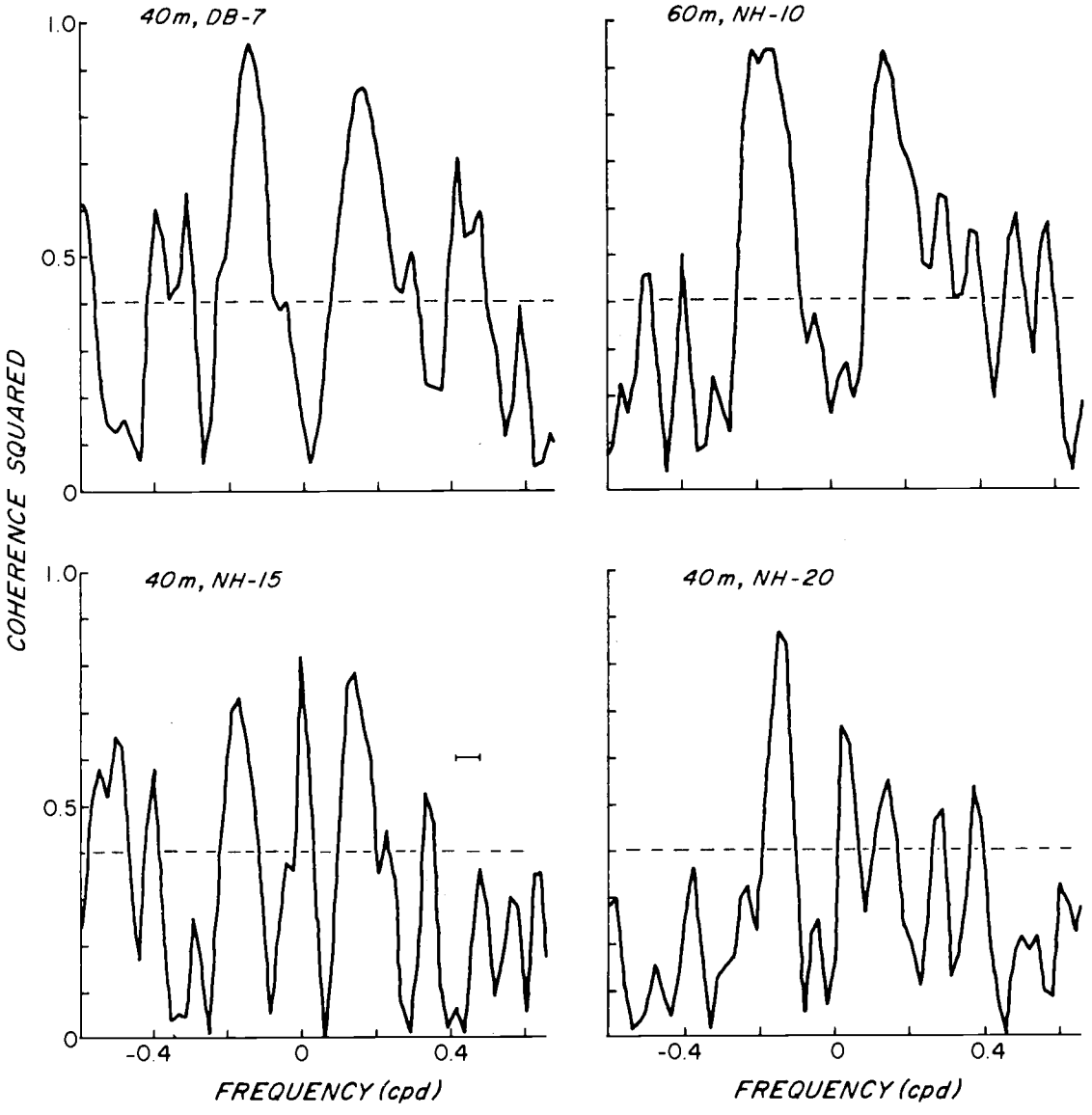

Figure 40. Coherence squared spectra for currents vs. wind at Newport, 10 July-27 August 1972. The dashed line shows coherence squared significantly different from zero at the 95% level.

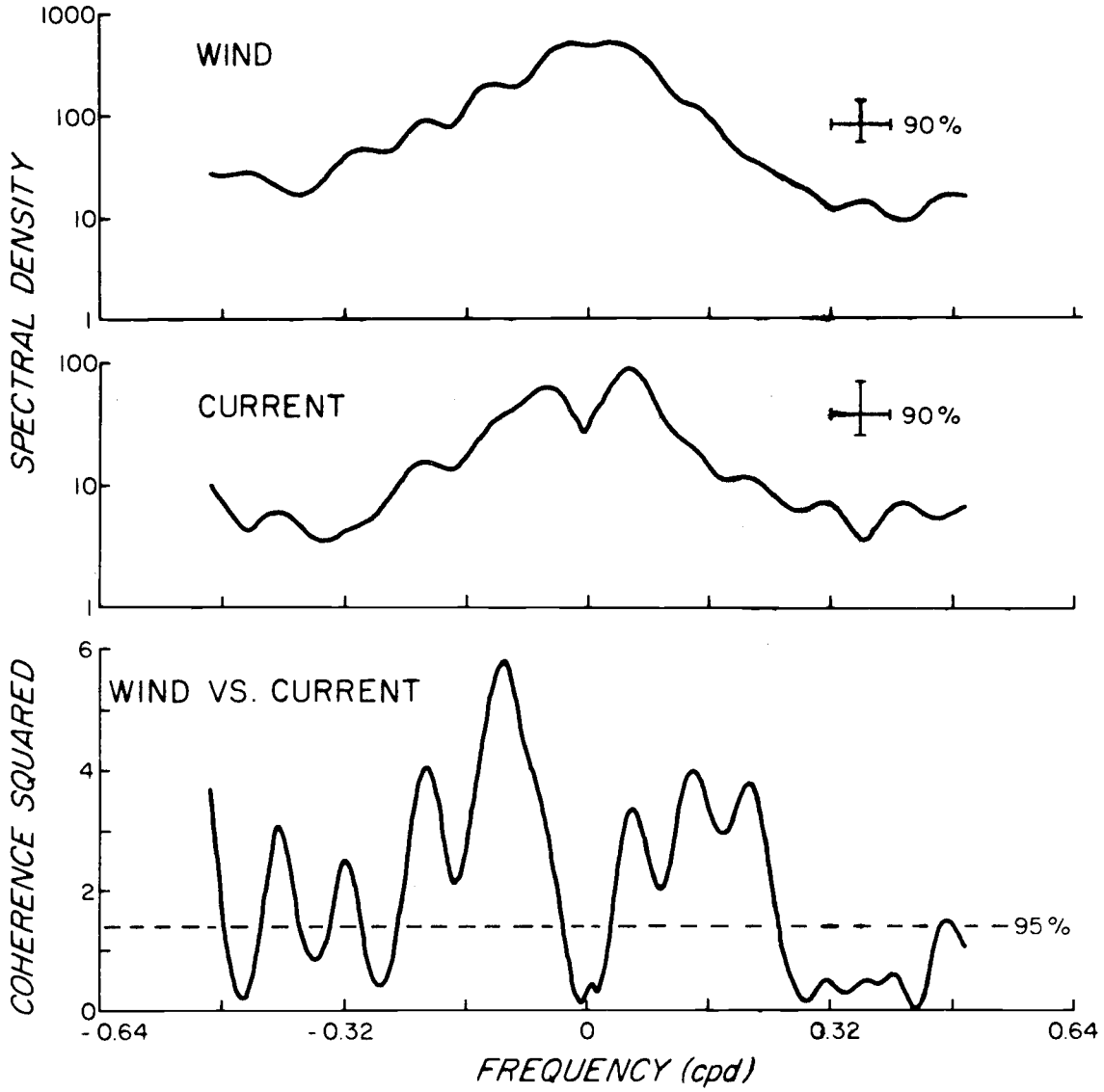

Figure 41. Autospectra and coherence squared spectrum for the wind at Newport and current at 40 m, NH-15, 23 June to 26 October 1972. The dashed line shows coherence squared different from zero at the 95% level.

clockwise component.

Sea Level

Brunson (1973) has described the annual variation of sea level at Newport, Oregon. He found the annual mean sea level to be at 274.6 cm at Newport. The mean annual range is about 30 cm, with sea level highest in December and lowest in May. The mean departure of sea level is positive from November to March, negative from April to September, and almost zero in October. The steric contribution to sea level accounts for about one-third of the annual range.

The sea level data shown in Figures 2, 22 and 23 show only relative changes in the sea level; they are not referred to the mean annual sea level. These observations were corrected for the "inverted barometer" effect of atmospheric pressure and were used to compare sea level to the wind and currents. Smith (1973) found very high correlation between current, wind and sea level at periods of several days, particularly in the clockwise component, during July and August 1972 at DB-7. Comparison between wind, sea level and current for the longest current record (40 m, NH-15) shows a similar result (Figures 41 and 42). Coherence is high for both components at periods of several days, and it is higher for the clockwise component. These results are consistent with the earlier interpretations by Mooers and Smith (1968) and Cutchin and Smith (1973) that continental

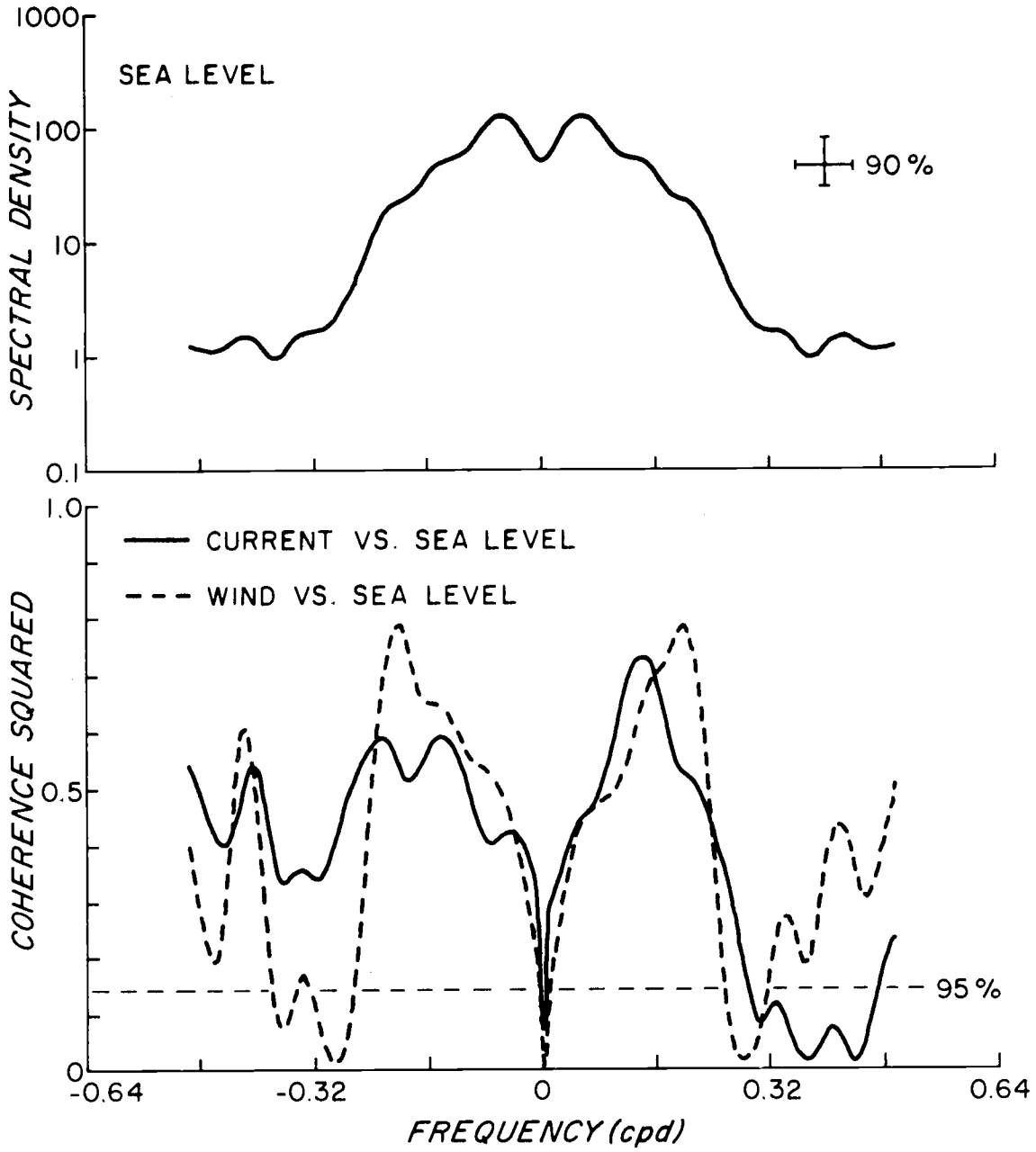

Figure 42. The spectrum of low passed sea level at Depoe Bay, 23 June to 26 October 1972, and the coherence squared spectra of Depoe Bay sea level vs. Newport wind and current at 40 m, NH-15, 23 June to 26 October 1972. The dashed line shows coherence squared significantly different from zero at the 95% level.

shelf waves may exist along the continental shelf off Oregon.

For two weeks during the 1972 upwelling season, the tide gauge at Newport malfunctioned. Comparison of the sea level data from Depoe Bay and Newport showed that fluctuations at the two locations were almost identical, and the Depoe Bay data was used to complete the Newport series. The monthly mean sea level at Newport was calculated for each month from April to October 1972. Results were compared (Figure 43) to the mean annual cycle determined by Brunson (1973). Sea level was somewhat higher than normal for much of the upwelling season. The general cycle observed in 1972 is similar to the normal except that sea level fell between September and October.

The annual range of the monthly sea level exceeds that of the oscillations with periods of several days observed during the upwelling season.

CONCLUSIONS

Seasonal development of the upwelling regime between April and October 1972 was observed for some aspects of the regime but was not observed or barely apparent for other aspects of the regime. The local wind was highly variable, and a seasonal trend was not apparent; the 1972 mean monthly upwelling indices show that the large seasonal changes did not occur between April and October, i.e. when observations were made.

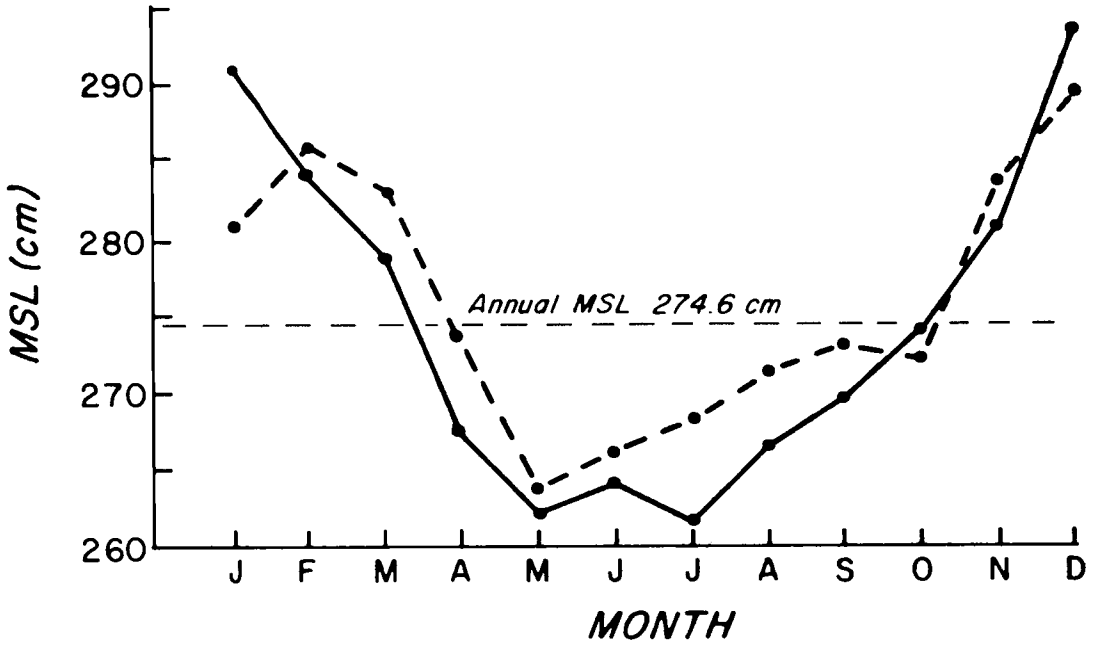

Figure 43. The monthly mean sea level at Newport, Oregon. Solid line shows the 10 year mean sea level (Brunson, 1973). Dashed line shows values from the 1972 upwelling season.

Although development was observed in the hydrographic regime, the contrast between any of the observations made between May and October and those made in January was much greater than between those made within the period from May to October. We conclude that most of the seasonal change occurred before May and after October 1972; this is consistent with the wind observations. Seasonal trends observed included the observing the lowest temperatures and the steepest isograms early in the upwelling season (June and July); the general decrease in the vertical and lateral density gradients from July to October; the observation of a well defined cool ribbon early in the upwelling season; the general warming of isohaline surfaces during the season; and the gradual increase in the temperature at the deepest current meters after early July.

As in the case of the wind, the high variability in the currents masks the seasonal trends. Also, the contrast between the observations and the inferred winter conditions are greater than among the observations. For instance, neither the development of the vertical shear, nor of the coastal jet was observed. A few seasonal trends are apparent: the vertical shear remains roughly constant over much of the upwelling season and decreases late in the season; no poleward undercurrent is observed early in the upwelling season; poleward flow at depth is observed later in the upwelling season and then diminishes.

The sea level was lowest in May and gradually increased through

September; it was higher than normal during most of the upwelling season.

Throughout the upwelling season, currents were mainly geostrophic. Wind, sea level, and currents were highly correlated at periods of several days. Temperature observations were not highly coherent with wind, currents or sea level at these frequencies. Current fluctuations were mainly barotropic throughout the season.

V. DISCUSSION

Descriptive physical oceanography is the art of describing as completely as possible the physical aspects of an oceanographic regime. Included in a complete description of any regime is a description of the boundaries, the density field, the velocity field, the distribution of water properties not uniquely determined by density, the exchange of mass and energy across the boundaries, and the time dependence of each of these. A description of this kind would result in determining the dominant length and time scales and would aid in understanding the balance of forces governing the regime.

No complete description of the upwelling regime is now available, nor will one be in the near future. Nonetheless, this framework can be used to provide a partial description and to provide perspective on the information that is available.

PARTIAL DESCRIPTION OF THE UPWELLING REGIME OFF OREGON

The results of Sections II, III and IV are combined here with other studies of CUE-1 and earlier data to provide a partial description of the upwelling regime. No attempt will be made to include phenomena with frequencies of tidal, inertial or higher periods, although these are

known to be an integral part of any oceanographic regime.

Boundaries

Off Oregon, the upwelling regime extends into the surf zone: the nearshore boundary is the coastline although the effects extend into coastal estuaries. The upper boundary is the sea surface. Near shore the lower boundary is the ocean bottom; further offshore in deeper water the lower boundary depends on the wind and ambient oceanographic conditions. The maximum depth influenced by the upwelling off Oregon clearly exceeds 175 m (see for example Figure 24) and may exceed 500 m (Park et al., 1972). The offshore limit should probably be beyond the coastal jet and other lateral features associated with upwelling; this would place it seaward of the area studied in CUE-I. The width of the regime seems to be related to the shelf width (Section III and Figure 10). The northern and southern limits of the upwelling regime are far beyond the area studied - it extends from northern Washington or Vancouver Island to Baja California. At present it is not feasible to study such a large region as a unit, and northern and southern limits have been rather arbitrarily placed.

There is some evidence (Section III) that the width of the upwelling regime increased from May through August in 1972. During most of the season, the survey grid was narrower and shallower than the

upwelling regime. No observations were available before the upwelling began, and very little is known in detail about the time dependence of the extent of the upwelling regime.

The Density Field

In the Subarctic Pacific, a typical vertical density profile shows a surface mixed layer, a seasonal pycnocline (due to the seasonal thermocline), a layer of weakly stratified water, a permanent pycnocline (due to the permanent halocline) and a deep layer in which the density increases slowly with depth (Dodimead and Pickard, 1967). The seasonal pycnocline is shallowest in late summer and disappears in winter. The bottom of the permanent halocline is at about 33.8‰. Temperature-salinity characteristics off Oregon (e.g. Figures 18 and 19) show that the permanent halocline there is between 32.5 and 33.8‰. The corresponding sigma-t range is 25.3 to 26.4. This is consistent with Collins' (1964) conclusion that sigma-t values between 25.3 and 26.3 were always within the permanent front.

The Columbia River plume modifies the near surface density structure off Oregon (Barnes, Duxbury and Morse (1972)). In winter the plume extends northward, and water off Oregon is not affected; in summer the plume extends southwards and offshore. Water in the plume is highly stratified, with the minimum surface salinity west of Newport often being about 28‰. Surface heating in this highly

stratified water causes further density stratification, and minimum values of sigma-t off Newport are frequently less than 23.0. The seasonal pycnocline off Oregon is the result of both salinity stratification due to the Columbia River plume and of temperature stratification. The seasonal pycnocline may have a much larger vertical density gradient (sigma-t increasing as much as 3.0 in 20 m) than the permanent pycnocline.

The density field exhibits a strong seasonal cycle. Pillsbury (personal communication) has computed the 10-year mean sigma-t values for a line of stations west of Newport. From November to February isopycnals are generally level inshore of 40 km except that very near shore (within 8 km) they slope downwards because of local runoff of the winter rainfall (see Figure 30). At NH-25 (40 km offshore) the surface sigma-t is very nearly 25.5 and the 200 m sigma-t is less than 26.5. Isopycnals begin to slope upward toward the coast in March and continue to steepen until July. In July the surface values of sigma-t at 8 and 40 km off shore are 25.6 and 23.5 respectively. The 200 m sigma-t value at NH-25 is maximum (26.74) in July. Isopycnal slopes remain steep in August and begin to decrease in September. The vertical range of sigma-t at NH-25 is greatest in July, decreases through September and October, and is smallest in winter.

During the upwelling season variations in the density field with periods of the order of a week are related to variations in the wind.

During July and August 1972 there were three separate occasions when there was a strong several day period in the wind: 9-18 July, 30 July - 3 August and 15 August - 2 September. The first of these periods is described in Section II and the others are described in detail by Halpern (1973). During each of these periods the major changes in the density field occurred at all depths inshore of 10 km and in about the upper 20 m further offshore. Sometimes changes in the density field occur further offshore and at greater depths as a result of changes in the wind (cf. Atlas, 1973). During northward winds, the surface density decreases and nearshore isopycnals descend; during southward winds, surface density increases and isopycnals near the coast rise.

The Velocity Field

Since the velocity field in an upwelling region is strongly anisotropic and inhomogeneous, it is partitioned into three orthogonal component fields - the vertical velocity field, the alongshore velocity field, and the onshore-offshore (or cross-stream) velocity field. Of the three, the vertical velocity field is of greatest interest and most difficult to observe.

Vertical current meters developed at Woods Hole Oceanographic Institution were used to measure the vertical velocity in the upwelling regime (Deckard, 1974) between 12 and 18 July 1972. Winds were

unfavorable for upwelling on 12 July, but became favorable on 13 July and remained so until 18 July. Changes in the hydrography were mainly in a near surface layer about 20 m thick, the near shore region about 10 km wide and near the bottom; the properties in the interior were largely unchanged by the wind (Section II). This suggests that the vertical velocities induced by the wind occurred mainly near shore and perhaps along the bottom. Each of the four vertical current meters deployed were well away from the surface and the very nearshore region. Isogram displacement, and associated vertical velocities, in the interior may be mainly a function of the speed and direction of the alongshore currents and the bottom topography (Section II). No large persistent vertical velocities were observed, and in two cases a net downward displacement was observed while the wind was favorable to upwelling. We concluded that the largest vertical velocities probably occurred inshore of the region where the vertical current meters were deployed.

The largest vertical velocities were estimated indirectly from the displacement of isopycnals. The assumption required to make these estimates (no mixing) always results in an underestimate of the vertical velocity. Halpern (1973) obtains estimates of 6.6×10^{-3} cm sec^{-1} and 1.25×10^{-2} cm sec^{-1} for the periods 2-6 August and 26-30 August respectively. Using the 26.0 isopycnal between 15 and 16 July (Figure 3), we obtain an estimate of about 2×10^{-2} cm sec^{-1} near

shore. These estimates are all for the region within 10 km of the coast. The estimates are of about the same order as the directly measured velocities in the interior. Since they are underestimates, we conclude that the vertical velocity is greater in the very near shore region than in the interior when the wind is favorable for upwelling.

There is almost certainly an annual cycle in the vertical velocity field, with greater upward velocities in summer, and perhaps sinking in winter when there is a surface convergence at the coast. In the very near shore region the vertical velocity probably has fluctuations with periods of the order of a week, as suggested by changes in the density regime.

Although the onshore-offshore component of velocity is much larger than the vertical velocity, its distribution is almost as difficult to determine. The surface Ekman flow is apparently restricted to the upper 20 m, while most moored current meters were at or below this depth. Flow in the near surface layer was measured by an array of eleven current meters placed at depths between 1.1 m and 28 m at the POL site (Halpern et al., 1973). The array was moored from 9 July and 27 August 1972. Data from current meters at 19 and 22 m agree well with observations obtained from the subsurface moored array at the site (Halpern, Pillsbury and Smith, 1973). During periods of sustained southward wind (13-18 July, 2-6 August and 23 August - 2 September) increased westward flow is observed at each of the current

meters between 1.1 and 28 m. Offshore velocities decrease with depth: from 14 to 17 July, the mean offshore velocity components were about 35, 30 and 10 cm sec^{-1} at depths of 4.4, 9.0, and 19 m respectively. Onshore flow in the surface layer is observed on only a few occasions and is very small. Taken over the whole summer, the shallower current meters show a larger offshore component than the deeper ones. This is consistent with Smith's (1973) observation that the offshore Ekman transport occurs mainly in the upper 20 m.

Convergence zones in the near surface layer were observed by surface drogues (Garvine, 1972) and from the NCAR aircraft and appear to coincide with thermal fronts (O'Brien, 1972 and personal communication). It is still unknown whether the convergence zones are isolated and short-lived or whether there is a single major convergence zone which lies roughly parallel to the coast and is a persistent feature. At least some of the convergence zones result from the sinking of surface water as it moves offshore over lighter water.

Below the upper 20 m, the onshore-offshore velocity component is small so its value depends on the choice of coordinate system. Comparisons between arrays are made in the common east-north system as well as in the local isobath system. Smith (1973) found the mean currents at DB-7 at all depths were onshore relative to the local isobath. Table VII shows the mean velocities for all current meters over a common period from 0000 Z, 25 July to 0000 Z, 5 August 1972.

Table VII. Mean velocities from the moored current meter array, 0000 Z, 25 July to 0000 Z, 5 August 1972. Components and eastward (u), northward (v), cross-isobath (u') and along-isobath (v').

Location	Local Direction of Isobath (°T)	Depth (m)	Velocity (cm sec^{-1}) u	v	u'	v'
NH-10	13	20	-7.1	-14.4	-3.7	-16.0
		60	-4.8	-3.4	-3.9	-4.4
NH-15	30	20	-4.6	-9.0	0.5	-10.1
		40	-0.4	-5.0	2.2	-4.5
		80	-0.1	4.2	-2.2	3.6
NH-20	12	20	-1.9	-6.7	-0.4	-7.0
		40	-0.9	-5.8	0.3	-5.9
		120	0.5	4.8	-0.5	4.8
DB-7	20	20	-1.8	-17.7	4.4	-17.2
		40	2.8	-9.8	6.0	-8.2
		60	2.3	-3.6	3.4	-2.6
		80	1.1	0.2	1.0	0.6
POL	40	40	0.1	-8.6	5.6	-6.5

DB-7 shows onshore flow relative to the isobaths for this shorter period as well as for the overall record length. Offshore flow is observed in both deep and shallow water at NH-10. At both NH-15 and NH-20, offshore flow in the deep water is associated with northward alongshore flow. Large day-to-day variations occurred in the eastward velocity field during the period of variable winds in early July (Section II). Eastward and northward velocity fields seemed to be closely related, suggesting that the dominant axis of flow was approximately southeast-

ward. We conclude that the onshore-offshore flow regime is as yet largely unknown.

The alongshore velocity field is relatively well understood and has been discussed extensively in Sections II and IV and by Smith (1973). During the upwelling season, the surface flow is southward with a maximum at about 15-20 km offshore; the jet is about 15 km wide. Very near shore, e.g. at NH-3 and NH-6 the mean flow is nearly zero and sometimes northward (Figure 22 and Stevenson, 1972 a, b). Late in the upwelling season, there is no mean vertical shear in the nearshore region. Beneath and seaward of the southward velocity maximum there is a persistent vertical shear with deeper water flowing northward relative to the surface. The shear appears to be mainly geostrophic and varies less than the current at a particular depth. A small poleward undercurrent is observed below and seaward of the coastal jet; at some arrays it is barely significant. There is no evidence that the undercurrent is restricted to the upwelling regime.

The spectrum of the longest low-passed current record (Figure 41) indicates that there are current fluctuations not only with periods of several days, but also with periods up to and probably exceeding 20 days. There is high coherence between the currents and the wind at periods of several days, but not at the longer periods.

There is a pronounced annual cycle in the alongshore velocity field. Surface flow is southward in summer except in the very near-

shore region; in winter, the mean surface flow is weakly northward. There is no mean vertical shear in winter; this was observed in January and February 1966 (Collins and Pattullo, 1970) and from December 1972 to June 1973 (Pillsbury, personal communication). Vertical shear is observed over the shelf very early in the upwelling season; the transition appears to occur very quickly. The shear remains relatively constant during the upwelling season but tends to decrease toward the end of the season. The shear is a function of distance offshore; no shear is observed at NH-3 and NH-6, it is greatest at DB-7 and NH-10 and still significant at NH-20.

In winter, there is no vertical shear over the continental shelf and hence no undercurrent there; it may exist further offshore. If the undercurrent is part of the California Current system, rather than of the upwelling regime, it may migrate shoreward seasonally.

Distribution of Tracers

Because of the high biological productivity of upwelling regions, the distribution and supply of nutrients is of very great interest. Kuo and Veronis (1970) have shown that the distribution of tracers can generally not be used to determine the mean flow regime; conversely, the velocity field does not determine the distribution of tracers unless even the smallest scales and shortest period motions are included.

From the CUE-I data, we found that subsurface temperature is

not particularly coherent with wind or current at periods of several days, although wind, sea level and current are very coherent with each other at these frequencies. Subsurface temperature is apparently determined more by larger scale and lower frequency motions; for example, the temperature reaches a minimum about the time the deep current becomes predominantly northward. Temperature may also be affected significantly by very high frequency motions, i.e., by turbulent diffusion. Both advection (very low frequency motions) and diffusion probably also affect the distribution of other tracers such as nutrients. The whole problem of the relative importance of advection, diffusion and decay (or generation) over the full range of length and time scales remains to be explored.

Exchange across Boundaries

Little is known about the exchange of mass and energy across the boundaries of the upwelling regime. Lane (1965) computed a heat budget for the area and concluded there is a positive heat transport from the atmosphere to the sea from April to late September; the annual mean heat exchange is usually positive.

The mean kinetic energy in the system appeared to decrease from April through August (Figure 22) while the wind stress remained significant (Table VI). Apparently the energy is dissipated faster than it can be provided by the wind stress. Presumably this would not be

true at the beginning of the upwelling season.

We assumed the water over the continental shelf to have no mean velocity on 13 April, i.e. at the beginning of the upwelling season. From Bakun's estimates of the zonal Ekman transport, we estimated the mean meridional component of the wind stress to be about -0.5 dynes cm^{-2} for the period 13-22 April 1972. We estimate the mean water velocity on 22 April to be about 10 cm sec^{-1} southward (from the observation of velocities greater than 20 cm sec^{-1} southward at NH-15; see Figure 23) in a depth of 100 m of water. This is a net change in momentum of 10^5 gm cm sec^{-1}. The change in momentum that could result from the mean wind stress over the ten day period is about 5×10^5 gm cm sec^{-1}. Even if the change in velocity is underestimated, the wind stress seems sufficient to cause the southward flow to begin.

COMPARISON WITH PREVIOUS DESCRIPTION

The manuscript by Mooers, Collins and Smith (1973) provides the most complete description of the upwelling regime of Oregon prior to the Coastal Upwelling Experiment. Their description has been widely referred to in theoretical upwelling models, and in chemical and biological studies of upwelling. Since the manuscript is as yet unpublished we quote their description of the regime and the conceptual model in its entirety, including their schematic of the upwelling regime

(Figure 44):

"A schematic of a coastal upwelling frontal zone, consistent with the data and analyses in this paper, is presented in Fig. 14 [Fig. 44]. The element of conjecture increases with depth and distance offshore. Note:

a. The undercurrent which flows poleward and which forms a jet under the steepest portion of the inclined frontal layer.

b. The surface current which flows equatorward and which forms a jet near the surface front.

c. The two anticlockwise rotating cells in the cross-stream circulation over the shelf. Exchange between the cells is implied at the one-sided divergence of the surface front, consistent with water mass formation there.

d. A similar circulation pattern is inferred for the continental slope regime, but with the lower cell rotating clockwise to attempt to conform with the downwarping of isopleths. Exchange between the offshore and shelf regimes is also implied.

e. The relatively high vertical shear in both the axial and cross-stream flows in the inclined frontal layer.

A synthesis of the frontal dynamics yields the following description for a physical model, which is an extension of the ideas presented in Mooers and Smith (1967):

a. Due to the near-surface, offshore Ekman drift induced by the winds, cold, salty water is upwelled from a depth of 100 to 200 meters offshore and arrives near the surface in a band from the coastline to 10 kilometers offshore.

b. The water in this nearshore band is separated from warmer, fresher water in the upper 100 meters offshore by an inclined frontal layer (pycnocline). Upwelling is set up in about a

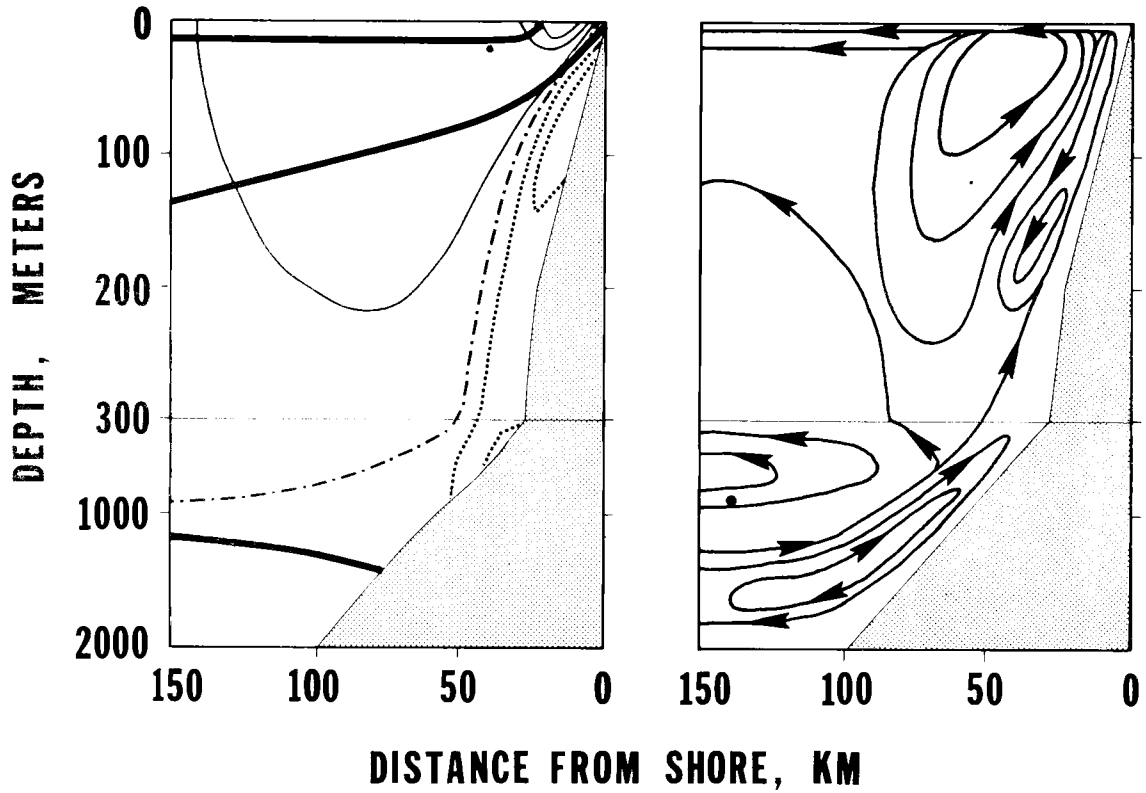

Figure 44. The conceptual model tested in the 1972 Coastal Upwelling Experiment (from Mooers et al., 1973, their Figure 14).

week, and the position of the inclined frontal layer remains approximately stationary for about 5 months. Though upwelling-favorable winds persist, the inclined frontal layer does not propagate further offshore, suggesting the formation of a one-sided surface divergence and a change in dynamics from essentially advective to diffusive and advective.

c. The water in the coastal band is modified by waves, wind, heating, evaporation, etc., and is mixed at the surface front (the one-sided surface divergence) with the offshore, surface water to form a water mass which sinks and flows offshore along the base of the inclined frontal layer. This water mass can be identified by a temperature inversion and by high particle content.

d. During the upwelling season, semidiurnal internal tides progress onshore. Hence, they must dissipate in the coastal region and may transfer energy to the mean flow.

e. There are three major sources of vertical shear in the current near the inclined frontal layer: the mean shear, the several-day shear, and the semi-diurnal shear. When they interfere constructively, shear instability can be induced, providing another energy source for mixing. The wind induced, near-surface mixing may cause the formation of the water mass, while the dissipation of internal tides may cause the disappearance of the water mass as it progresses seaward.

f. Frontal mixing, and the subsequent offshore flow along the base of the inclined frontal layer, may play a significant role in the development of the northward undercurrent observed beneath the inclined frontal layer."

Each of these points is compared to the corresponding aspect of the present partial description of the upwelling regime. A few terms used

in the Mooers, Collins and Smith description have specific meanings: the "frontal layer" is the layer of water with sigma-t between 25.5 and 26.0, believed to represent the permanent pycnocline; the "surface front" is where the "frontal layer" intersects the sea surface, i.e. the band where the surface sigma-t lies between 25.5 and 26.0.

First, the present results are compared to the description of the schematic (Figure 44):

(a) A mean poleward undercurrent is observed at the height of the upwelling season. There is no evidence that it has a jet-like structure, and it appears to increase with distance offshore. The poleward flow may be part of the California Current system and may not be an integral part of the upwelling regime.

(b) The surface current does flow equatorward and does have a nearshore velocity maximum (jet) centered about 15 km or so from shore. The jet is near the maximum horizontal density gradient (the surface front).

(c) There is no evidence for two semi-permanent anti-clockwise rotating cells in the cross-stream direction. Water mass formation at the surface is observed, and sinking of surface water does occur as the surface water moves offshore into a region of less dense surface water. The lack of continuity of the resulting warm anomaly both in time and space implies the surface convergence is not due to semi-permanent rotating cells but rather due to the local density gradients.

(d) There is no evidence for a two-celled circulation for the continental slope regime. Only a few of the 1972 observations went near the bottom over the continental slope, and it is unknown whether isograms there sloped upward or downward toward the coast.

(e) Relatively high shear is observed in the alongshore flow regime. There is little evidence of high shear in the mean onshore-offshore flow regime except in the upper 20 or 30 m. High shears due to internal tides are present in both the alongshore and onshore-offshore velocity fields.

Present results are also compared to the description of the physical model presented by Mooers et al. (1973):

(a) Near-surface offshore Ekman drift is induced by the wind and causes upwelling. Although the resulting nearshore water properties correspond approximately to those observed at depths of 150 to 200 m in winter, it is believed that water is upwelled from much greater depths, perhaps exceeding 500 m. There is undoubtedly mixing, with resulting dilution of tracers, as the water is advected upward. Rapid changes in properties (with periods of a few days) are apparently limited to the band within 10 km of shore. However, all of the water within 50 km of shore above 200 m (except the very near surface water) is 2C cooler in summer than in winter.

(b) The water in the near shore band is not separated from warmer, fresher water by the inclined frontal layer. All of the water

to at least 50 km offshore is cooled as a result of upwelling. The time in which "upwelling is set up" is rather ambiguous; this is discussed more fully in the subsection about defining upwelling.

The position of the "frontal layer" (25.5 to 26.0 sigma-t) is relatively stationary but the stratification (both vertical and lateral density gradients) continues to decrease as the upwelling season progresses. Also, although the position of the frontal layer is relatively constant its composition changes during the upwelling season, becoming progressively warmer and saltier.

(c) The surface water is modified as it moves offshore and sinks when it approaches lighter surface water. However, there is little continuity either in time or space. Another feature, an alongshore cool ribbon, also results in a temperature inversion. The cool ribbon results from alongshore advection and appears to be at about the top of the permanent pycnocline and has a salinity of about 32.5‰. The warm temperature anomaly frequently has a salinity of about 33.4‰, while the bottom of the permanent pycnocline occurs at about 33.8‰. It is not surprising that the sinking occurs somewhere within the range corresponding to the permanent pycnocline, as tilting it results in large horizontal density gradients. High turbidity is frequently associated with the warm temperature anomalies.

(d) No analysis of the tides is included in the present description.

(e) The vertical shear is great enough to achieve very low

Richardson numbers (Section II) and shear instabilities probably occur. Their relation to the mixing processes is not known at this time.

(f) Since there is no evidence for mean offshore flow at the base of the frontal layer, and since it is not clear what frontal mixing is, it is not clear that they play any role in the development of the undercurrent, particularly since it does not seem to be related to the inclined frontal layer.

COMPLETING THE DESCRIPTION

Many kinds of studies are required to complete the description of the upwelling regime off Oregon. Some of the studies require no additional field work. Much information can still be gleaned from CUE-I data, and analysis of CUE-II data has barely begun. Studies which would have high priority are:

(1) determining the seaward and the lower extent of the upwelling regime,

(2) observing the spring transition period from essentially level to sloped isograms, and from no vertical shear in the current to a well-established shear,

(3) determining the role of tidal and inertial phenomena in the upwelling regime,

(4) determining the onshore-offshore velocity field,

(5) determining the vertical velocity field, and

(6) determining which length and time scales of motion are important in determining tracer distributions.

DEFINING UPWELLING

Oceanographers studying upwelling all agree that the definition of upwelling presented by Smith (1968) is a reasonable one, namely: upwelling is ascending motion of some minimum duration and extent by which water from subsurface layers is brought into the surface layer and is removed from the area of upwelling by horizontal flow. However, there is heated debate among CUE participants about whether the onset and decay of upwelling occurs only once or frequently during a particular upwelling season. Some say that upwelling begins and ends several times during a season, with the time required for onset being a few days or less. Others say that in 1972 upwelling began before observations were begun and that it continued until after observations ceased in late October, although large perturbations with periods of a week or so occurred during the upwelling season.

The confusion stems largely from the present inability to measure vertical velocities. The definition of upwelling is in terms of upward vertical velocity but because we have not yet succeeded in measuring them directly, almost all observational studies are in terms of the effects of upwelling, e.g. sloped isopycnals, modified water properties, and a modified flow regime. It is difficult to distinguish

between the time required to establish significant vertical velocities, and the time required to produce all the characteristics of a typical upwelling regime; both are referred to as "the onset of upwelling". Similarly, there is confusion between the cessation of significant ascending motion and the removal of all the effects of upwelling.

It is clear from the CUE-I data that at least in the very near-shore region vertical velocity can be greatly enhanced and reduced in a few days (in so-called "upwelling events"). It is not clear whether small but significant upward velocities persist during the upwelling season even during periods when the wind is not particularly favorable for upwelling (between the "events"). It is also clear that some of the effects of upwelling, e.g., the cool temperatures, sloped isopycnals, vertical shear, and the coastal jet, are established very early in the upwelling season, persist, and do not disappear until very late in the upwelling season; these effects have time scales much longer than a week. There is some suggestion that the effects of upwelling are easier to create than to destroy; the regime with sloped isopycnals and a coastal jet seems to be rather stable. The effects of upwelling do not disappear during several day periods when the wind is unfavorable to upwelling. It remains to be seen whether the properties of the upwelling regime are the result only of bursts of upward velocity during rather brief periods of favorable winds (upwelling events) or whether small upward velocities persist throughout the upwelling season.

VI. CONCLUSIONS

The 1972 Coastal Upwelling Experiment has already contributed significantly to our understanding of the coastal upwelling regime. It has been possible to study the behavior of the regime during periods of variable winds as well as the development of the regime during a single upwelling season. A mesoscale feature in the hydrographic regime, a ribbon of relatively cool water, was identified and related to the velocity field. Combining these and other studies of the CUE-I data we obtained a partial description of the upwelling regime and compared it to the conceptual model developed prior to CUE-I.

We have not yet been successful in determining either the vertical velocity field or the onshore-offshore velocity field. The alongshore velocity field is relatively well understood: the alongshore flow is mainly geostrophic, but significant departures from geostrophy were observed; there is a persistent vertical shear, with deeper currents always being northward relative to the surface; there is a nearshore maximum in the southward surface current; and several day period fluctuations in the current are highly coherent with both wind and sea level. It is still not clear whether a poleward undercurrent is a result of upwelling, or whether one is frequently observed in upwelling regions

because both tend to occur along eastern boundaries of the ocean. Poleward flow at depth was observed but its mean was usually smaller than the standard deviation, and its velocity seemed to increase with distance from shore.

The hydrographic regime shows the effect of upwelling in the entire region, and during the entire time span covered by CUE-I. The seasonal signal is much stronger than the shorter period variations except in the very near surface layer. Minimum temperatures were observed in June and July. At most depths, both salinity and temperature increased during most of the season; the position of the 25.5 and 26.0 sigma-t band remained relatively constant during the season. The difference between any two sections occupied between April and October 1972 was less than between any of these sections and the section occupied in January 1973. Subsurface temperature is not highly coherent with the wind at periods of a few days.

A ribbon of relatively cool water was observed early in the upwelling season. It was well defined in May, June and early July, but less so later in the season, perhaps because it widened and moved offshore. The ribbon appears to result from the rapid advection of Subarctic water, which has a temperature minimum at the same salinity, by the coastal jet associated with the upwelling regime. A warm temperature anomaly, generally observed shoreward of the ribbon, results from the sinking of modified upwelled water as it moves

offshore. The warm anomaly seems less continuous than the cool ribbon, both in time and in space. The cool ribbon seems related to the alongshore flow regime, while the warm temperature anomaly appears to be associated with the offshore-onshore velocity field.

The comparison with the earlier conceptual model indicates that it was essentially correct in some respects, but likely erroneous in other respects. The CUE-I results show no evidence of a jet-like structure in the undercurrent; the undercurrent may not be an integral part of the upwelling regime; there is no evidence for two celled cross-stream circulation, either over the continental shelf or slope; and the source of upwelled water is almost certainly deeper than 200 m. CUE-I results support the presence of southward surface flow with a coastal jet, geostrophic alongshore flow, persistent vertical shear, the formation of a warm temperature anomaly, and the likely occurrence of shear instabilities.

A number of further studies are required, especially to determine the vertical and the onshore-offshore velocity fields.

VII. REFERENCES

Allen, J. S. 1973. Upwelling and coastal jets in a continuously stratified ocean. J. Phys. Oceanogr., 3, 245-257.

Anonymous, 1972a. CUE-I Preliminary Hydrographic Data Report, YAQUINA cruise Y7206C, 19-23 June 1972. School of Oceanography, Oregon State University. CUEA Data Report No. 1. 96 pp.

_____. 1972b. CUE-I Hydrographic Data Report, YAQUINA Cruise Y7207A, 5-9 July 1972. School of Oceanography, Oregon State University. CUEA Data Report No. 2. 104 pp.

_____. 1972c. CUE-I Hydrographic Data Report, YAQUINA Cruise Y7207B, 10-18 July 1972. School of Oceanography, Oregon State University. CUEA Data Report 3. 93 pp.

_____. 1972d. CUE-I Hydrographic Data Report, YAQUINA Cruise Y7207E, 31 July-7 August 1972. School of Oceanography, Oregon State University, CUEA Data Report No. 5. 83 pp.

_____. 1972e. CUE-I Hydrographic Data Report, YAQUINA cruise Y7208C, 22-23 August 1972. School of Oceanography, Oregon State University. CUEA Data Report No. 6. 50 pp.

_____. 1973a. CUE-I Hydrographic Data Report, YAQUINA Cruise Y7208E, 26-30 August 1972. School of Oceanography, Oregon State University. CUEA Data Report No. 7. 115 pp.

_____. 1972b. CUE-I Hydrographic Data Report, YAQUINA Cruise Y7205A, 17-22 May 1972. School of Oceanography, Oregon State University. CUEA Data Report No. 8. 92 pp.

_____. 1973c. CUE-I Hydrographic Data Report, YAQUINA Cruises Y7209A, 11-13 September 1972 and Y7210B, 28-30 October 1972. School of Oceanography, Oregon State University. CUEA Data Report 10. 95 pp.

Atlas, E. L. 1973. Changes in chemical distributions and relationships during an upwelling event off the Oregon coast. M. S. Thesis. Oregon State University. 100 pp.

Bakun, A. 1972. The PEG upwelling index off Oregon during 1972. CUE Notes, No. 10, 8-12.

_____. 1973. Coastal upwelling indices, west coast of North America, 1946-1971. U. S. Dept. of Commerce. Nat'l. Ocean. and Atmos. Admin. Nat'l. Mar. Fish. Serv. NOAA Tech. Rept. NMFS SSRF-671. 103 pp.

Ball, D. S. 1970. Seasonal distribution of nutrients off the coast of Oregon, 1968. M. S. Thesis. Oregon State University. 71 pp.

Barnes, C. A., A. C. Duxbury and B. A. Morse. 1972. Circulation and selected properties of the Columbia River effluent at sea. In: The Columbia River Estuary and Adjacent Ocean Waters, edited by A. T. Pruter and D. L. Alverson. Univ. of Wash. Press. Seattle: 41-80.

Barstow, D., W. Gilbert, K. Park, R. Still and B. Wyatt. 1968. Hydrographic data from Oregon waters, 1966. Dept. of Oceanography, Oregon State University. Ref. 68-34, 109 pp.

Barstow, D., W. Gilbert and B. Wyatt. 1969a. Hydrographic data from Oregon waters, 1967. Dept. of Oceanography, Oregon State University. Ref. 69-3. 77 pp.

_____. 1969b. Hydrographic data from Oregon waters, 1968. Dept. of Oceanography, Oregon State University. Ref. 69-6, 84 pp.

Bennett, E. B. 1959. Some oceanographic features of the northeast Pacific Ocean during August 1955. J. Fish. Res. Bd. Canada. 16(5): 565-633.

Brunson, B. A. 1973. Steric contributions to the seasonal oscillation in sea level off Oregon. In: Studies on Oceanography, pp. 156-165. Editor K. Yoshida. University of Washington Press, Seattle. 560 pp.

Cissell, M. C. 1969. Chemical features of the Columbia River plume off Oregon. M. S. Thesis. Oregon State University. 45 pp.

Collins, C. A. 1964. Structure and kinematics of the permanent oceanic front off the Oregon coast. M. S. Thesis. Oregon State University. 53 pp.

Collins, C. A., C. N. K. Mooers, M. R. Stevenson, R. L. Smith and J. G. Pattullo. 1968. Direct current measurements in the frontal zone of a coastal upwelling region. J. Oceanog. Soc. Japan. 24(6): 295-306.

Collins, C. A. and J. G. Pattullo. 1970. Ocean currents above the continental shelf off Oregon as measured with a single array of current meters. J. Mar. Res. 28(1): 51-68.

Cutchin, D. L. and R. L. Smith. 1973. Continental shelf waves: Low-frequency variations in sea level and currents over the Oregon continental shelf. J. Phys. Oceanogr. 3(1): 73-82.

Deckard, D. E. 1974. Vertical current measurement in the Oregon coastal upwelling region. M. S. Thesis. Oregon State University. 57 pp.

Dodimead, A. J., F. Favorite and T. Hirano. 1963. Review of oceanography of the subarctic Pacific region. International North Pacific Fisheries Commission. Bulletin 13, 195 pp.

Dodimead, A. J. and G. L. Pickard. 1967. Annual changes in the oceanic-coastal waters of the eastern Subarctic Pacific. J. Fish. Res. Bd. Canada, 24(11): 2207-2227.

Fisher, C. W. 1970. A statistical study of winds and sea water temperatures during Oregon coastal upwelling. M. S. Thesis. Oregon State University. 67 pp.

Garvine, R. 1972. Surface drogues. CUE Notes. No. 5: 2-4.

Gonella, J. 1972. A rotary-component method for analyzing meteorological and oceanographic vector time series. Deep-Sea Res. 19: 833-846.

Gordon, L. I. 1973. A study of carbon dioxide partial pressures in surface waters of the Pacific Ocean. Ph. D. Thesis. Oregon State University. 216 pp.

Hager, S. W. 1969. Processes determining silicate concentrations in the northeastern Pacific Ocean. M. S. Thesis. Oregon State University. 58 pp.

Halpern, D. 1973. Variations in the density field during coastal upwelling. Tethys. In press.

Halpern, D. and J. R. Holbrook. 1972. STD measurements off the Oregon coast, July/August 1972. Coastal Upwelling Ecosystems Analysis. International Decade of Ocean Exploration. CUEA Data Report 4. 381 pp.

Halpern, D., J. R. Holbrook and R. M. Reynolds. 1973. Physical oceanographic observations made by the Pacific Oceanographic Laboratory off the Oregon coast during July and August 1972. Coastal Upwelling Ecosystems Analysis. International Decade of Ocean Exploration. Tech. Rept. 3. 205 pp.

Halpern, D., R. D. Pillsbury and R. L. Smith. 1973. An intercomparison of three current meters in shallow water. Submitted to Deep-Sea Res.

Huyer, A. 1973. Vertical distributions of temperature, salinity and sigma-t from observations from R/V YAQUINA during Coastal Upwelling Experiment, 1972. School of Oceanography, Oregon State University. Ref. 73-6, 59 pp.

Huyer, A. and J. G. Pattullo. 1972. A comparison between wind and current observations over the continental shelf off Oregon, summer 1969. J. Geophys. Res. 77(18): 3215-3220.

Huyer, A., R. L. Smith and R. D. Pillsbury. 1973. Observations in a coastal upwelling region during a period of variable winds (Oregon coast, July 1972). Tethys (in press).

Kantz, K. W. 1973. Chemistry and hydrography of Oregon coastal waters and the Willamette and Columbia Rivers; March and June, 1971. M. S. Thesis. Oregon State University. 70 pp.

Kuo, H.-H. and G. Veronis. 1970. Distributions of tracers in the deep oceans of the world. Deep-Sea Res. 17(1): 29-46.

Lane, R. K. 1965. Climate and heat exchange in the oceanic region adjacent to Oregon. Ph. D. Thesis. Oregon State University. 115 pp.

McNider, R. T. and J. J. O'Brien. 1973. A multi-layer model of coastal upwelling. (To appear in J. Phys. Oceanogr.)

Mooers, C. N. K. 1970. The interaction of an internal tide with the frontal zone of a coastal upwelling region. Ph. D. Thesis. Oregon State University. 480 pp.

Mooers, C. N. K., L. M. Bogert, R. L. Smith and J. G. Pattullo. 1968. A compilation of observations from moored current meters and thermographs (and of complementary oceanographic and atmospheric data), Vol. II: Oregon continental shelf, August-September, 1966. School of Science, Oregon State University. Ref. 68-5. 98 pp.

Mooers, C. N. K., C. A. Collins and R. L. Smith. 1973. The dynamic structure of the frontal zone in the coastal upwelling region off Oregon. Submitted to J. Phys. Oceanogr.

Mooers, C. N. K. and Robert L. Smith. 1968. Continental shelf waves off Oregon. J. Geophys. Res. 73(2): 549-557.

O'Brien, J. J. 1972. CUE-I meteorological atlas. Vol. I. Coastal Upwelling Ecosystems Analysis. International Decade of Ocean Exploration. Atlas I. 309 pp.

O'Brien, J. J. and H. E. Hurlburt. 1972. A numerical model of coastal upwelling. J. Phys. Oceanogr. 2(1): 14-26.

Pak, H., G. F. Beardsley, Jr. and R. L. Smith. 1970. An optical and hydrographic study of a temperature inversion off Oregon during upwelling. J. Geophys. Res. 75(3): 629-636.

Park, Kilho. 1967a. Chemical features of the subarctic boundary near 170°W. J. Fish. Res. Bd. Canada 24(5): 899-908.

_____. 1967b. Nutrient regeneration and preformed nutrients off Oregon. Limnol. Oceanogr. 12(2): 353-357.

_____. 1968. Alkalinity and pH off the coast of Oregon. Deep-Sea Res. 15: 171-183.

Park, K., J. G. Pattullo and B. Wyatt. 1962. Chemical properties as indicators of upwelling along the Oregon coast. Limnology and Oceanography 7(3): 435-437.

Pattullo, J. G , W. V. Burt and S. A. Kulm. 1969. Oceanic heat content off Oregon: its variation and their causes. Limnology and Oceanography, 14(2): 279-287.

Pattullo, J. and W. Denner. 1965. Processes affecting seawater characteristics along the Oregon coast.

Pattullo, J. G. and W. B. McAlister. 1962. Evidence for oceanic frontogenesis off Oregon. Science 135: 106-107.

Pavlova, Yu. V. 1966. Seasonal variations of the California Current. Oceanology. 6(6): 806-814.

Phillips, O. M. 1966. The dynamics of the upper ocean. Cambridge University Press. Cambridge. 621 pp.

Pillsbury, R. D. 1972. A description of hydrography, winds and currents during the upwelling season near Newport, Oregon. Ph. D. Thesis. Oregon State University. 163 pp.

Pillsbury, R. D., J. S. Bottero and R. E. Still. 1973. A compilation of moored current meter observations. Oregon continental shelf, April-October 1972. In preparation.

Plank, W. S. and H. Pak. 1973. Observations of light scattering and suspended particulate matter off the Oregon coast, June-October 1972. School of Oceanography, Oregon State University. Ref. 73-11. 318 pp.

Pytkowicz, R. M. 1964. Oxygen exchange rates off the Oregon coast. Deep-Sea Res., 11: 381-389.

Reed, R. K. and D. Halpern. 1973. STD observations in the Northeast Pacific, September-October, 1972. U. S. Dept. of Commerce. Nat'l. Oc. and Atmos. Admin. Envir. Res. Lab. NOAA Tech. Rept. ERL 271-POL 19. 58 pp.

Reid, J. L., G. I. Roden and J. G. Wyllie. 1958. Studies of the California Current system. Calif. Coop. Oceanic Fisheries Investigations. Progress Rept. VI: 27: 57.

Roden, G. I 1964. Shallow temperature inversions in the Pacific Ocean. J. Geophys. Res., 69: 2899-2914.

Rosenberg, D. H. 1962. Characteristics and distribution of water masses of the Oregon coast. M. S. Thesis. Oregon State University. 45 pp.

Small, L. F. 1972. Phytoplankton pigment data in CUE-I experimental area. Data Report. Oregon State University. Unpublished manuscript.

Smith, R. L. 1968. Upwelling. Oceanogr. Mar. Biol. Ann. Rev. 6: 11-46.

_____. 1973. A description of current, wind and sea level variations during coastal upwelling (Oregon coast, July-August 1972). Submitted to J. Geophys. Res.

Smith, R. L., C. N. K. Mooers and D. B. Enfield. 1971. Mesoscale studies of the physical oceanography in two coastal upwelling regions: Oregon and Peru. In: Fertility of the Sea. Vol. 2. Editor: J. D. Costlow, Jr. pp. 513-535. Gordon and Breach Science Publishers. New York.

Smith, R. L., J. G. Pattullo and R. K. Lane. 1966. An investigation of the early stage of upwelling along the Oregon coast. J. Geophys. Res. 71(4): 1135-1140.

Stefansson, U. and F. A. Richards. 1964. Distributions of dissolved oxygen, density and nutrients off the Washington and Oregon coasts. Deep-Sea Res. 11: 355-380.

Stevenson, M. 1972a. Subsurface drogues. CUE Notes. No. 5: 4-7.

_____. 1972b. Preliminary results from subsurface drogue experiment, August 23-26, 1972. CUE Notes. No. 7: 1-4.

Stevenson, M. R., J. G. Pattullo and Bruce Wyatt. 1969. Subsurface currents off the Oregon coast as measured by parachute drogues. Deep-Sea Res. 16: 449-461.

Stevenson, M. and B. Wyatt. 1973. STD measurements off the Oregon coast, August 1972. Coastal Upwelling Ecosystems Analysis. International Decade of Ocean Exploration. CUEA Data Report 9. 77 pp.

Stommel, H. 1965. The Gulf Stream. University of California Press. Berkeley. 248 pp.

Tomlinson, R. D., L. Barstow, D. R. Standley, S. Williams, L. I. Gordon and P. K. Park. 1973. Chemical data from Oregon waters, 1972. School of Oceanography, Oregon State University. Data Report No. 56. Ref. 73-15.

Uda, M. 1963. Oceanography of the Subarctic Pacific Ocean. J. Fish. Res. Bd. Canada. 20(1):119-179.

Wyatt, B. and N. F. Kujala. 1962. Hydrographic data from Oregon coastal waters, June 1960 through May 1961. School of Science, Oregon State University. Ref. 62-6, 77 pp.

_____. 1963. Hydrographic data from Oregon waters, June through December 1961. Dept. of Oceanography, Oregon State University. Ref. 63-33. 36 pp.

Wyatt, B. and W. E. Gilbert. 1967. Hydrographic data from Oregon waters, 1962 through 1964. Dept. of Oceanography, Oregon State University. Ref. 67-1. 175 pp.

Wyatt, B., W. Gilbert, L. Gordon and D. Barstow. 1970. Hydrographic data from Oregon waters, 1969. Dept. of Oceanography, Oregon State University. Ref. 70-12. 155 pp.

Wyatt, B., R. Still, D. Barstow and W. Gilbert. 1967. Hydrographic data from Oregon waters, 1965. Dept. of Oceanography, Oregon State University. Ref. 67-28. 56 pp.

Wyatt, B., R. Tomlinson, W. Gilbert, L. Gordon and D. Barstow. 1971. Hydrographic data from Oregon waters, 1970. Dept. of Oceanography, Oregon State University. Ref. 71-23. 134 pp.

_____. 1972. Hydrographic data from Oregon waters, 1971. Dept. of Oceanography, Oregon State University. Ref. 72-14. 77 pp.